(Supporting Information)

Teaching an Old Scaffold New Recognition Tricks: Oligopyrrolamide Antagonists of IAPP Aggregation

Sunil Kumar*, Maria C. Vogel, and Andrew D. Hamilton*

Chemistry Department, New York University, Silver Center, 100 Washington Square E, New York, NY 10003

Table of Contents

MATERIALS AND METHODS

Materials. Thioflavin T (ThT) was purchased from Acros Organics (Fair Lawn, NJ). Lipids [dioleoylphosphatidylglycerol (DOPG) and dioleoylphosphatidylcholine (DOPC)] were purchased from Avanti Polar Lipids, Inc. (Alabaster, AL). The 96-well plates (black, w/flat bottom) were bought from Greiner Bio-One (Monroe, NC). All of the chemicals were purchased from commercial suppliers and used without further purification. Silica plates (w/UV254, aluminum backed, 200 micron) and silica gel (standard grade, particle size = 40-63 micron, 230 × 400 mesh) for flash column chromatography were purchased from Sorbent Technologies (Atlanta, GA). Dry solvents were purchased from Sigma Aldrich (St. Louis, MI) or VWR (Bridgeport, NJ). Ethyl 4-nitro-1*H*-pyrrole-2-carboxylate, Alkyl iodides, triethylamine (dry), *PyBOP* (benzotriazol-1-yl-oxytripyrrolidinophosphonium hexafluorophosphate), *tert*-butyl bromoacetate, tetra-n-butylammonium iodide, trifluoroacetic acid (TFA), and triethylsilane (TES) were purchased from Sigma Aldrich (St. Louis, MI). Human islet amyloid polypeptide (IAPP) and $A\beta_{42}$ were purchased from Anaspec (Fremont, CA) with >98% purity. $A\beta_{42}$ was used without further purification while IAPP was re-purified using in-house purification method.

Preparation of IAPP. IAPP (~2 mg) was solubilized in 7 M guanidinium hydrochloride. The solution was filtered (0.2 micron) and transferred to C-18 spin column, washed twice with water (400 µL each) followed by 10% acetonitrile in water, 0.1% formic acid (v/v) and then eluted into 200 µL of 50% acetonitrile in water, 0.1% formic acid (v/v). The concentration of IAPP (oxidized form) was calculated using absorbance measurements at 280 nm (ε = 1400 $M^{-1}cm^{-1}$). The IAPP solution was divided into several aliquots (20-50 µL, 1-2 mM), lyophilized, and stored as a white solid at -80 ºC. Fresh stock solution of IAPP was prepared in water for each experiment.

ThT-based Kinetic Assay. Kinetic assays were conducted on a FlexStation 3 Multi-Mode Microplate reader from Molecular Devices (Sunnyvale, CA). Experiments were conducted in triplicate in a 96-well plate with a final volume of 200 µL per well. Every measurement was an average of 50 readings. The aggregation of IAPP was initiated by its addition from a stock solution (1 mM in DMSO) to phosphate buffer. The stoichiometry ratio for ThT to IAPP was 0.5:1. Peptide aggregation were monitored by ThT fluorescence (λ_{ex} = 445 nm and λ_{em} = 485 nm). The blank sample contained everything except peptide. The sample data were processed by subtracting the

blank and renormalizing the fluorescence intensity by setting the maximum value to one. Buffer conditions: 100 mM KCl, 50 mM NaPi, pH 7.4.

Kinetic assays in the presence of small molecules were conducted under the same conditions except that the small molecules were added from a stock solution (1 mM or 10 mM in DMSO) to keep the final concentration of DMSO less than 1.0% (v/v). Small molecules were added to the wells with ThT and buffer and mixed gently with a pipette before adding IAPP. To keep the conditions identical, an equal amount of DMSO was added to the wells with IAPP only reactions. For the aggregation kinetics of $A\beta_{42}$, the peptide was dissolved in 1N NaOH (0.5-1 mM) and vortexed for 2 min. to ensure the complete solubility. The aggregation of 3 μM $A\beta_{42}$ was initiated by addition of peptide from a stock solution (in 1 N NaOH, 0.5-1 mM) to phosphate buffer.
Kinetic profiles were processed using Origin (version 9.1). Kinetic curves were fit using the built-in sigmoidal fit. Each run was fit independently to extract the t_{50} (time required to reach 50% of the maximum fluorescence intensity). Error bars represent standard deviations from the mean of at least three independent experiments.

Seed-Catalyzed Kinetic Assay. Seeds of IAPP were prepared by incubating 100 μM of IAPP in phosphate buffer at r.t. and aged for 24 h. The formation of fibers was confirmed by TEM and ThT stain before storage at -20 °C until use. For the seed catalyzed aggregation kinetics of IAPP, 10% (based on the monomeric IAPP, v/v) seeds were added with ThT in phosphate buffer to the 96-well plate. The aggregation was initiated by the addition of fresh IAPP followed by gentle mixing. Kinetic assays in the presence of small molecules were conducted under the same conditions except that the small molecules were added from a stock solution (1 mM or 10 mM in DMSO) to keep the final concentration of DMSO less than 1.0% (v/v). Error bars represent standard deviations from the mean of at least three independent experiments. Buffer conditions: 100 mM KCl, 50 mM NaPi, pH 7.4.

Preparation of Large Unilamellar Vesicles (LUVs). LUVs were prepared using DOPG and DOPC at stoichiometric ratio of 3:7 (DOPG:DOPC). The solution of DOPG and DOPC (6 mg and 14 mg) in chloroform (10 mg/L) was mixed, dried over a stream of argon (g) for 2 h, and then lyophilized for 12 h (0.1×10^{-3} bar). The solid was rehydrated in 1 mL phosphate buffer for 30 min. The turbid solution (6 mg:14 mg, 3:7, DOPG:DOPC) was then extruded (21 times) through 100 nm diameter filters (Whatman, GE Healthcare, Marlborough, MA). The concentration of the

phospholipid content in the extruded material was confirmed by calculating total phosphorus using total phosphate assay.[1] Buffer conditions: 100 mM KCl, 50 mM NaPi, pH 7.4.

Liposome leakage assay. The kinetics of liposome leakage induced by IAPP was monitored on QuantaMaster C-61 fluorescence spectrometer (Photon Technology International, Edison, NJ) at 25 ºC. The excitation and emission were observed at 480 nm and 526 nm respectively with 3 nm slit widths. The stock solution of IAPP used in the measurements was kept in water at a concentration of 1 mM. The stock solution of water soluble quencher, DPX (*p*-xylene-bis-pyridinium bromide) was prepared in buffer (100 mM KCl, 50 mM NaPi, pH 7.4) at a concentration of 100 mM. The small molecules used in the leakage assay were dissolved in DMSO with a concentration range of 10-20 mM. The final concentration of dye encapsulating liposome (LUVs: DOPG:DOPC, 3:7, d = 100 nm), DPX, human IAPP, and small molecules were 200, 6000, 4, and 4 μM respectively. The final buffer concentration was corrected using higher concentration of buffer to keep the osmolality balanced. The final concentration of DMSO used in the assay was less than 0.4%. The negative control (no leakage) sample contained everything except IAPP. For positive control (100% leakage), the negative control sample was treated with Triton X-100 (Sigma-Aldrich, St. Louis, MO). To determine the leakage rate constant, first the fluorescence was normalized and corrected by subtracting it from normalized fluorescence of control reaction. The corrected fluorescence was fit using equation given below (using Origin 9.1). All the experiments were performed in triplicate and the error values presented are standard deviations.

$$a*\exp(-b*x)+c \qquad (2)$$

a = amplitude from 100% unleaked to 0% leaked

c = final fraction of unleaked liposome

y = change in fluorescence

b = leakage rate constant

Transmission Electron Microscopy (TEM) Analysis. IAPP was incubated in phosphate buffer in the absence and presence of ADH-101 at equimolar ratio for 12 or 24 h. Aliquots of these samples were then applied to glow-discharged carbon-coated 300-mesh copper grids for 2 min and dried. Grids were negatively stained with uranyl acetate (2%, w/v) and dried. Micrographs of grids

were examined on a Phillips CM12 Cryoelectron Microscope equipped with Gatan 4k × 2.7k CCD camera at 120-kV accelerating voltage. Buffer conditions: 100 mM KCl, 50 mM NaPi, pH 7.4.

Circular Dichroism (CD) Spectroscopy. A freshly prepared stock solution of IAPP (500 μM in water) was diluted to 15 μM in phosphate buffer for CD measurements. The spectra of IAPP were recorded at 0.5 nm intervals from 190 to 260 nm with an averaging time of 10 sec. and an average of three repeats on a Aviv Stopped Flow CD Spectropolarimeter (Model 202SF). Spectra were recorded using the identical method as described above, except ADH-101 was added to the solution of IAPP at an equimolar ratio. The CD spectra of lipid catalyzed IAPP kinetics were recoded under the same conditions with the addition of DOPG:DOPC (3:7, 750 μM, d=100 nm). Buffer conditions: 100 mM KCl, 50 mM NaPi, pH 7.4.

Photoinduced cross-linking of unmodified proteins (PICUP) analysis. A stock solution of IAPP (1 mM) in water was diluted (15 μM) and incubated with the cross-linking agent, ammonium persulphate (20 mM, 1 μL) and tris (2,2'-bipyridyl) dichlororuthenium (II) hexahydrate (1 mM, 1 μL) for time intervals of 30 min., 60 min., 120 min., and 300 min. The reaction mixture was then exposed to filament lamp for 20 s. followed by the addition of dithiothreitol (1 M, 1 μL) to quench the reaction. The samples were incubated on ice for 15 min. followed by the addition of SDS buffer. The samples were heated at 90 ° C for 5 min. and then centrifuged. Similar process was repeated in the presence of the oligopyrrolamides at equimolar ratio (IAPP:oligopyrroleamide). The samples were employed to Nu-PAGE electrophoresis in 12% Bis-Tris gels with SDS-PAGE buffer. The protein samples, in the absence and presence of the oligopyrroleamides, were then analyzed by staining them with silver stain kit from Sigma Aldrich (St. Louis, MI, USA). All the experiments were performed in triplicate to validate the results.

Fluorescence Titration. N^{α}-amino-terminal fluorescein-labeled IAPP ($IAPP_F$) was purchased from Anaspec (Fremont, CA, USA) and used without further purification. To ensure the monomeric state of $IAPP_F$, the peptide was treated similarly to other peptides and stored at -80 °C in the dark until use. Fluorescence measurements were performed on a FlexStation 3 Multi-Mode Microplate reader from Molecular Devices (Sunnyvale, CA, USA). Fluorescence titrations were conducted in triplicate in a 96-well plate with a final well volume of 200 μL. For fluorescence measurements, the fluorescein dye was excited at 492 nm and the spectra were recorded from 500 nm to 600 nm. A 50 nM $IAPP_F$ solution in fluorescence assay buffer (20 mM NaPi, 1% TFE, pH

7.4) was titrated with incremental amounts of ADH-101 (in DMSO, 0.5-2 mM) and the spectra were recorded from 500 nm to 600 nm. A number of high concentration stock solutions of ADH-101 were prepared to minimize the amount of DMSO in the fluorescence titrations (<3%). The addition of ADH-101 was continued until no further change in the fluorescence was observed. To determine the binding affinity of ADH-101 against IAPP, the change in the fluorescence intensity (λ_{max} = 522 nm) was plotted as a function of the concentration of ADH-101. The plot was fitted using a sigmoidal fit to extract the apparent binding affinity.

Cell Culture. Rat insulinoma RIN-m cells (ATCC, Manassas, VA) were cultured in RPMI medium supplemented with 10% fetal bovine serum, 1% penicillin/streptomycin, 100 mM sodium pyruvate, and 50 mM β-mercaptoethanol (Life Technologies, Carlsbad, CA) at 37 ° C and 5% CO_2. Upon reaching ~95% confluence, cells were washed with phosphate buffered saline (VWR, Radnor, PA), split using 0.25% Trypsin-EDTA (Life Technologies), and plated in clear 96-well plates (Corning, Glenview, IL) for cell viability assays.

Cell Viability. Cell viability was measured using the CellTiter Blue (CTB, Promega, Madison, WI) fluorescence-based assay. Cells were plated at a density of 20,000 cells per well in 96 well plates. After 48 h of incubation at 37 ° C and 5% CO_2, cells were washed with 100 μL of PBS. ADH-101 and hIAPP were pre-mixed in 1xPBS (ThermoFisher, Waltham, MA) for 5 min and added to cells with complete RPMI growth medium. Cells were incubated for an additional 48 h. 20 μL of CellTiter Blue reagent was added to each well and incubated for 2.5 – 3.5 h. Fluorescence of the dye was measured on a FlexStation3 microplate reader (Molecular Devices, Sunnyvale, CA). Positive control wells contained 10% DMSO, whereas negative control wells contained water and 0.3% DMSO to account for the peptide and ADH-101 vehicles, respectively. Percent viability was calculated as per the following equation:

$$\% \text{ Viability} = 100*[(<S>-<P>)/(<N>-<P>)]$$

Where <S>, <P>, and <N> are the average fluorescence intensities of the sample, positive control, and negative control, respectively. Error bars reflect variability across 4–8 technical replicates within a single execution of the assay.

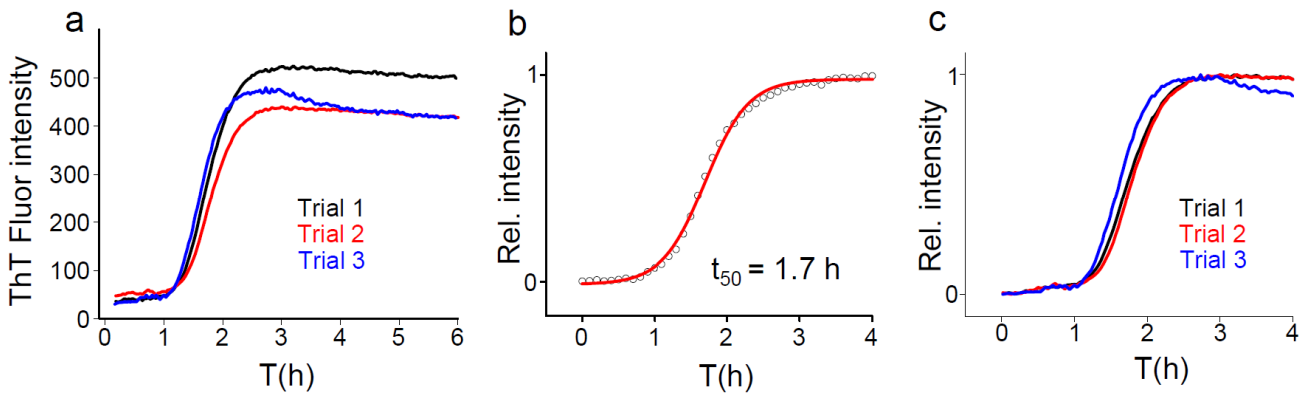

Figure S1. a, Representative kinetic profiles of IAPP fibrillation probed by the change in the fluorescence intensity of ThT dye as a function of time. **b**, A sigmoidal fit to extract the t_{50} of one of the traces presented in (c). **c**, Normalized profiles of three independent readings of lipid catalyzed aggregation (750 μM, LUVs, DOPG:DOPC, 3:7, d=100 nm) of 15 μM IAPP in phosphate buffer. The error bars reported for the kinetic assays in the main text Figure 2, 4 were the standard deviations from three independent experiments. Buffer conditions: 50 mM NaPi, 150 mM KCl, pH 7.4. [ThT] = 7.5 μM.

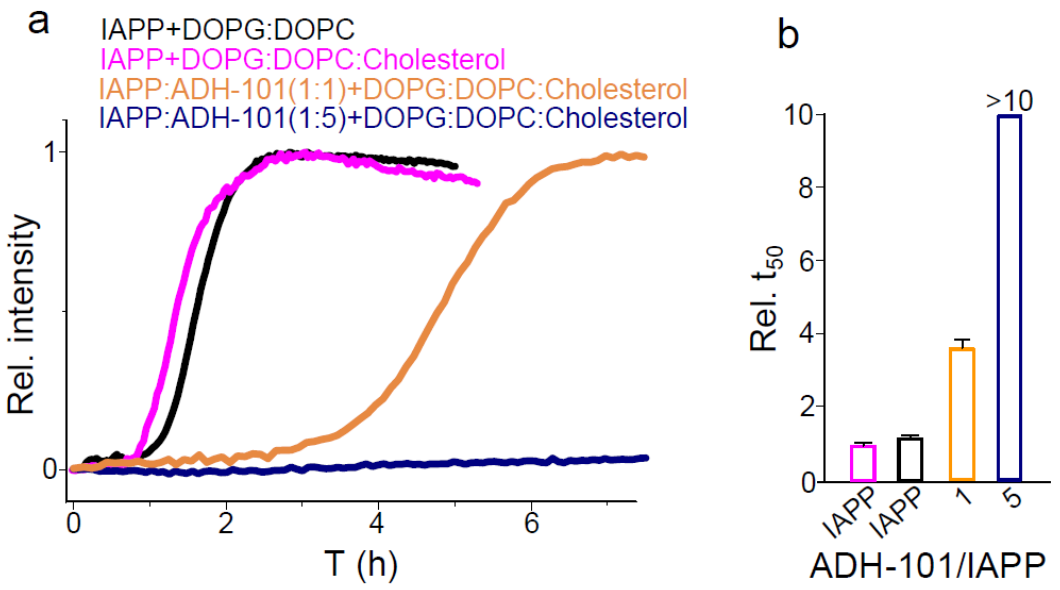

Figure S2. **a**, Representative normalized amyloid kinetic profiles of 15 μM IAPP in the presence of LUVs (750 μM) and ADH-101 at an equimolar ratio. LUVs were synthesized in the absence and presence of Cholesterol. LUVs without Cholesterol were synthesized using a mixture of DOPG:DOPC (3:7, d=100 nm) and LUVs with Cholesterol were synthesized using a mixture of DOPG:DOPC (3:7, 30% Cholesterol, w/w, d=100 nm). **b**, Statistical analysis of the amyloid kinetics performed in Figure a. The error bars reported for the kinetic assays are the standard deviations from three independent experiments. Buffer conditions: 50 mM NaPi, 150 mM KCl, pH 7.4. [ThT] = 7.5 μM.

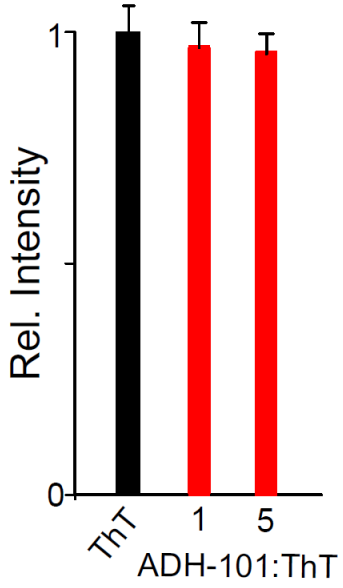

Figure S3. Effect of ADH-101 on the fluorescence intensity of ThT. All the conditions are identical as described in Figure 2 (main text) except protein (IAPP). Buffer conditions: 150 mM KCl, 50 mM NaPi, pH 7.4, [ThT] = 7.5 μM.

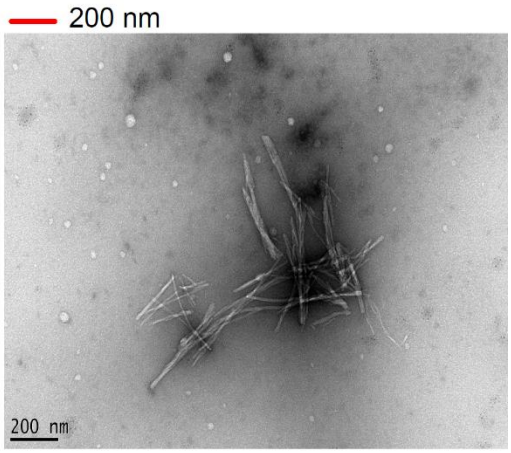

Figure S4. Visual analysis of the effect of ADH-101 on the kinetics of IAPP fibrillation using TEM. TEM image of 15 μM IAPP under lipid membrane conditions (750 μM, LUVs, DOPG:DOPC, 3:7, d=100 nm) in the presence of ADH-101 at an equimolar ratio after 24 h. Buffer conditions: 150 mM KCl, 50 mM NaPi, pH 7.4.

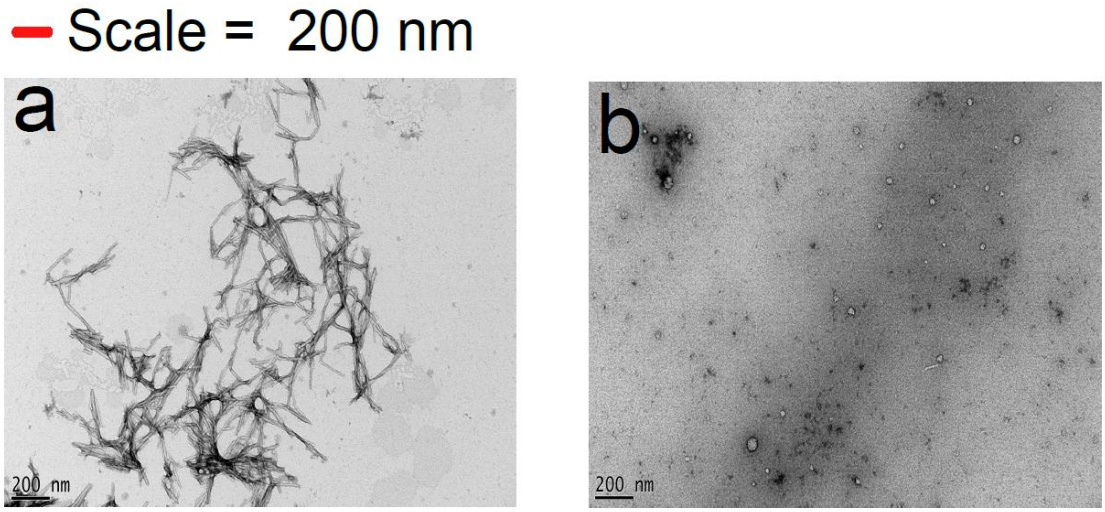

Figure S5. Visual analysis of the effect of ADH-101 on the kinetics of IAPP fibrillation using TEM. TEM image of 15 μM IAPP in the absence (a) and presence (b) of ADH-101 at an equimolar ratio after 12 h. Buffer conditions: 150 mM KCl, 50 mM NaPi, pH 7.4.

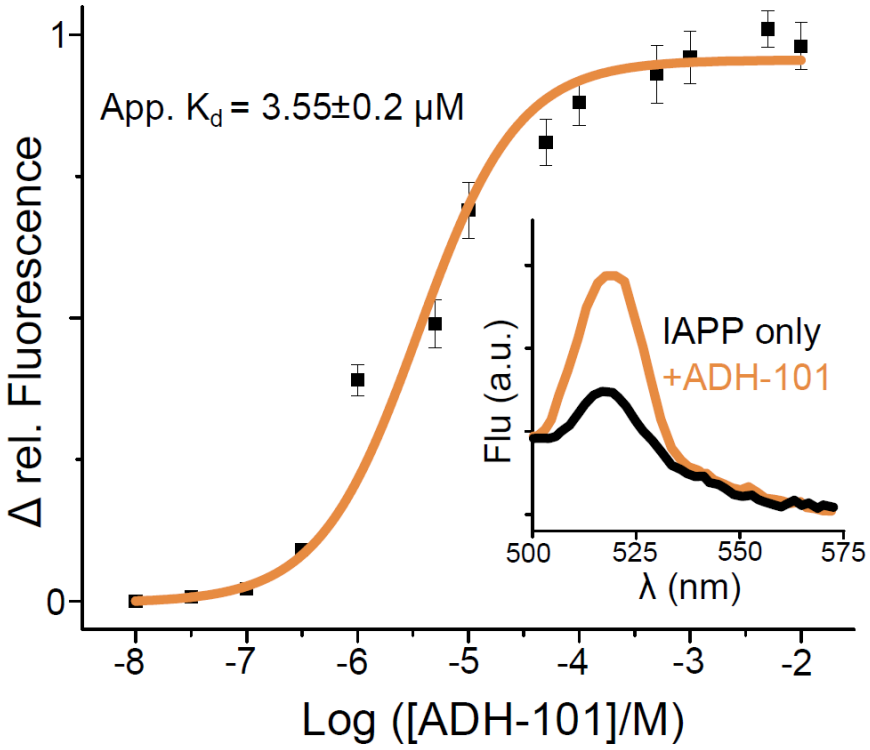

Figure S6. Determination of the binding affinity between IAPP and ADH-101 using fluorescence titration. The plot results from a fluorescence titration between $IAPP_F$ and ADH-101. A concentrated solution of ADH-101 was continually added to a solution of 20 nM $IAPP_F$ until no more change in the fluorescence observed. Inset, The fluorescence spectra of $IAPP_F$ in the absence (black) and presence (blue) of ADH-101 recorded from 500 nm to 575 nm (λ_{ex} = 492 nm).

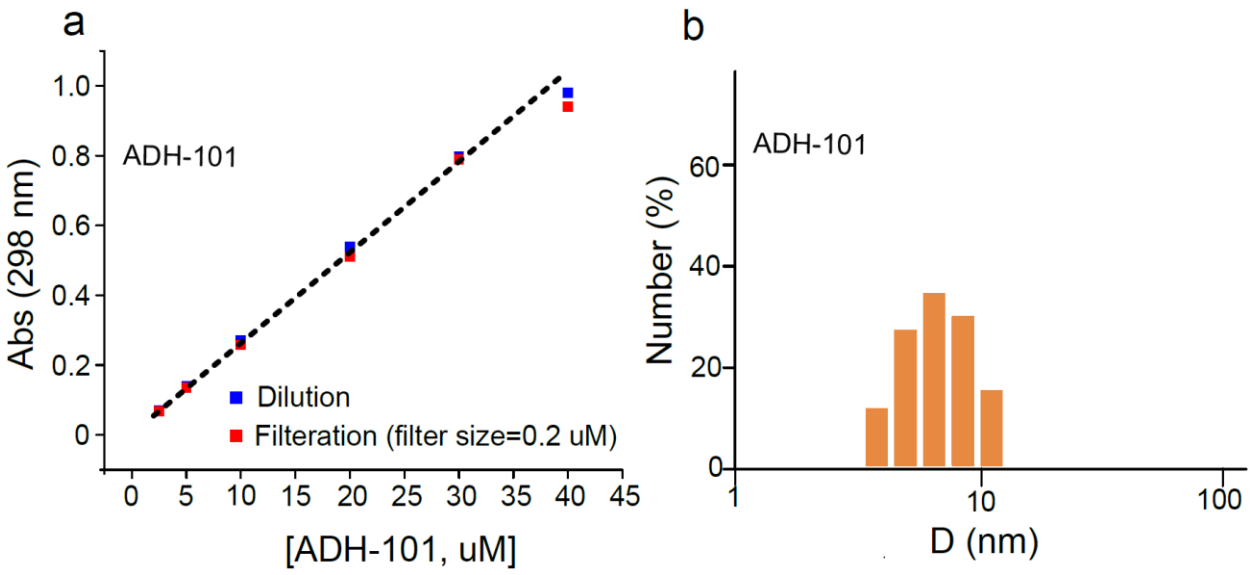

Figure S7. Analysis of the self-aggregation of ADH-101 using absorbance and DLS. **a**, The plot of absorption values with increasing concentrations of ADH-41 under indicated conditions. **b**, DLS plot of 25 μM ADH-101 under the identical conditions used in Figure a. Buffer conditions: 150 mM KCl, 50 mM NaPi, pH 7.4.

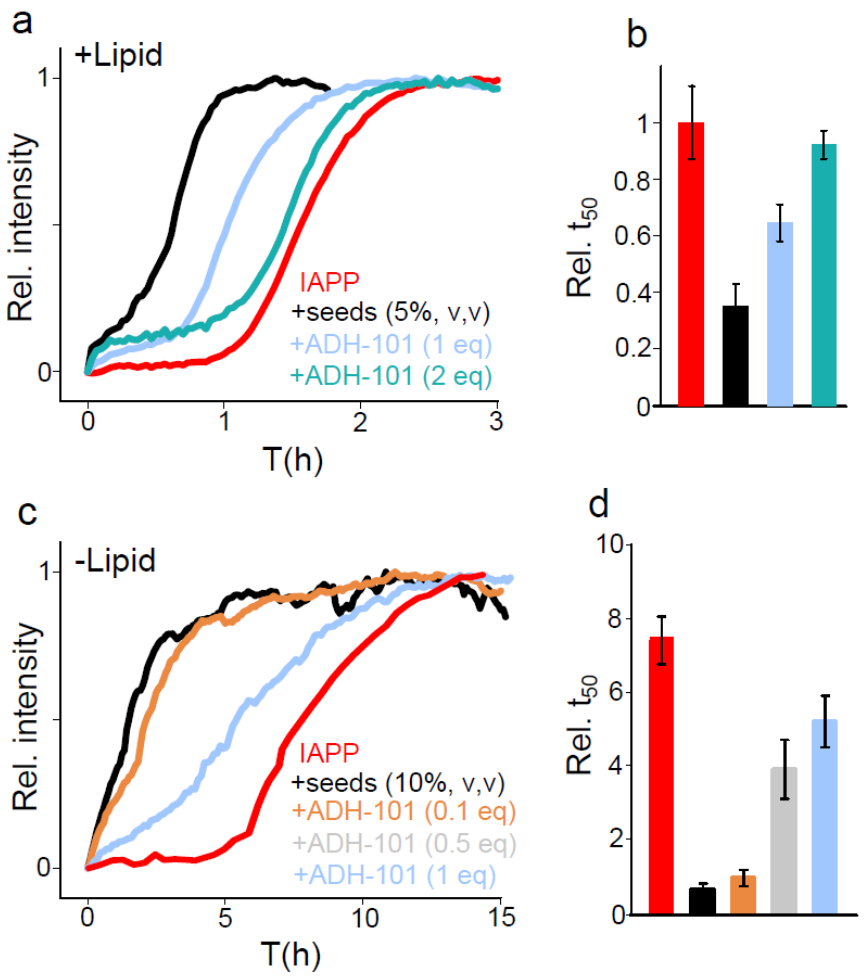

Figure S8. Dose dependent effect of ADH-101 on IAPP fibrillation. (a) The representative kinetic curves of seed catalyzed (5% v,v) fibrillation of 15 μM IAPP in the absence and presence of various doses of ADH-101 under lipid catalyzed conditions (750 μM, LUVs, DOPG:DOPC, 3:7, d=100 nm) at the indicated stoichiometric ratios. (b) The statistics of the repeats of seeded kinetics of IAPP fibrillation. The representative kinetic curves (c) and the statistics of the repeats (d) of seeded kinetics of IAPP (10 μM) fibrillation (seeds, 10% v,v) in the absence and presence of ADH-101 at the indicated stoichiometric ratios. All error bars represent SDs from a minimum of three independent experiment. Buffer conditions: 50 mM NaPi, 150 mM KCl, pH 7.4.

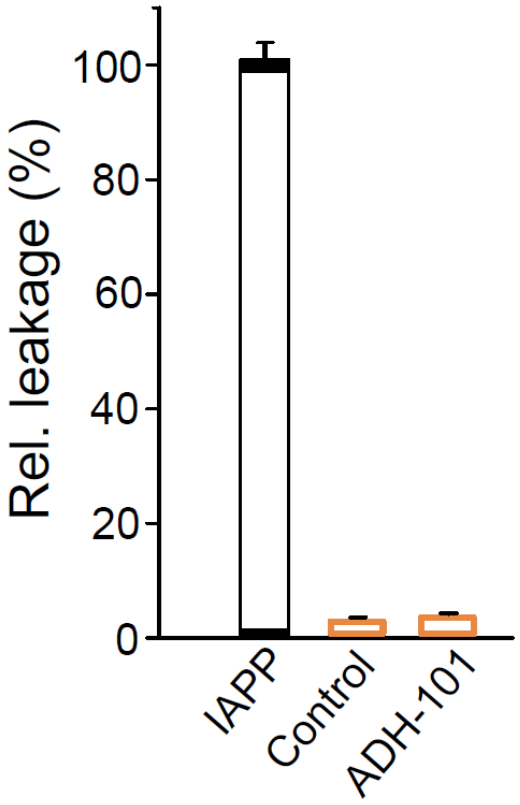

Figure S9. Effect of ADH-101 on the liposome leakage. A sample of 4 μM of ADH-101 in buffer was added to 200 μM LUVs used in our leakage assay (see Materials and Methods). For reference, leakage induced by 4 μM IAPP and by the control (buffer only) is also shown. All kinetic experiments were conducted at least in triplicate with errors reported as standard deviations (SD).

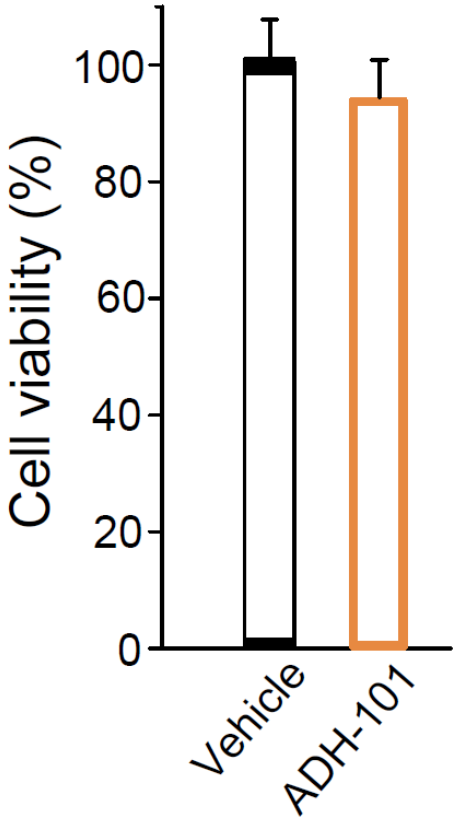

Figure S10. Effect of ADH-101 on the cell viability. Comparison of the effect of IAPP-free solution and ADH-101 on the cell viability of RIN-m cells. The experimental conditions were similar to the cell-viability assay presented in Figure 6 (in the main text) except that no IAPP was added to the cells. Error bars reflect variability across 4–8 technical replicates within a single execution of the assay.

General method for the *N*-substitution of pyrroles.

To a solution of ethyl 4-nitro-1*H*-pyrrole-2-carboxylate (184 mg, 1 mmol) in acetone (25 mL), K_2CO_3 (415 mg, 3 mmol) and alkyl (or benzyl) iodide (3 mmol) were added and the reaction started at 65° C with constant stirring for 12 h. The reaction mixture was then cooled at to r.t. and concentrated on rotovap. The reaction mixture was then partitioned between water (100 mL) and ethylacetate (100 mL), and extracted with ethylacetate (3×100 mL). The organic layer was dried over Na_2SO_4 and concentrated on rotovap. Column chromatography (0 to 25% ethylacetate in hexane, v/v) afforded the desired product as an off white solid (Table 1 for % yield).

General method for the reduction of pyrroles.

To a solution of nitropyrrole (0.3 mmol) in EtOAc (10 mL), Pd/C (10% by wt.) was added and the reaction started with constant stirring in the atmosphere of H_2 (g) at room temperature. The progress of the reaction was monitored using TLC. The disappearance of the starting material confirms the completion of the reaction. The reaction mixture was filtered and the filtrate was dried over rotovap to afford the desired product as a brown oil, which is used in next step without further characterization.

General method for the saponification of ester pyrroles

To a solution of pyrrole (1 mmol) in methanol (5 mL), 1M NaOH (5 mL) was added and the reaction was stirred for 6 h at 60 °C. The reaction solution was allowed to equilibrate at r.t. The solution was then poured into water (20 mL). The pH of the reaction solution was adjusted to 4. The aqueous layer was extracted with EtOAc (2×30 mL). The organic layers were combined, dried over Na_2SO_4, and concentrated on rotovap to afford the desired product as a yellow solid (The % yields for saponification reaction were varied from 85-95%).

General method for the amide coupling.

To a solution of 6-(O-alkyl/amine/benzyl/carboxylic acid)-5-nitropicolinic acid (0.5 mmol) in dimethylformamide (10 mL, anhydrous), PyBOP (1 mmol) and diisopropylethylamine (0.48 mmol) were added and the reaction stirred for 20 min. at r.t. 5-amino-6-(O-alkyl/amine/benzyl/carboxylic acid) picolinic acid (0.4 mmol) in dimethylformamide (10 mL,

anhydrous) was added and the reaction mixture was stirred at r.t. for 4 h in the atm. of argon. The reaction solution was poured in water (30 mL) and extracted with ethylacetate (30 mL × 3). The volatiles were removed on rotovap. Column chromatography (0 to 40% ethylacetate in hexane, v/v) afforded the desired product as a yellow solid (see Table S1 for % yield).

General method for the deprotection of N-substituted oligopyrroles.

To a solution of N-substituted oligopyrrole (mmol) in dichloromethane (mL), triethylsilane (mL) was added followed by the addition of trifluoroacetic acid (mL) and the reaction started with constant stirring. The progress of the reaction was monitored using TLC and the disappearance of the starting material confirms the deprotection of the acid sensitive tert-butyl group. The reaction solution was dried on rotovap and washed with cold diethyl ether (3×5 mL) which afforded the desired product as a yellow solid (see Table S1 for % yield).

***The synthesis and characterization of ADH-201 will be presented elsewhere.**

***N-Tert*-Butyl ADH-117**

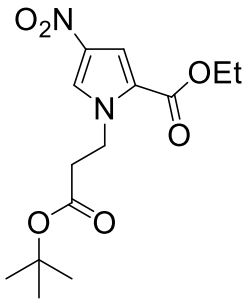

To a solution of ethyl 2-(4-nitro-1H-pyrrol-2-yl)-2-oxoacetate (1 gm, 5.43 mmol) in acetone (35 mL), K_2CO_3 (2.6 g, 18.5 mmol), tert-butyl 3-bromopropanoate (3.62 mL, 20 mmol), and tetra-n-butylammonium iodide (166.2 mg, 0.5 mmol) were added and the reaction started at 65° C with constant stirring for 12 h. The reaction mixture was then cooled at to r.t. and concentrated on rotovap. The reaction mixture was then partitioned between water (100 mL) and ethylacetate (100 mL), and extracted with ethylacetate (3×100 mL). The organic layer was dried over Na_2SO_4 and concentrated on rotovap. Column chromatography (0 to 30% ethylacetate in hexane, v/v) afforded the desired product as a yellow solid (Table 1 for % yield). ^{1}H NMR (600 MHz, Chloroform-*d*) δ 7.78 – 7.73 (d, *J* = 2.0 Hz, 1H), 7.46 – 7.43 (d, *J* = 2.0 Hz, 1H), 4.64 – 4.56 (t, *J* = 6.3 Hz, 2H), 4.36 – 4.28 (q, *J* = 7.1 Hz, 2H), 2.80 – 2.74 (t, *J* = 6.3 Hz, 2H), 1.45 – 1.41 (s, 9H), 1.40 – 1.36 (t, *J* = 7.1 Hz, 3H). ^{13}C NMR (151 MHz, $CDCl_3$) δ 169.8, 160.0, 135.3, 127.9, 122.2, 113.2, 81.8, 77.2, 77.0, 76.8, 61.0, 46.1, 36.6, 28.0, 14.2. MS-ESI (*m/z*): calculated for $C_{14}H_{21}N_2O_6$ (M+H): 312.1321, found 312.1321.

ADH-113

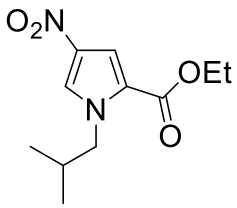

^{1}H NMR (600 MHz, Chloroform-*d*) δ 7.60 – 7.58 (d, *J* = 2.0 Hz, 1H), 7.47 – 7.43 (d, *J* = 2.0 Hz, 1H), 4.35 – 4.27 (q, *J* = 7.1 Hz, 2H), 4.18 – 4.14 (d, *J* = 7.4 Hz, 2H), 2.16 – 2.05 (dt, *J* = 13.5, 6.8

Hz, 1H), 1.40 – 1.34 (t, *J* = 7.1 Hz, 3H), 0.94 – 0.90 (d, *J* = 6.7 Hz, 6H). ^{13}C NMR (151 MHz, $CDCl_3$) δ 160.1, 135.2, 127.2, 122.6, 113.1, 77.2, 77.0, 76.8, 60.9, 57.5, 29.9, 19.7, 14.2, 14.1. MS-ESI (*m/z*): calculated for $C_{11}H_{16}N_2O_4$ (M+H): 241.1188, found 241.1181. Anal. Calcd for $C_{11}H_{16}N_2O_4$: C, 54.99; H, 6.71; N, 11.66; O, 26.64. Found: C, 55.11; H, 6.79; N, 11.51.

ADH-113_COOH

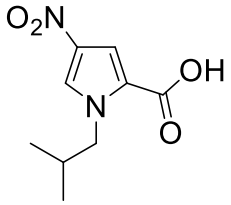

^{1}H NMR (600 MHz, DMSO-d_6) δ 13.27 – 13.07 (s, 1H), 8.28 – 8.23 (d, *J* = 2.0 Hz, 1H), 7.32 – 7.28 (d, *J* = 2.1 Hz, 1H), 4.24 – 4.17 (d, *J* = 7.4 Hz, 2H), 2.09 – 1.99 (hept, *J* = 6.9 Hz, 1H), 0.86 – 0.80 (d, *J* = 6.7 Hz, 6H). ^{13}C NMR (151 MHz, $CDCl_3$) δ 161.4, 134.6, 129.4, 123.8, 112.5, 56.4, 29.8, 19.7. MS-ESI (*m/z*): calculated for $C_9H_{12}N_2O_4$ (M-H): 211.0719, found 211.0717. Anal. Calcd for $C_9H_{12}N_2O_4$: C, 50.94; H, 5.70; N, 13.20; O, 30.16. Found: C, 51.20; H, 5.81; N, 13.11.

ADH-117

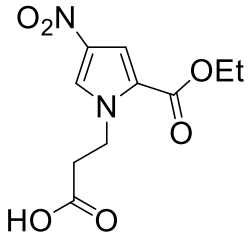

^{1}H NMR (600 MHz, DMSO-d_6) δ 12.59 – 12.39 (s, 1H), 8.31 – 8.17 (d, *J* = 2.1 Hz, 1H), 7.40 – 7.24 (d, *J* = 2.1 Hz, 1H), 4.62 – 4.50 (t, *J* = 7.0 Hz, 2H), 4.34 – 4.21 (q, *J* = 7.1 Hz, 2H), 2.86 – 2.70 (t, *J* = 7.1 Hz, 2H), 1.36 – 1.24 (t, *J* = 7.1 Hz, 3H). ^{13}C NMR (151 MHz, DMSO) δ 172.3, 159.7, 134.8, 129.6, 122.7, 112.5, 65.4, 61.2, 15.6, 14.5. MS-ESI (*m/z*): calculated for $C_{10}H_{13}N_2O_6$ (M+H): 257.0774 found 257.0769. Anal. Calcd for $C_{10}H_{13}N_2O_6$: C, 46.88; H, 4.72; N, 10.93; O, 37.47. Found: C, 46.99; H, 4.81; N, 10.81.

ADH-102

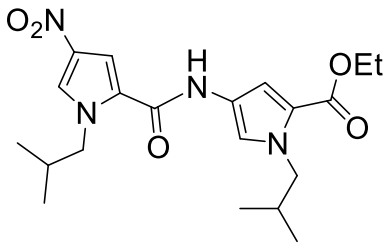

^{1}H NMR (600 MHz, Chloroform-*d*) δ 7.61 – 7.58 (d, *J* = 1.9 Hz, 1H), 7.39 – 7.34 (d, *J* = 2.1 Hz, 1H), 7.19 – 7.15 (d, *J* = 1.9 Hz, 1H), 6.88 – 6.84 (d, *J* = 2.0 Hz, 1H), 4.30 – 4.25 (q, *J* = 7.2 Hz, 2H), 4.24 – 4.20 (d, *J* = 7.4 Hz, 2H), 4.12 – 4.08 (d, *J* = 7.4 Hz, 2H), 2.20 – 2.06 (m, 2H), 1.37 – 1.32 (t, *J* = 7.1 Hz, 3H), 0.95 – 0.89 (dd, *J* = 12.5, 6.7 Hz, 12H). ^{13}C NMR (151 MHz, $CDCl_3$) δ 160.9, 157.4, 135.0, 126.5, 126.0, 120.7, 120.5, 120.0, 108.8, 107.2, 60.0, 57.3, 56.5, 30.2, 30.0, 19.9, 19.7, 14.4. MS-ESI (*m/z*): calculated for $C_{20}H_{28}N_4O_5$ (M+H): 405.2138 found 405.2133. Anal. Calcd for $C_{20}H_{28}N_4O_5$: C, 59.39; H, 6.98; N, 13.85; O, 19.78. Found: C, 59.55; H, 7.04; N, 13.69.

ADH-102_COOH

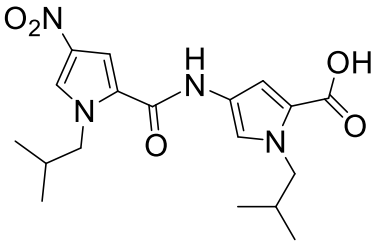

^{1}H NMR (600 MHz, DMSO-d_6) δ 12.41 – 12.01 (s, 1H), 10.53 – 10.09 (s, 1H), 8.24 – 8.18 (d, *J* = 2.0 Hz, 1H), 7.61 – 7.55 (d, *J* = 2.0 Hz, 1H), 7.44 – 7.39 (d, *J* = 2.0 Hz, 1H), 6.89 – 6.84 (d, *J* = 2.0 Hz, 1H), 4.29 – 4.24 (d, *J* = 7.4 Hz, 2H), 4.14 – 4.08 (d, *J* = 7.3 Hz, 2H), 2.10 – 2.03 (dq, *J* = 13.8, 7.0, 6.5 Hz, 1H), 2.02 – 1.94 (m, 1H), 0.85 – 0.78 (dd, *J* = 6.7, 4.5 Hz, 12H). ^{13}C NMR (151 MHz, DMSO) δ 162.2, 157.4, 134.3, 128.4, 126.3, 122.2, 120.5, 119.8, 109.4, 108.6, 56.3, 55.3, 30.4, 29.8, 20.0, 19.8. MS-ESI (*m/z*): calculated for $C_{18}H_{24}N_4O_5$ (M+H): 377.1825 found

377.1820. Anal. Calcd for $C_{18}H_{24}N_4O_5$: C, 57.44; H, 6.43; N, 14.88; O, 21.25. Found: C, 57.66; H, 6.51; N, 14.75.

***N-Tert*-Butyl ADH-104**

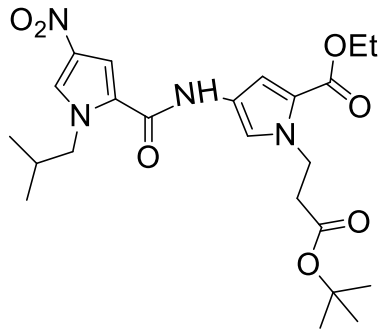

^{1}H NMR (600 MHz, Chloroform-*d*) δ 7.64 – 7.60 (s, 1H), 7.60 – 7.58 (d, *J* = 1.9 Hz, 1H), 7.45 – 7.41 (d, *J* = 2.1 Hz, 1H), 7.20 – 7.16 (d, *J* = 1.9 Hz, 1H), 6.88 – 6.86 (d, *J* = 2.0 Hz, 1H), 4.57 – 4.50 (t, *J* = 6.9 Hz, 2H), 4.31 – 4.25 (q, *J* = 7.1 Hz, 2H), 4.24 – 4.20 (d, *J* = 7.3 Hz, 2H), 2.80 – 2.68 (t, *J* = 6.9 Hz, 2H), 2.19 – 2.00 (dt, *J* = 13.5, 6.8 Hz, 1H), 1.45 – 1.43 (s, 10H), 1.38 – 1.33 (t, *J* = 7.1 Hz, 3H), 0.94 – 0.89 (d, *J* = 6.6 Hz, 7H). ^{13}C NMR (151 MHz, $CDCl_3$) δ 170.4, 160.7, 157.4, 135.0, 126.5, 125.9, 121.0, 120.5, 119.7, 109.2, 107.2, 81.1, 60.2, 57.3, 45.2, 37.4, 30.0, 28.1, 19.7, 14.4. MS-ESI (*m/z*): calculated for $C_{23}H_{32}N_4O_7$ (M+Na): 499.2169 found 499.2160.

ADH-104

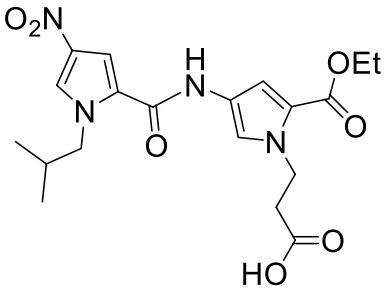

^{1}H NMR (600 MHz, DMSO-d_6) δ 12.50 – 12.22 (s, 1H), 10.34 – 10.21 (s, 1H), 8.24 – 8.16 (d, *J* = 1.9 Hz, 1H), 7.60 – 7.54 (d, *J* = 2.0 Hz, 1H), 7.50 – 7.40 (d, *J* = 2.0 Hz, 1H), 6.99 – 6.92 (d, *J* = 2.0 Hz, 1H), 4.49 – 4.43 (t, *J* = 6.9 Hz, 2H), 4.28 – 4.24 (d, *J* = 7.4 Hz, 2H), 4.25 – 4.18 (q, *J* = 7.1 Hz, 2H), 2.73 – 2.65 (t, *J* = 7.0 Hz, 2H), 2.09 – 2.00 (hept, *J* = 6.9 Hz, 1H), 1.31 – 1.26 (t, *J* = 7.1 Hz, 3H), 0.86 – 0.79 (d, *J* = 6.7 Hz, 6H). ^{13}C NMR (151 MHz, DMSO) δ 172.7, 160.5, 157.4, 134.4, 128.5, 126.2, 122.7, 120.6, 118.8, 109.5, 108.6, 60.1, 56.3, 44.8, 36.3, 29.8, 19.8, 14.7. MS-ESI (*m/z*): calculated for $C_{19}H_{24}N_4O_7$ (M+H): 421.1723 found 421.1719. Anal. Calcd for $C_{19}H_{24}N_4O_7$: C, 54.28; H, 5.75; N, 13.33; O, 26.64. Found C, 54.44; H, 5.87; N, 13.19.

ADH-105

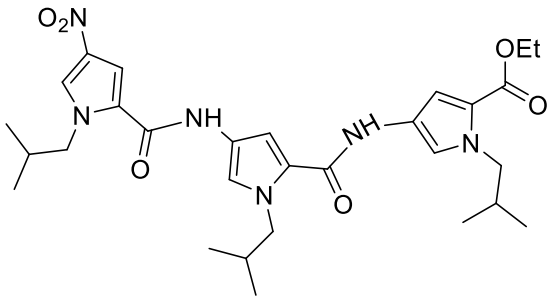

^{1}H NMR (600 MHz, Chloroform-*d*) δ 7.64 – 7.62 (d, *J* = 1.9 Hz, 1H), 7.59 – 7.55 (s, 1H), 7.50 – 7.46 (s, 1H), 7.43 – 7.39 (d, *J* = 2.1 Hz, 1H), 7.22 – 7.19 (d, *J* = 1.9 Hz, 1H), 7.19 – 7.15 (d, *J* = 1.9 Hz, 1H), 6.85 – 6.83 (d, *J* = 2.0 Hz, 1H), 6.74 – 6.71 (d, *J* = 1.9 Hz, 1H), 4.32 – 4.27 (q, *J* = 7.1 Hz, 2H), 4.27 – 4.24 (d, *J* = 7.5 Hz, 2H), 4.22 – 4.18 (d, *J* = 7.5 Hz, 2H), 4.14 – 4.10 (d, *J* = 7.3 Hz, 2H), 2.24 – 2.08 (dddt, *J* = 29.7, 20.6, 13.8, 6.9 Hz, 3H), 1.39 – 1.36 (t, *J* = 7.1 Hz, 3H), 0.97 – 0.95 (d, *J* = 6.7 Hz, 6H), 0.94 – 0.91 (d, *J* = 6.6 Hz, 12H). MS-ESI (*m/z*): calculated for $C_{29}H_{40}N_6O_6$ $(M+H_2O)^+$: 585.3037 found 585.3030. Anal. Calcd for $C_{29}H_{40}N_6O_6$: C, 61.25; H, 7.09; N, 14.78; O, 16.88. Found C, 61.42; H, 7.11; N, 14.74.

***N-Tert*-Butyl ADH-101**

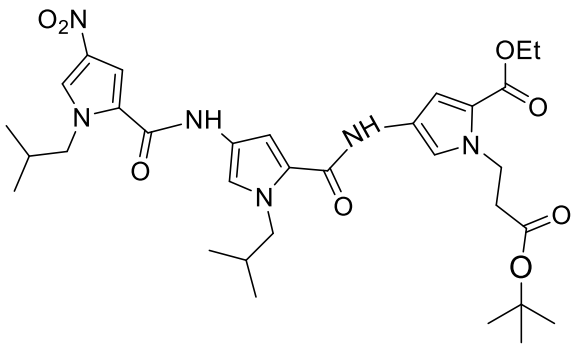

^{1}H NMR (600 MHz, Chloroform-*d*) δ 7.82 – 7.71 (s, 1H), 7.65 – 7.60 (d, *J* = 1.9 Hz, 1H), 7.54 – 7.49 (s, 1H), 7.49 – 7.44 (d, *J* = 2.2 Hz, 1H), 7.27 – 7.23 (d, *J* = 1.9 Hz, 1H), 7.21 – 7.17 (d, *J* = 1.9 Hz, 1H), 6.88 – 6.85 (d, *J* = 2.1 Hz, 1H), 6.78 – 6.73 (s, 1H), 4.58 – 4.51 (t, *J* = 7.0 Hz, 2H), 4.33 – 4.28 (q, *J* = 7.1 Hz, 2H), 4.27 – 4.24 (d, *J* = 7.4 Hz, 2H), 4.20 – 4.15 (d, *J* = 7.4 Hz, 2H), 2.80 – 2.73 (t, *J* = 7.0 Hz, 2H), 2.26 – 2.07 (ddq, *J* = 27.5, 13.8, 6.9 Hz, 2H), 1.48 – 1.41 (s, 9H), 1.40 – 1.34 (t, *J* = 7.1 Hz, 3H), 0.99 – 0.93 (d, *J* = 6.7 Hz, 6H), 0.93 – 0.90 (d, *J* = 6.7 Hz, 6H). MS-ESI (*m/z*): calculated for $C_{32}H_{44}N_6O_8$ (M+H): 641.3299 found 641.3297.

ADH-101

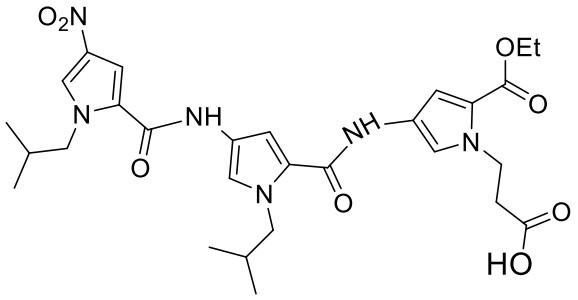

^{1}H NMR (600 MHz, Chloroform-*d*) δ 7.82 – 7.71 (s, 1H), 7.65 – 7.60 (d, *J* = 1.9 Hz, 1H), 7.54 – 7.49 (s, 1H), 7.49 – 7.44 (d, *J* = 2.2 Hz, 1H), 7.27 – 7.23 (d, *J* = 1.9 Hz, 1H), 7.21 – 7.17 (d, *J* = 1.9 Hz, 1H), 6.88 – 6.85 (d, *J* = 2.1 Hz, 1H), 6.78 – 6.73 (s, 1H), 4.58 – 4.51 (t, *J* = 7.0 Hz, 2H), 4.33 – 4.28 (q, *J* = 7.1 Hz, 2H), 4.27 – 4.24 (d, *J* = 7.4 Hz, 2H), 4.20 – 4.15 (d, *J* = 7.4 Hz, 2H), 2.80 – 2.73 (t, *J* = 7.0 Hz, 2H), 2.26 – 2.07 (ddq, *J* = 27.5, 13.8, 6.9 Hz, 2H), 1.48 – 1.41 (s, 9H),

1.40 – 1.34 (t, *J* = 7.1 Hz, 3H), 0.99 – 0.93 (d, *J* = 6.7 Hz, 6H), 0.93 – 0.90 (d, *J* = 6.7 Hz, 6H). MS-ESI (*m/z*): calculated for $C_{28}H_{37}N_6O_8$ (M+H): 585.2673 found 585.2676. Anal. Calcd for $C_{28}H_{37}N_6O_8$: C, 57.52; H, 6.21; N, 14.38; O, 21.89. Found C, 57.63; H, 6.32; N, 14.34.

***N-Tert*-Butyl ADH-103**

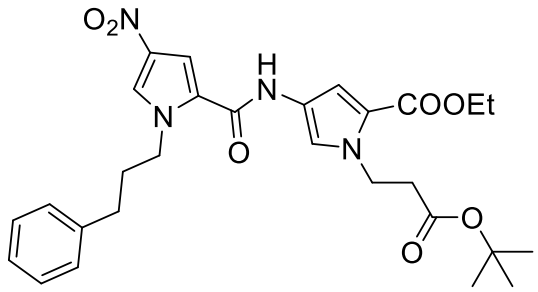

^{1}H NMR (600 MHz, Chloroform-*d*) δ 7.75 – 7.71 (s, 1H), 7.61 – 7.58 (d, *J* = 1.8 Hz, 1H), 7.48 – 7.43 (d, *J* = 2.1 Hz, 1H), 7.34 – 7.27 (dd, *J* = 14.3, 6.8 Hz, 3H), 7.25 – 7.16 (m, 4H), 6.94 – 6.89 (d, *J* = 2.0 Hz, 1H), 4.59 – 4.53 (t, *J* = 6.9 Hz, 2H), 4.51 – 4.41 (t, *J* = 7.3 Hz, 2H), 4.37 – 4.25 (q, *J* = 7.1 Hz, 2H), 2.81 – 2.73 (t, *J* = 6.9 Hz, 2H), 2.73 – 2.65 (t, *J* = 7.6 Hz, 2H), 2.27 – 2.15 (p, *J* = 7.5 Hz, 2H), 1.48 – 1.43 (s, 9H), 1.42 – 1.35 (t, *J* = 7.1 Hz, 3H). ^{13}C NMR (151 MHz, $CDCl_3$) δ 170.4, 160.7, 157.3, 140.3, 135.1, 128.6, 128.3, 126.3, 126.1, 125.7, 121.1, 120.5, 119.7, 109.3, 107.3, 81.2, 60.2, 49.9, 45.2, 37.4, 32.6, 32.5, 29.7, 28.1, 14.4. MS-ESI (*m/z*): calculated for $C_{28}H_{34}N_4O_7$ (M+H): 539.2506 found 539.2501.

ADH-103

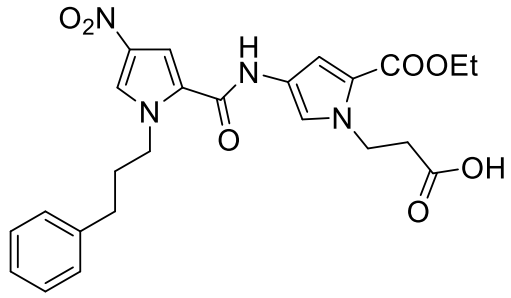

^{1}H NMR (600 MHz, DMSO-d_6) δ 12.70 – 12.13 (s, 1H), 10.40 – 10.20 (s, 1H), 8.26 – 8.23 (d, *J* = 2.0 Hz, 1H), 7.61 – 7.54 (d, *J* = 2.0 Hz, 1H), 7.50 – 7.43 (d, *J* = 2.0 Hz, 1H), 7.31 – 7.24 (m, 2H), 7.22 – 7.14 (m, 3H), 6.98 – 6.94 (d, *J* = 2.0 Hz, 1H), 4.52 – 4.43 (q, *J* = 6.7 Hz, 2H), 4.27 – 4.17 (q, *J* = 7.1 Hz, 2H), 2.70 – 2.65 (t, *J* = 7.1 Hz, 2H), 2.60 – 2.56 (dd, *J* = 9.3, 6.7 Hz, 2H), 2.10 – 2.02 (ddt, *J* = 13.0, 10.3, 3.9 Hz, 2H). ^{13}C NMR (151 MHz, DMSO) δ 172.7, 160.5, 157.3, 141.4, 134.6, 128.8, 128.6, 128.1, 126.3, 126.0, 122.7, 120.6, 118.8, 109.5, 108.6, 60.1, 55.4, 49.6, 44.8, 36.2, 32.7, 32.5, 14.7. MS-ESI (*m/z*): calculated for $C_{24}H_{26}N_4O_7$ (M+H): 483.1880 found 483.1885. Anal. Calcd for $C_{24}H_{26}N_4O_7$: C, 59.74; H, 5.43; N, 11.61; O, 23.21. Found C, 59.77; H, 5.49; N, 11.57.

***N-Tert*-Butyl-ADH-106**

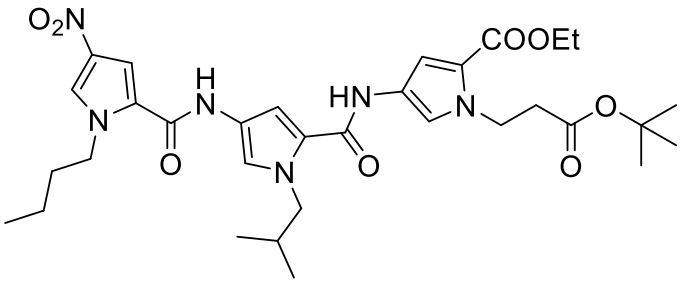

^{1}H NMR (600 MHz, Chloroform-*d*) δ 7.77 – 7.71 (s, 1H), 7.69 – 7.64 (d, *J* = 1.7 Hz, 1H), 7.53 – 7.50 (s, 1H), 7.48 – 7.44 (d, *J* = 2.1 Hz, 1H), 7.24 – 7.22 (d, *J* = 1.8 Hz, 1H), 7.22 – 7.20 (d, *J* = 1.8 Hz, 1H), 6.88 – 6.85 (d, *J* = 2.0 Hz, 1H), 6.77 – 6.69 (s, 1H), 4.58 – 4.51 (t, *J* = 7.0 Hz, 2H), 4.47 – 4.42 (t, *J* = 7.3 Hz, 2H), 4.33 – 4.27 (q, *J* = 7.1 Hz, 2H), 4.20 – 4.16 (d, *J* = 7.4 Hz, 2H), 2.80 – 2.72 (t, *J* = 7.0 Hz, 2H), 2.19 – 2.10 (dt, *J* = 13.7, 6.9 Hz, 1H), 1.90 – 1.82 (m, 2H), 1.56 – 1.50 (dq, *J* = 13.1, 6.5 Hz, 1H), 1.47 – 1.46 (s, 9H), 1.39 – 1.35 (t, *J* = 7.1 Hz, 5H), 1.00 – 0.96 (t, *J* = 7.4 Hz, 3H), 0.90 – 0.87 (d, *J* = 4.1 Hz, 6H). MS-ESI (*m/z*): calculated for $C_{32}H_{45}N_6O_8$ (M+H): 641.3299 found 641.3306.

ADH-106

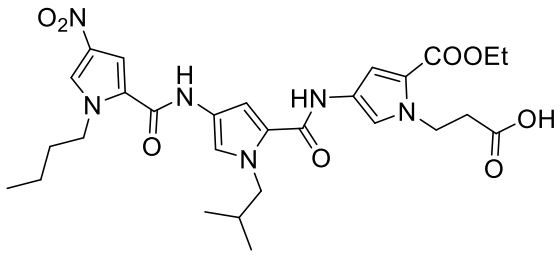

^{1}H NMR (600 MHz, DMSO-d_6) δ 12.38 – 11.88 (s, 1H), 9.10 – 9.03 (s, 1H), 8.01 – 7.94 (d, *J* = 8.4 Hz, 1H), 7.78 – 7.66 (d, *J* = 8.3 Hz, 1H), 7.59 – 7.49 (t, *J* = 7.6 Hz, 1H), 7.45 – 7.38 (m, 1H), 7.12 – 7.06 (m, 1H), 6.98 – 6.77 (m, 1H), 6.63 – 6.54 (d, *J* = 2.0 Hz, 1H), 4.28 – 4.24 (t, *J* = 7.1 Hz, 2H), 4.23 – 4.19 (t, *J* = 7.1 Hz, 4H), 4.10 – 4.06 (d, *J* = 7.3 Hz, 2H), 2.72 – 2.64 (t, *J* = 7.1 Hz, 2H), 2.02 – 1.91 (dq, *J* = 13.7, 6.8 Hz, 1H), 0.89 – 0.85 (m, 9H), 0.84 – 0.79 (d, *J* = 6.8 Hz, 6H). MS-ESI (*m/z*): calculated for $C_{28}H_{37}N_6O_8$ (M+H): 585.2673 found 585.2676. Anal. Calcd for $C_{28}H_{36}N_6O_8$: C, 57.52; H, 6.21; N, 14.38; O, 21.89. Found C, 57.60; H, 6.28; N, 14.34.

***N*-*Tert*-Butyl-ADH-107**

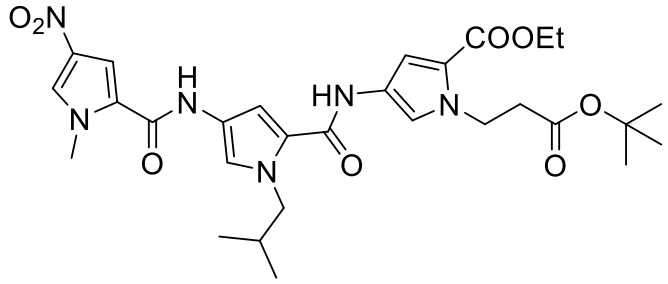

^{1}H NMR (600 MHz, Chloroform-*d*) δ 8.89 – 8.83 (s, 1H), 8.74 – 8.69 (d, *J* = 2.8 Hz, 1H), 8.62 – 8.58 (s, 1H), 8.57 – 8.53 (d, *J* = 3.2 Hz, 1H), 8.35 – 8.32 (d, *J* = 2.7 Hz, 1H), 8.32 – 8.29 (d, *J* = 3.0 Hz, 1H), 7.97 – 7.91 (q, *J* = 2.3 Hz, 1H), 7.84 – 7.77 (s, 1H), 5.67 – 5.61 (q, *J* = 5.5, 3.9 Hz, 2H), 5.41 – 5.35 (qd, *J* = 7.1, 2.1 Hz, 2H), 5.29 – 5.24 (d, *J* = 7.5 Hz, 2H), 5.17 – 5.14 (m, 3H), 3.87 – 3.82 (m, 2H), 3.32 – 3.15 (m, *J* = 11.1, 9.8 Hz, 1H), 2.56 – 2.53 (m, 9H), 2.01 – 1.97 (m, 6H). MS-ESI (*m/z*): calculated for $C_{28}H_{37}N_6O_8$ (M+H): 599.2829 found 599.2826.

ADH-107

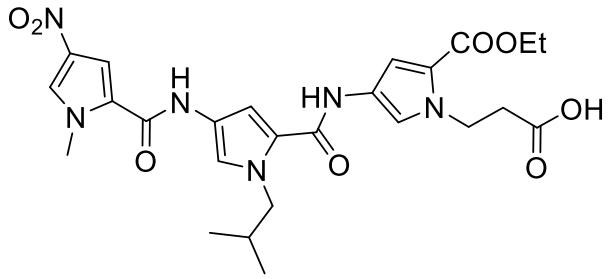

^{1}H NMR (600 MHz, DMSO-d_6) δ 12.46 – 12.24 (s, 1H), 10.36 – 10.26 (s, 1H), 10.04 – 9.93 (s, 1H), 8.22 – 8.18 (d, *J* = 1.9 Hz, 1H), 7.62 – 7.59 (d, *J* = 2.0 Hz, 1H), 7.51 – 7.47 (d, *J* = 2.0 Hz, 1H), 7.30 – 7.27 (d, *J* = 1.8 Hz, 1H), 7.07 – 7.04 (d, *J* = 1.9 Hz, 1H), 6.99 – 6.95 (d, *J* = 2.0 Hz, 1H), 4.49 – 4.43 (t, *J* = 7.0 Hz, 2H), 4.25 – 4.19 (q, *J* = 7.1 Hz, 2H), 4.17 – 4.13 (d, *J* = 7.3 Hz, 2H), 4.00 – 3.95 (s, 3H), 2.74 – 2.66 (t, *J* = 7.0 Hz, 2H), 2.04 – 1.95 (dp, *J* = 13.8, 6.9 Hz, 1H), 1.32 – 1.26 (t, *J* = 7.1 Hz, 3H), 0.85 – 0.76 (d, *J* = 6.6 Hz, 6H). MS-ESI (*m/z*): calculated for $C_{25}H_{31}N_6O_8$ (M+H): 543.2203 found 543.2206. Anal. Calcd for $C_{25}H_{30}N_6O_8$: C, 55.35; H, 5.57; N, 15.49; O, 23.59. Found C, 55.36; H, 5.63; N, 15.43.

ADH-108

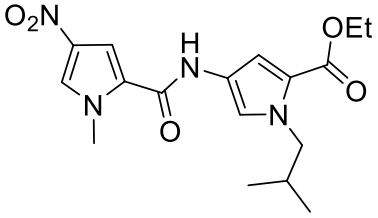

^{1}H NMR (600 MHz, Chloroform-*d*) δ 7.91 – 7.82 (s, 1H), 7.65 – 7.58 (s, 1H), 7.46 – 7.38 (s, 1H), 7.29 – 7.28 (s, 1H), 7.27 – 7.25 (s, 1H), 6.95 – 6.87 (s, 1H), 4.33 – 4.27 (q, *J* = 7.1 Hz, 2H), 4.15 – 4.09 (d, *J* = 7.3 Hz, 2H), 4.08 – 4.04 (s, 3H), 2.16-2.07 (m, 1H), 1.77 – 1.66 (m, 9H), 0.92 – 0.91 (d, *J* = 5.5 Hz, 6H), 0.90 – 0.88 (s, 3H). ^{13}C NMR (151 MHz, $CDCl_3$) δ 160.8, 157.4, 135.1, 127.0, 126.1, 120.6, 120.4, 120.0, 108.7, 106.9, 60.0, 56.5, 38.0, 30.2, 19.9, 14.4. MS-ESI (*m/z*): calculated for $C_{17}H_{23}N_4O_5$ (M+H): 363.1668 found 363.1675. Anal. Calcd for $C_{17}H_{22}N_4O_5$: C, 56.35; H, 6.12; N, 15.46; O, 22.07. Found C, 56.31; H, 6.15; N, 15.50.

ADH-108_COOH

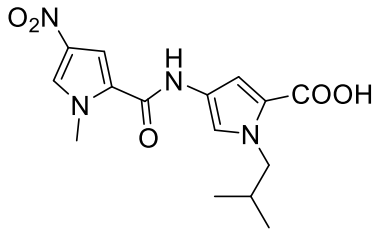

^{1}H NMR (600 MHz, DMSO-d_6) δ 12.25 – 12.12 (s, 1H), 10.29 – 10.20 (s, 1H), 8.24 – 8.12 (d, *J* = 1.9 Hz, 1H), 7.60 – 7.53 (d, *J* = 2.0 Hz, 1H), 7.48 – 7.38 (d, *J* = 2.0 Hz, 1H), 6.89 – 6.82 (d, *J* = 2.0 Hz, 1H), 4.12 – 4.08 (d, *J* = 7.3 Hz, 2H), 3.98 – 3.94 (s, 3H), 2.03 – 1.95 (hept, *J* = 6.9 Hz, 1H), 0.84 – 0.79 (d, *J* = 6.7 Hz, 6H). ^{13}C NMR (151 MHz, DMSO) δ 162.3, 157.4, 134.3, 128.8, 126.7, 122.2, 120.5, 119.8, 109.2, 108.1, 55.4, 37.9, 30.4, 20.0. MS-ESI (*m/z*): calculated for $C_{15}H_{19}N_4O_5$ (M+H): 335.1355 found 335.1363.

ADH-109

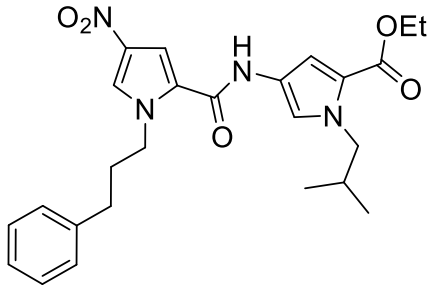

^{1}H NMR (600 MHz, Chloroform-*d*) δ 8.17 – 8.10 (d, *J* = 8.4 Hz, 1H), 8.01 – 7.95 (d, *J* = 1.8 Hz, 1H), 7.89 – 7.85 (d, *J* = 2.0 Hz, 1H), 7.63 – 7.58 (m, 1H), 7.53 – 7.44 (m, 4H), 5.34 – 5.26 (s, 2H), 4.25 – 4.07 (d, *J* = 7.4 Hz, 2H), 3.85 – 3.79 (t, *J* = 6.4 Hz, 2H), 2.72 – 2.47 (m, 2H), 2.21 – 2.05 (dp, *J* = 13.8, 6.9 Hz, 1H), 0.97 – 0.93 (d, *J* = 6.7 Hz, 6H). ^{13}C NMR (151 MHz, $CDCl_3$) δ 160.9,

157.2, 140.3, 135.2, 128.6, 128.3, 126.3, 126.1, 125.7, 120.7, 120.5, 120.0, 108.7, 107.2, 65.9, 60.0, 56.5, 49.8, 32.6, 32.5, 30.3, 29.7, 19.9, 14.4. MS-ESI (*m/z*): calculated for $C_{25}H_{31}N_4O_5$ (M+H): 467.2294 found 467.2290. Anal. Calcd for $C_{25}H_{30}N_4O_5$: C, 64.36; H, 6.48; N, 12.01; O, 17.15. Found C, 64.42; H, 6.50; N, 11.97.

ADH-109_COOH

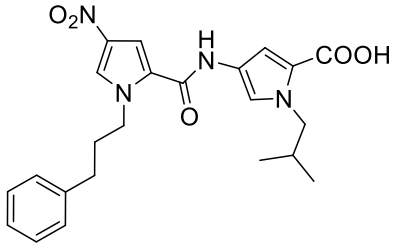

^{1}H NMR (600 MHz, DMSO-d_6) δ 12.31 – 12.00 (s, 1H), 10.33 – 10.25 (s, 1H), 8.27 – 8.19 (d, *J* = 2.0 Hz, 1H), 7.59 – 7.55 (d, *J* = 2.0 Hz, 1H), 7.44 – 7.41 (d, *J* = 2.0 Hz, 1H), 7.29 – 7.24 (m, 2H), 7.20 – 7.14 (m, 3H), 6.89 – 6.86 (d, *J* = 2.0 Hz, 1H), 4.50 – 4.44 (t, *J* = 7.2 Hz, 2H), 4.14 – 4.07 (d, *J* = 7.3 Hz, 2H), 2.60 – 2.55 (m, 2H), 2.11 – 2.04 (tt, *J* = 7.9, 6.2 Hz, 2H), 2.03 – 1.95 (hept, *J* = 6.9 Hz, 1H), 0.84 – 0.80 (d, *J* = 6.6 Hz, 6H). ^{13}C NMR (151 MHz, DMSO) δ 162.3, 157.3, 141.4, 134.5, 128.8, 128.6, 128.1, 126.4, 126.2, 122.2, 120.5, 119.8, 109.3, 108.5, 55.4, 49.6, 32.7, 32.5, 30.4, 20.0. MS-ESI (*m/z*): calculated for $C_{23}H_{27}N_4O_5$ (M+H): 439.1981 found 439.1991.

***N-Tert*-Butyl-ADH-110**

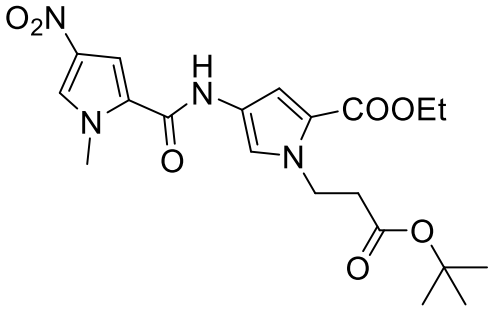

^{1}H NMR (600 MHz, Chloroform-*d*) δ 7.73 – 7.68 (s, 1H), 7.63 – 7.59 (d, *J* = 1.9 Hz, 1H), 7.48 – 7.41 (d, *J* = 2.0 Hz, 1H), 7.23 – 7.18 (d, *J* = 1.9 Hz, 1H), 6.94 – 6.89 (d, *J* = 2.1 Hz, 1H), 4.63 – 4.50 (t, *J* = 6.9 Hz, 2H), 4.36 – 4.26 (q, *J* = 7.1 Hz, 2H), 2.80 – 2.72 (t, *J* = 6.9 Hz, 2H), 1.47 – 1.44 (s, 9H), 1.40 – 1.35 (t, *J* = 7.1 Hz, 3H). ^{13}C NMR (151 MHz, $CDCl_3$) δ 160.2, 135.3, 127.5, 123.2, 112.7, 61.0, 38.0, 14.3. MS-ESI (*m/z*): calculated for $C_{20}H_{27}N_4O_7$ (M+H): 435.1880 found 435.1882.

ADH-110

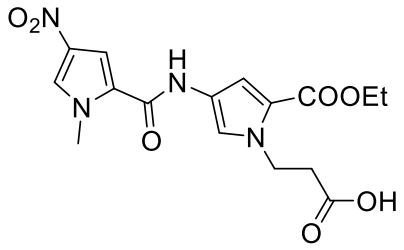

^{1}H NMR (600 MHz, DMSO-d_6) δ 12.43 – 12.34 (s, 1H), 10.33 – 10.24 (s, 1H), 8.23 – 8.18 (d, *J* = 1.9 Hz, 1H), 7.59 – 7.54 (d, *J* = 1.8 Hz, 1H), 7.50 – 7.45 (d, *J* = 1.9 Hz, 1H), 6.98 – 6.92 (d, *J* = 1.8 Hz, 1H), 4.52 – 4.40 (t, *J* = 6.8 Hz, 2H), 4.27 – 4.17 (q, *J* = 7.1 Hz, 2H), 3.97 – 3.94 (s, 3H), 2.73 – 2.65 (t, *J* = 6.9 Hz, 2H), 1.32 – 1.26 (t, *J* = 7.1 Hz, 3H). ^{13}C NMR (151 MHz,) δ 172.7, 160.5, 157.4, 134.3, 128.8, 126.5, 122.7, 120.5, 118.8, 109.5, 108.1, 60.1, 44.8, 38.0, 36.2, 14.7. MS-ESI (*m/z*): calculated for $C_{16}H_{19}N_4O_7$ (M+H): 379.1254 found 379.1258. Anal. Calcd for $C_{16}H_{18}N_4O_7$: C, 50.79; H, 4.80; N, 14.81; O, 29.60. Found C, 50.86; H, 4.85; N, 14.75.

***N*-*Tert*-Butyl-ADH-111**

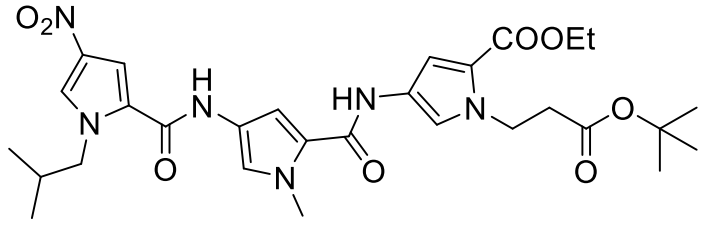

^{1}H NMR (600 MHz, Chloroform-*d*) δ 8.21 – 8.16 (s, 1H), 7.75 – 7.70 (s, 1H), 7.64 – 7.60 (d, *J* = 1.8 Hz, 1H), 7.47 – 7.43 (d, *J* = 2.2 Hz, 1H), 7.32 – 7.31 (d, *J* = 1.9 Hz, 1H), 7.24 – 7.22 (d, *J* = 1.8 Hz, 1H), 6.91 – 6.87 (d, *J* = 2.0 Hz, 1H), 6.80 – 6.73 (m, 1H), 4.55 – 4.50 (t, *J* = 7.0 Hz, 2H), 4.31 – 4.27 (q, *J* = 7.1 Hz, 2H), 4.26 – 4.23 (d, *J* = 7.3 Hz, 2H), 3.97 – 3.93 (s, 3H), 2.78 – 2.73 (t, *J* = 7.1 Hz, 2H), 2.21 – 2.13 (dt, *J* = 13.8, 6.9 Hz, 1H), 1.46 – 1.45 (s, 9H), 0.95 – 0.93 (d, *J* = 6.6 Hz, 6H). MS-ESI (*m/z*): calculated for $C_{28}H_{37}N_6O_8$ (M+H): 599.2829 found 599.2835.

ADH-111

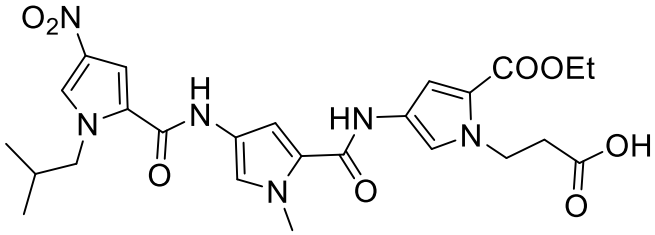

^{1}H NMR (600 MHz, DMSO-d_6) δ 12.49 – 12.24 (m, 1H), 10.35 – 10.28 (s, 1H), 10.01 – 9.95 (s, 1H), 8.27 – 8.18 (d, *J* = 2.0 Hz, 1H), 7.62 – 7.56 (d, *J* = 2.0 Hz, 1H), 7.53 – 7.48 (d, *J* = 2.0 Hz, 1H), 7.28 – 7.24 (d, *J* = 1.8 Hz, 1H), 7.09 – 7.03 (d, *J* = 1.9 Hz, 1H), 7.00 – 6.93 (d, *J* = 1.9 Hz, 1H), 4.49 – 4.43 (t, *J* = 6.9 Hz, 2H), 4.30 – 4.25 (d, *J* = 7.4 Hz, 2H), 4.25 – 4.19 (q, *J* = 7.1 Hz, 2H), 3.89 – 3.85 (s, 3H), 2.73 – 2.65 (t, *J* = 6.9 Hz, 2H), 2.12 – 2.00 (hept, *J* = 6.9 Hz, 1H), 1.32 – 1.24 (t, *J* = 7.1 Hz, 3H), 0.86 – 0.79 (d, *J* = 6.6 Hz, 6H). MS-ESI (*m/z*): calculated for $C_{25}H_{31}N_6O_8$ (M+H): 543.2203 found 543.2204. Anal. Calcd for $C_{25}H_{30}N_6O_8$: C, 55.35; H, 5.57; N, 15.49; O, 23.59. Found C, 55.42; H, 5.61; N, 15.45.

***N-Tert*-Butyl ADH-112**

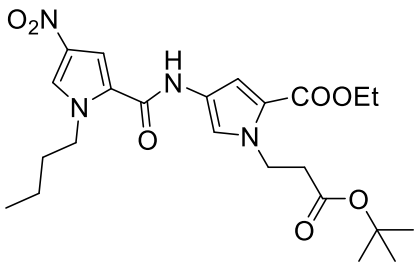

^{1}H NMR (600 MHz, Chloroform-*d*) δ 7.78 – 7.71 (s, 1H), 7.67 – 7.62 (d, *J* = 1.9 Hz, 1H), 7.50 – 7.44 (d, *J* = 2.1 Hz, 1H), 7.22 – 7.19 (d, *J* = 1.9 Hz, 1H), 6.93 – 6.90 (d, *J* = 2.1 Hz, 1H), 4.60 – 4.52 (t, *J* = 6.9 Hz, 2H), 4.46 – 4.40 (t, *J* = 7.3 Hz, 2H), 4.34 – 4.27 (q, *J* = 7.1 Hz, 2H), 2.82 – 2.72 (t, *J* = 6.9 Hz, 2H), 1.88 – 1.76 (p, *J* = 7.5 Hz, 2H), 1.47 – 1.44 (s, 9H), 1.41 – 1.34 (m, 5H), 1.00 – 0.92 (t, *J* = 7.3 Hz, 3H). ^{13}C NMR (151 MHz, $CDCl_3$) δ 170.5, 160.7, 157.4, 135.1, 126.1, 125.8, 121.2, 120.5, 119.7, 114.4, 109.3, 107.3, 81.2, 60.2, 50.1, 45.1, 37.4, 33.3, 28.1, 19.7, 14.4, 13.6. MS-ESI (*m/z*): calculated for $C_{23}H_{33}N_4O_7$ (M+H): 477.2349 found 477.2358.

ADH-112

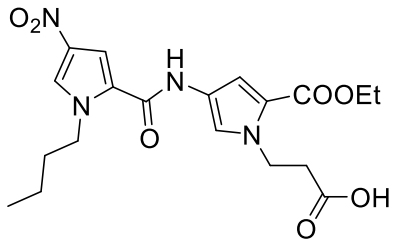

^{1}H NMR (600 MHz, DMSO-d_6) δ 12.55 – 12.12 (s, 1H), 10.35 – 10.24 (s, 1H), 8.27 – 8.23 (d, *J* = 2.0 Hz, 1H), 7.58 – 7.55 (d, *J* = 2.0 Hz, 1H), 7.50 – 7.45 (d, *J* = 2.1 Hz, 1H), 6.99 – 6.92 (d, *J* = 2.0 Hz, 1H), 4.51 – 4.44 (t, *J* = 6.9 Hz, 2H), 4.44 – 4.38 (t, *J* = 7.2 Hz, 2H), 4.26 – 4.18 (q, *J* = 7.1 Hz, 2H), 2.73 – 2.64 (t, *J* = 6.9 Hz, 2H), 1.75 – 1.66 (m, 2H), 1.31 – 1.27 (t, *J* = 7.1 Hz, 3H), 1.27 – 1.20 (p, *J* = 7.5 Hz, 2H), 0.92 – 0.84 (t, *J* = 7.4 Hz, 3H). ^{13}C NMR (151 MHz, DMSO) δ 172.7, 160.5, 157.3, 134.5, 128.1, 125.9, 122.7, 120.6, 118.8, 109.5, 108.6, 60.1, 49.5, 44.8, 36.2, 33.4, 19.6, 14.7, 14.0. MS-ESI (*m/z*): calculated for $C_{19}H_{25}N_4O_7$ (M+H): 421.1723 found 421.1724. Anal. Calcd for $C_{19}H_{24}N_4O_7$: C, 54.28; H, 5.75; N, 13.33; O, 26.64. Found C, 54.38; H, 5.78; N, 13.26.

ADH-114

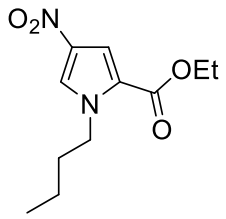

^{1}H NMR (600 MHz, Chloroform-*d*) δ 7.66 – 7.62 (q, *J* = 1.9 Hz, 1H), 7.47 – 7.42 (q, *J* = 1.8 Hz, 1H), 4.40 – 4.36 (m, 2H), 4.36 – 4.30 (m, 2H), 1.84 – 1.76 (m, 2H), 1.42 – 1.33 (m, 5H), 1.01 – 0.94 (td, *J* = 7.4, 2.1 Hz, 3H). ^{13}C NMR (151 MHz, $CDCl_3$) δ 13.5, 14.2, 19.7, 33.1, 50.2, 60.9, 113.0, 122.5, 126.7, 135.3, 159.9. MS-ESI (*m/z*): calculated for $C_{11}H_{17}N_2O_4$ (M+H): 241.1188 found 241.1190. Anal. Calcd for $C_{11}H_{16}N_2O_4$: C, 54.99; H, 6.71; N, 11.66; O, 26.64. Found C, 55.06; H, 6.73; N, 11.64.

ADH-114_COOH

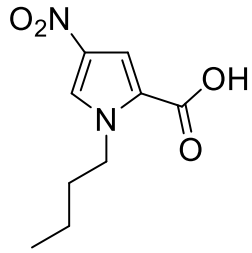

^{1}H NMR (600 MHz, Chloroform-*d*) δ 11.34 – 9.39 (s, 1H), 7.73 – 7.68 (d, *J* = 1.7 Hz, 1H), 7.65 – 7.56 (s, 1H), 4.49 – 4.29 (t, *J* = 6.9 Hz, 2H), 1.92 – 1.75 (p, *J* = 7.2 Hz, 2H), 1.45 – 1.34 (h, *J* = 7.3 Hz, 2H), 1.02 – 0.96 (t, *J* = 7.4 Hz, 3H). ^{13}C NMR (151 MHz, DMSO) δ 161.3, 134.7, 129.0, 123.5, 112.4, 49.5, 33.1, 19.5, 13.9. MS-ESI (*m/z*): calculated for $C_9H_{13}N_2O_4$ (M+H): 213.0875 found 213.0883. Anal. Calcd for $C_9H_{12}N_2O_4$: C, 50.94; H, 5.70; N, 13.20; O, 30.16. Found C, 51.01; H, 5.73; N, 13.16.

ADH-115

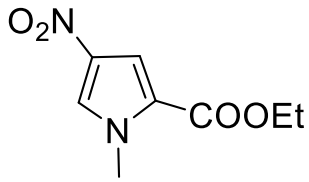

^{1}H NMR (600 MHz, Chloroform-*d*) δ 7.64 – 7.58 (d, *J* = 2.0 Hz, 1H), 7.47 – 7.43 (d, *J* = 2.0 Hz, 1H), 4.37 – 4.32 (q, *J* = 7.1 Hz, 2H), 4.03 – 4.00 (s, 3H), 1.43 – 1.36 (t, *J* = 7.1 Hz, 3H). ^{13}C NMR (151 MHz, $CDCl_3$) δ 160.2, 135.3, 127.5, 123.2, 112.7, 61.0, 38.0, 14.3. MS-ESI (*m/z*): calculated for $C_8H_{11}N_2O_4$ (M+H): 199.0719 found 199.0725. Anal. Calcd for $C_8H_{10}N_2O_4$: C, 48.49; H, 5.09; N, 14.14; O, 32.29. Found C, 48.59; H, 5.04; N, 14.10.

ADH-115_COOH

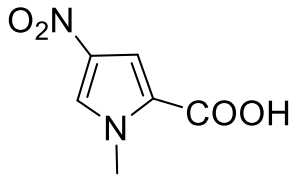

^{1}H NMR (600 MHz, DMSO-d_6) δ 13.80 – 12.57 (s, 1H), 8.24 – 8.18 (d, *J* = 2.1 Hz, 1H), 7.29 – 7.20 (d, *J* = 2.1 Hz, 1H), 3.95 – 3.89 (s, 3H). ^{13}C NMR (151 MHz, DMSO) δ 161.5, 134.5, 129.5, 124.6, 111.7, 38.0. MS-ESI (*m/z*): calculated for $C_6H_7N_2O_4$ (M+H): 171.0406 found 171.0415. Anal. Calcd for $C_6H_6N_2O_4$: C, 42.36; H, 3.56; N, 16.47; O, 37.62. Found C, 42.28; H, 3.60; N, 16.40.

ADH-116

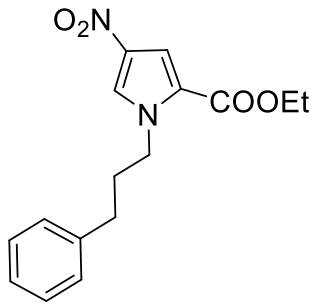

^{1}H NMR (600 MHz, Chloroform-*d*) δ 7.62 – 7.59 (d, *J* = 2.0 Hz, 1H), 7.49 – 7.47 (dd, *J* = 2.1, 0.9 Hz, 1H), 7.36 – 7.31 (td, *J* = 7.5, 5.6 Hz, 3H), 7.27 – 7.19 (m, 4H), 4.38 – 4.33 (m, 2H), 3.24 – 3.18 (t, *J* = 6.8 Hz, 2H), 2.79 – 2.74 (t, *J* = 7.3 Hz, 2H), 2.73 – 2.68 (m, 2H), 1.44 – 1.38 (t, *J* = 7.1 Hz, 3H). ^{13}C NMR (151 MHz, $CDCl_3$) δ 170.4, 160.7, 157.3, 140.3, 135.1, 128.3, 126.3, 120.5, 119.7, 109.3, 107.3, 81.2, 60.2, 49.9, 37.4, 28.1. MS-ESI (*m/z*): calculated for $C_{16}H_{19}N_2O_4$ (M+H): 303.1345 found 303.1352. Anal. Calcd for $C_{16}H_{18}N_2O_4$: C, 63.56; H, 6.00; N, 9.27; O, 21.17. Found C, 63.62; H, 6.04; N, 9.20.

ADH-116_COOH

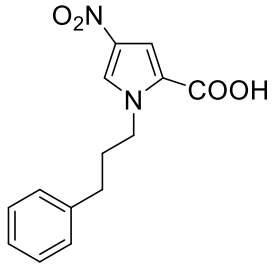

^{1}H NMR (600 MHz, Chloroform-*d*) δ 7.66 – 7.62 (d, *J* = 1.9 Hz, 1H), 7.60 – 7.56 (s, 1H), 7.35 – 7.30 (t, *J* = 7.5 Hz, 2H), 7.27 – 7.22 (m, 1H), 7.21 – 7.18 (m, 2H), 4.43 – 4.35 (t, *J* = 7.3 Hz, 2H), 2.74 – 2.65 (t, *J* = 7.6 Hz, 2H), 2.23 – 2.17 (p, *J* = 7.3 Hz, 2H). MS-ESI (*m/z*): calculated for $C_{14}H_{15}N_2O_4$ (M+H): 275.1032 found 275.1038.

ADH-118

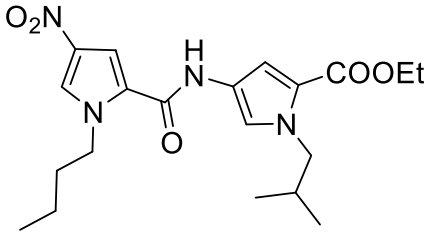

^{1}H NMR (600 MHz, Chloroform-*d*) δ 7.84 – 7.78 (s, 1H), 7.67 – 7.64 (d, *J* = 1.8 Hz, 1H), 7.43 – 7.39 (d, *J* = 2.1 Hz, 1H), 7.30 – 7.27 (s, 1H), 7.26 – 7.22 (d, *J* = 2.0 Hz, 1H), 6.93 – 6.91 (d, *J* = 2.1 Hz, 1H), 4.47 – 4.39 (t, *J* = 7.3 Hz, 2H), 4.32 – 4.27 (q, *J* = 7.1 Hz, 2H), 4.14 – 4.08 (d, *J* = 7.4 Hz, 2H), 2.19 – 2.05 (hept, *J* = 6.9 Hz, 1H), 1.89 – 1.79 (m, 2H), 1.40 – 1.33 (q, *J* = 7.3 Hz, 5H), 1.00 – 0.94 (t, *J* = 7.4 Hz, 3H), 0.93 – 0.90 (d, *J* = 6.7 Hz, 6H). ^{13}C NMR (151 MHz, $CDCl_3$) δ 160.9, 157.3, 135.1, 126.0, 125.9, 120.9, 120.5, 120.0, 108.9, 107.3, 60.0, 56.5, 50.0, 33.3, 30.2, 29.7, 29.4, 19.9, 19.7, 14.4, 13.6. MS-ESI (*m/z*): calculated for $C_{20}H_{29}N_4O_5$ (M+H): 405.2138 found 405.2139. Anal. Calcd for $C_{20}H_{28}N_4O_5$: C, 59.39; H, 6.98; N, 13.85; O, 19.78. Found C, 59.46; H, 7.01; N, 13.80.

ADH-118_COOH

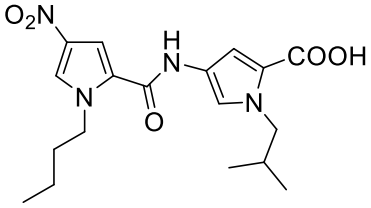

^{1}H NMR (600 MHz, DMSO-d_6) δ 12.26 – 12.15 (s, 1H), 10.34 – 10.16 (s, 1H), 8.28 – 8.19 (s, 1H), 7.60 – 7.53 (d, *J* = 2.2 Hz, 1H), 7.48 – 7.39 (s, 1H), 6.91 – 6.79 (d, *J* = 2.0 Hz, 1H), 4.46 – 4.38 (t, *J* = 7.2 Hz, 2H), 4.13 – 4.07 (d, *J* = 7.2 Hz, 2H), 2.03 – 1.93 (dq, *J* = 13.8, 7.0 Hz, 1H), 1.75 – 1.65 (p, *J* = 7.4 Hz, 2H), 1.31 – 1.20 (h, *J* = 8.5, 7.5 Hz, 2H), 0.92 – 0.85 (t, *J* = 7.4 Hz, 3H), 0.84 – 0.78 (d, *J* = 6.5 Hz, 6H). ^{13}C NMR (151 MHz, DMSO) δ 162.3, 157.3, 134.5, 128.0, 126.1, 122.2,

120.5, 119.8, 109.3, 108.5, 55.3, 49.5, 33.3, 30.4, 20.0, 19.6, 14.0. MS-ESI (*m/z*): calculated for $C_{18}H_{25}N_4O_5$ (M+H): 377.1825 found 377.1832.

ADH-119

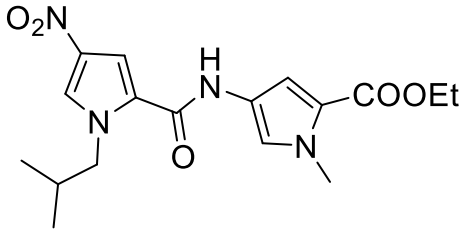

^{1}H NMR (600 MHz, Chloroform-*d*) δ 7.72 – 7.68 (s, 1H), 7.63 – 7.60 (d, *J* = 1.9 Hz, 1H), 7.39 – 7.36 (d, *J* = 2.1 Hz, 1H), 7.24 – 7.20 (d, *J* = 1.9 Hz, 1H), 6.88 – 6.83 (d, *J* = 2.0 Hz, 1H), 4.34 – 4.28 (q, *J* = 7.1 Hz, 2H), 4.27 – 4.22 (d, *J* = 7.4 Hz, 2H), 3.96 – 3.92 (s, 3H), 2.21 – 2.11 (hept, *J* = 6.9 Hz, 1H), 1.40 – 1.34 (t, *J* = 7.1 Hz, 3H), 0.95 – 0.92 (d, *J* = 6.7 Hz, 6H). ^{13}C NMR (151 MHz, $CDCl_3$) δ 161.1, 157.5, 135.0, 126.6, 125.9, 121.0, 120.8, 120.6, 108.6, 107.4, 60.1, 57.3, 36.9, 30.0, 19.7, 14.4. MS-ESI (*m/z*): calculated for $C_{17}H_{23}N_4O_5$ (M+H): 363.1668 found 363.1670. Anal. Calcd for $C_{17}H_{22}N_4O_5$: C, 56.35; H, 6.12; N, 15.46; O, 22.07. Found C, 56.43; H, 6.10; N, 15.38.

ADH-119_COOH

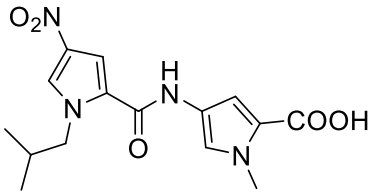

^{1}H NMR (600 MHz, DMSO-d_6) δ 12.39 – 12.17 (s, 1H), 10.33 – 10.21 (s, 1H), 8.25 – 8.19 (d, *J* = 1.9 Hz, 1H), 7.60 – 7.53 (d, *J* = 1.9 Hz, 1H), 7.46 – 7.41 (d, *J* = 2.0 Hz, 1H), 6.85 – 6.79 (d, *J* = 1.9 Hz, 1H), 4.31 – 4.21 (d, *J* = 7.4 Hz, 2H), 3.89 – 3.81 (s, 3H), 2.08 – 2.00 (hept, *J* = 6.9 Hz, 1H), 0.85 – 0.78 (d, *J* = 6.7 Hz, 6H). ^{13}C NMR (151 MHz, DMSO) δ 162.4, 157.4, 134.3, 128.4,

126.3, 122.3, 120.9, 120.3, 108.8, 108.6, 56.3, 36.7, 29.8, 19.8. MS-ESI (*m/z*): calculated for $C_{15}H_{19}N_4O_5$ (M+H): 335.1355 found 335.1359.

***N-Tert*-Butyl-ADH-120**

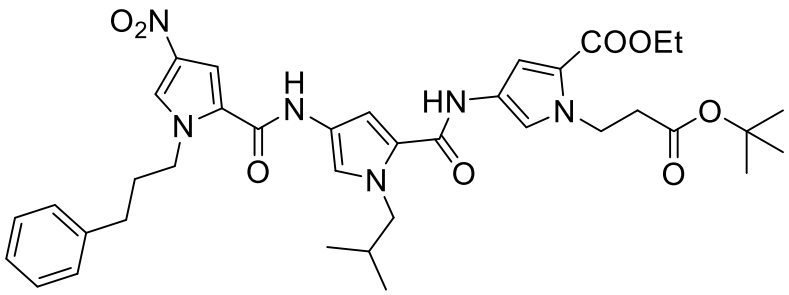

^{1}H NMR (600 MHz, Chloroform-*d*) δ 7.73 – 7.69 (s, 1H), 7.63 – 7.60 (d, *J* = 1.9 Hz, 1H), 7.52 – 7.48 (s, 1H), 7.48 – 7.45 (d, *J* = 2.0 Hz, 1H), 7.33 – 7.30 (dd, *J* = 8.2, 6.9 Hz, 2H), 7.25 – 7.21 (m, 2H), 7.21 – 7.19 (m, 2H), 7.19 – 7.18 (d, *J* = 1.1 Hz, 1H), 6.88 – 6.85 (d, *J* = 2.1 Hz, 1H), 6.76 – 6.71 (s, 1H), 4.58 – 4.53 (t, *J* = 7.0 Hz, 2H), 4.50 – 4.45 (m, 2H), 4.34 – 4.27 (q, *J* = 7.1 Hz, 2H), 4.21 – 4.18 (d, *J* = 7.4 Hz, 2H), 2.79 – 2.74 (t, *J* = 7.0 Hz, 2H), 2.74 – 2.68 (m, 2H), 2.27 – 2.21 (m, 2H), 2.18 – 2.12 (p, *J* = 7.0 Hz, 1H), 1.48 – 1.43 (s, 9H), 0.91 – 0.90 (d, *J* = 4.8 Hz, 6H). MS-ESI (*m/z*): calculated for $C_{37}H_{47}N_6O_8$ (M+H): 703.3455 found 703.3463.

ADH-120

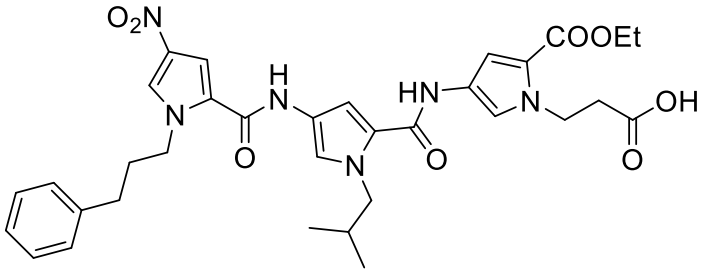

^{1}H NMR (600 MHz, DMSO-d_6) δ 12.64 – 12.04 (s, 1H), 10.40 – 10.27 (s, 1H), 10.04 – 9.92 (s, 1H), 8.27 – 8.22 (d, *J* = 2.0 Hz, 1H), 7.61 – 7.58 (d, *J* = 2.0 Hz, 1H), 7.50 – 7.47 (d, *J* = 2.0 Hz, 1H), 7.30 – 7.24 (m, 3H), 7.21 – 7.15 (m, 3H), 7.08 – 7.04 (d, *J* = 1.9 Hz, 1H), 6.99 – 6.95 (d, *J* = 1.9 Hz, 1H), 4.52 – 4.42 (dt, *J* = 19.0, 7.1 Hz, 4H), 4.25 – 4.19 (q, *J* = 7.1 Hz, 2H), 4.18 – 4.13 (d, *J* = 7.3 Hz, 2H), 2.71 – 2.66 (t, *J* = 7.0 Hz, 2H), 2.60 – 2.56 (dd, *J* = 9.3, 6.7 Hz, 2H), 2.13 – 2.05 (qd, *J* = 7.8, 6.1 Hz, 2H), 2.04 – 1.95 (hept, *J* = 6.8 Hz, 1H), 1.32 – 1.26 (t, *J* = 7.1 Hz, 3H), 0.83 – 0.80 (d, *J* = 6.7 Hz, 6H). MS-ESI (*m/z*): calculated for $C_{33}H_{39}N_6O_8$ (M+H): 647.2829 found 647.2834. Anal. Calcd for $C_{33}H_{38}N_6O_8$: C, 61.29; H, 5.92; N, 13.00; O, 19.79. Found C, 61.38; H, 5.90; N, 13.01.

Compound	% yield
N-Tert-Butyl ADH-117	80
ADH-113	86
ADH-113_COOH	95
ADH-117	98
ADH-102	91
ADH-102_COOH	94
N-Tert-Butyl ADH-104	88
ADH-104	96
ADH-105	85
N-Tert-Butyl ADH-101	82
ADH-101	93
N-Tert-Butyl ADH-103	78
ADH-103	81
N-Tert-Butyl ADH-106	84
ADH-106	85

N-Tert-Butyl ADH-107	82
ADH-107	83
ADH-108	87
ADH-108_COOH	81
ADH-109	79
ADH-109_COOH	82
N-Tert-Butyl ADH-110	87
ADH-110	89
N-Tert-Butyl ADH-111	83
ADH-111	91
N-Tert-Butyl ADH-112	90
ADH-112	92
ADH-114	93
ADH-114_COOH	89
ADH-115	88
ADH-115_COOH	86
ADH-116	81
ADH-116_COOH	76
ADH-118	87

ADH-118_COOH	90
ADH-119	87
ADH-119_COOH	89
N-*Tert*-Butyl ADH-120	81
ADH-120	84

Table S1. % yields of the compounds used in the study.

References

1. P.S. Chen, T.Y. Toribara, H. Warner, *Anal. Chem.* 1956, **28**, 1756-1758.

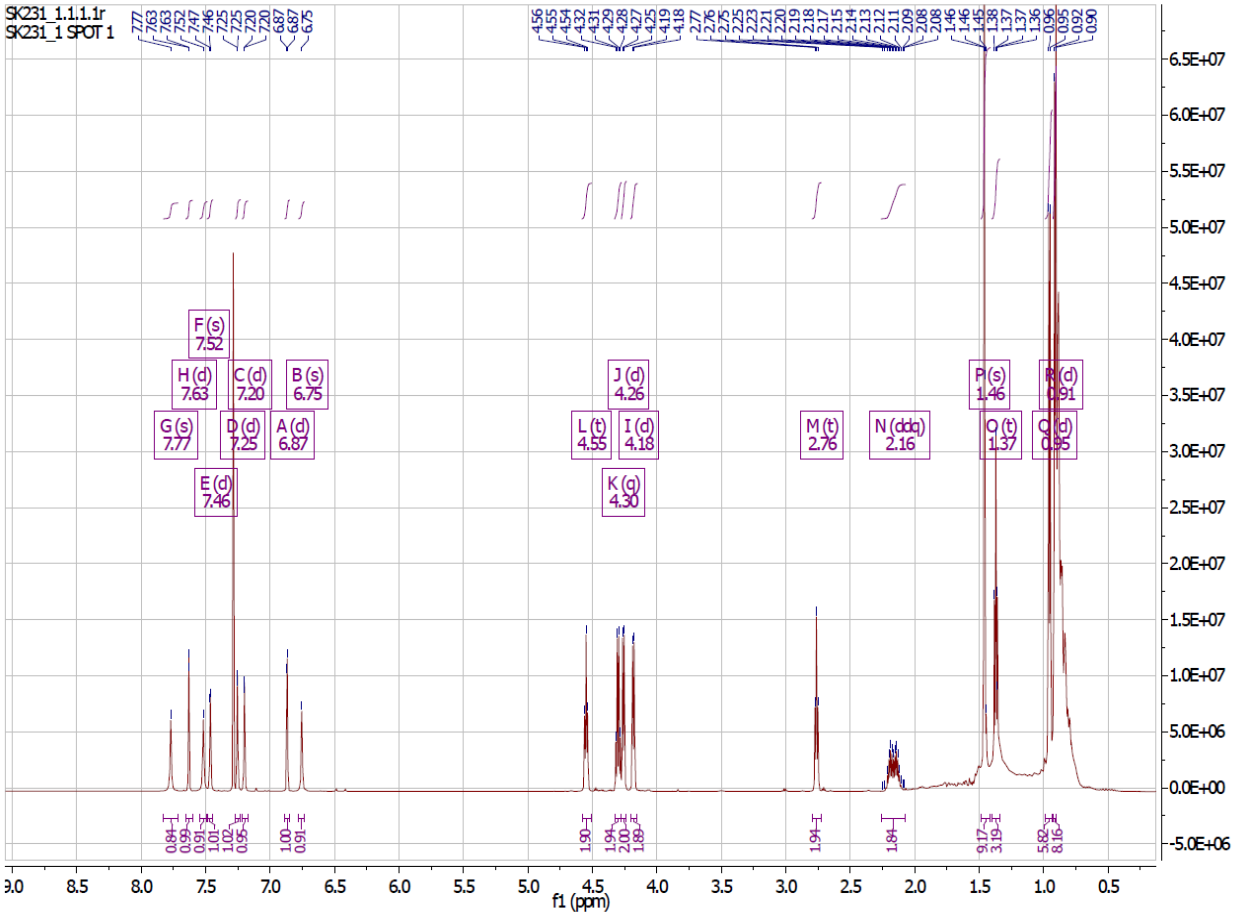

Figure S. ^{1}H of N-tert-butyl ADH-101.

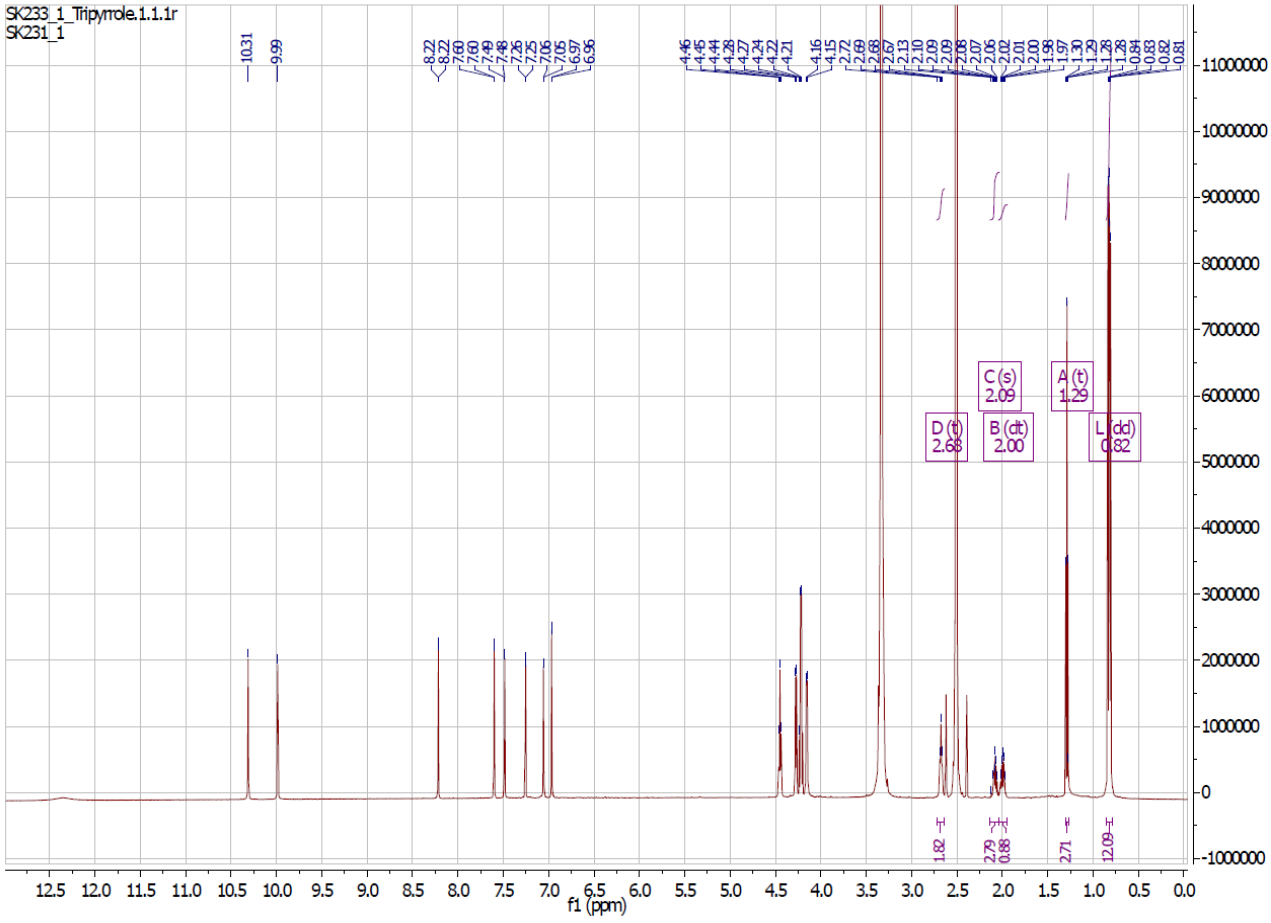

Figure S. ^{1}H of ADH-101.

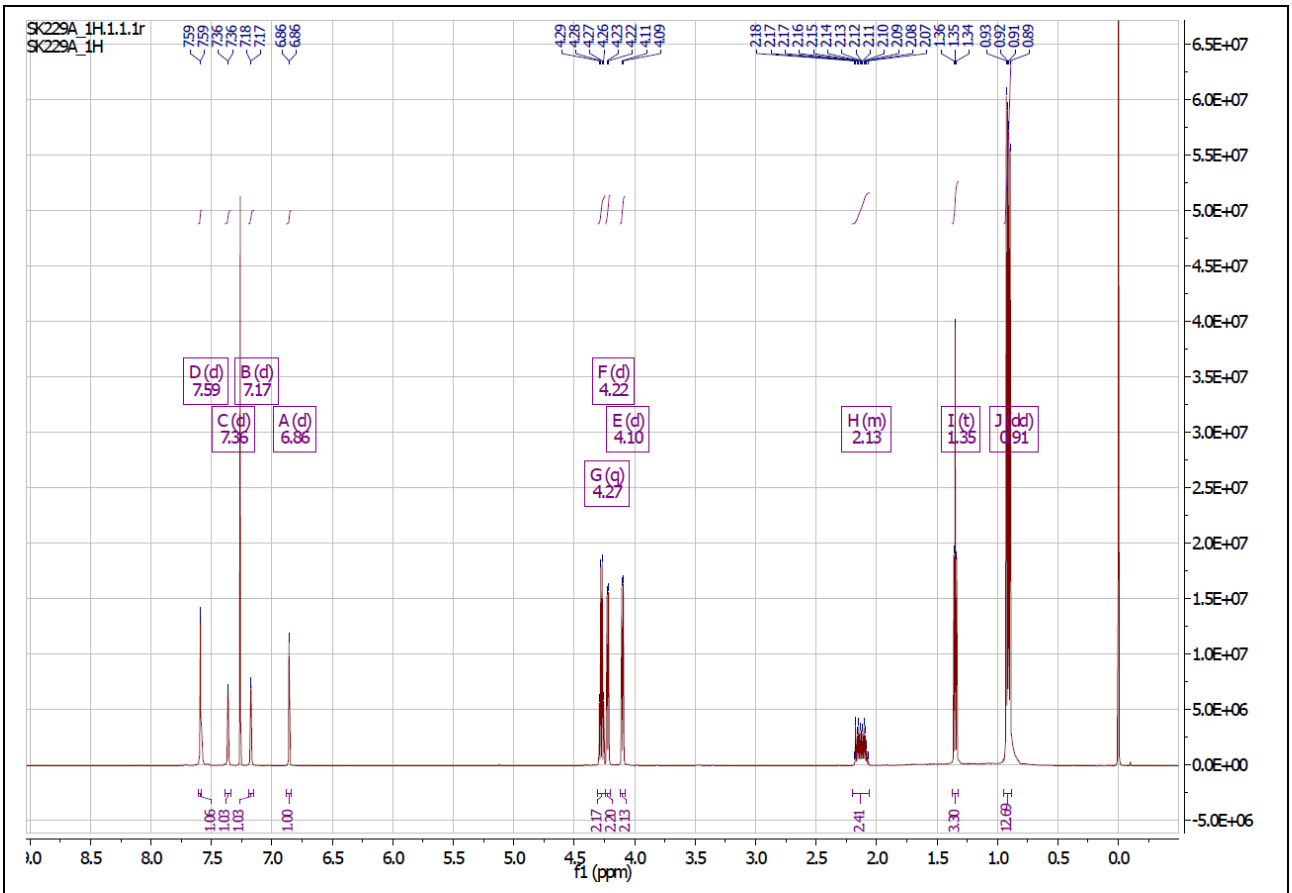

Figure S. ^{1}H of ADH-102.

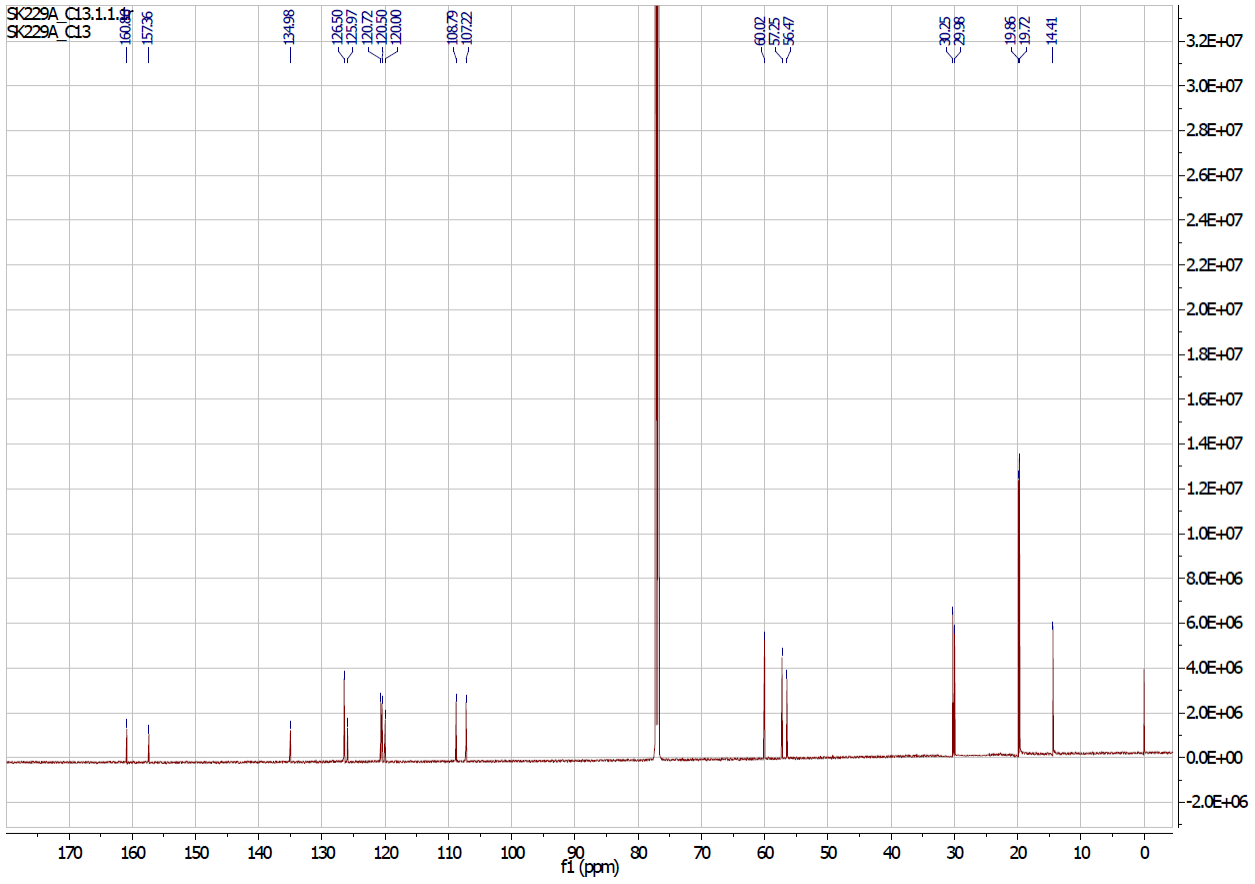

Figure S. ^{13}C of ADH-102.

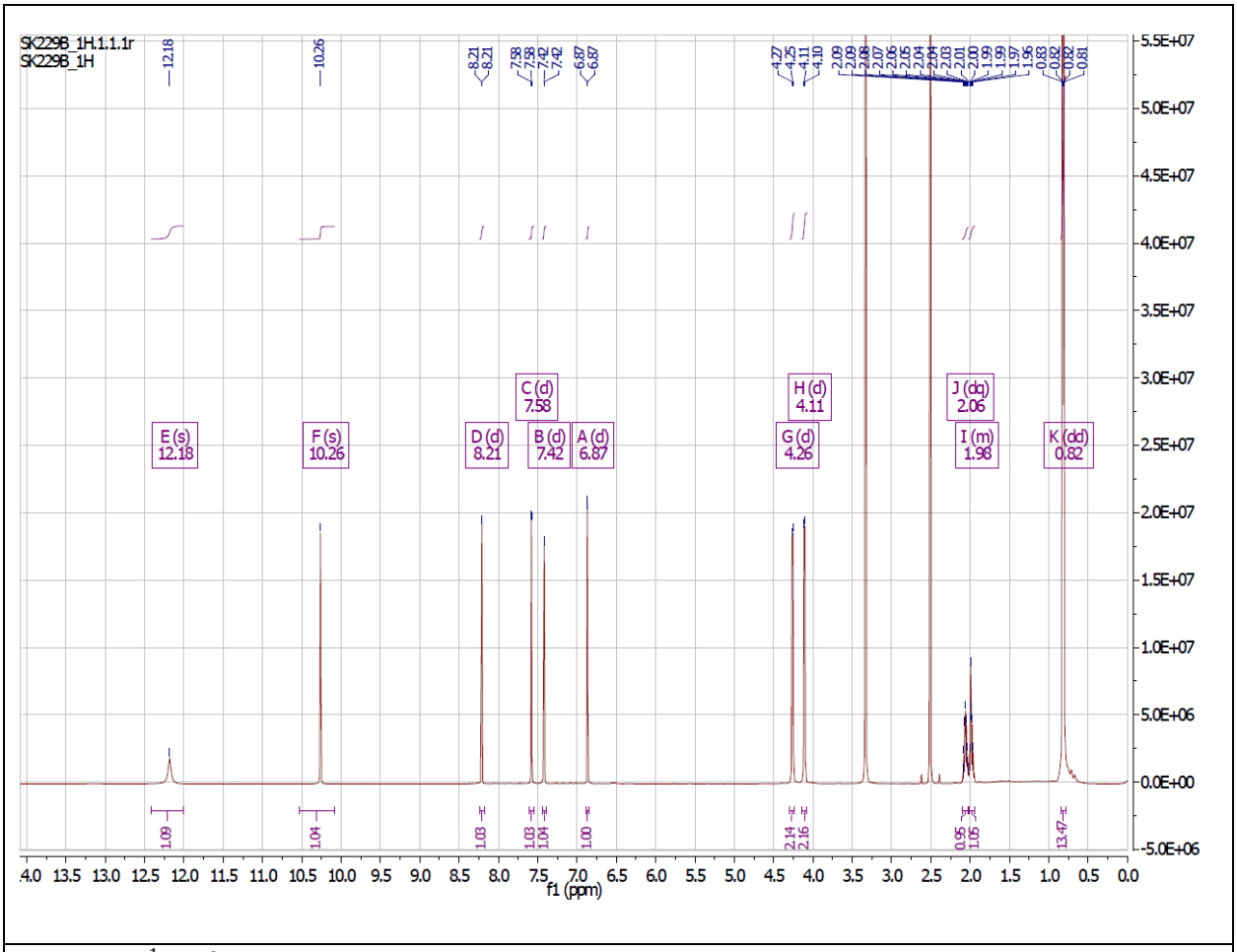

Figure S. ^{1}H of ADH-102_COOH

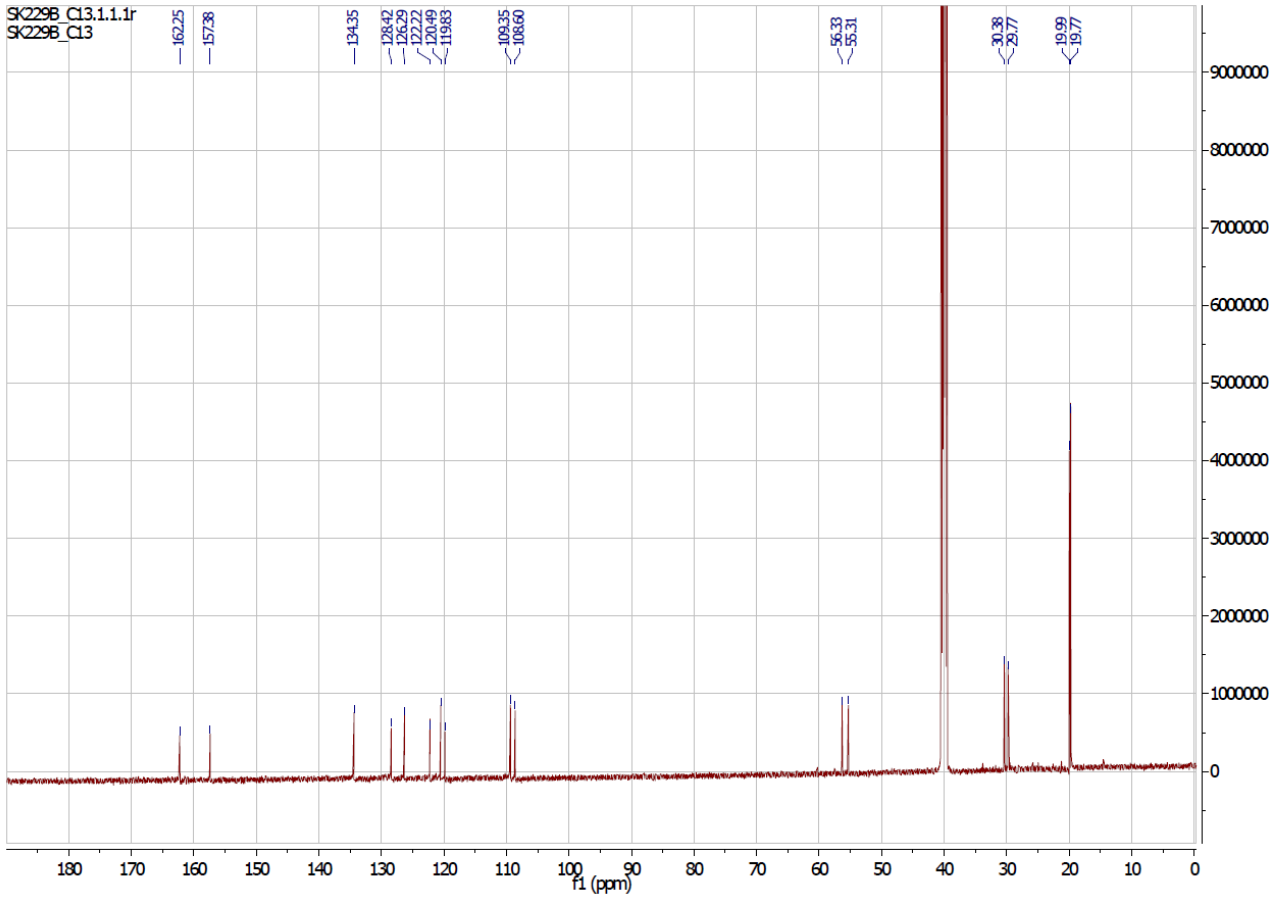

Figure S. ^{13}C of ADH-102_COOH

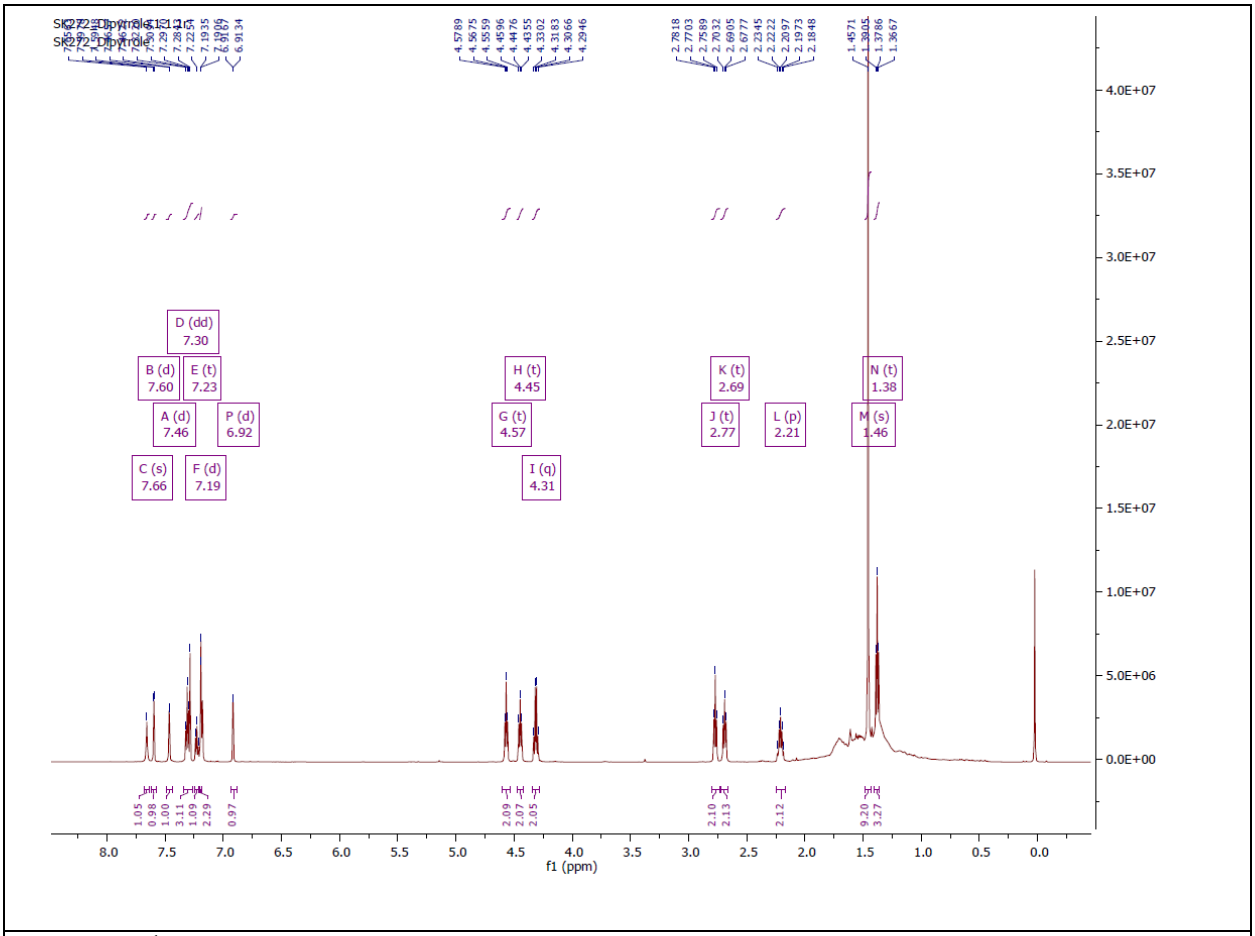

Figure S. ^{1}H of N-tert Butyl ADH-103

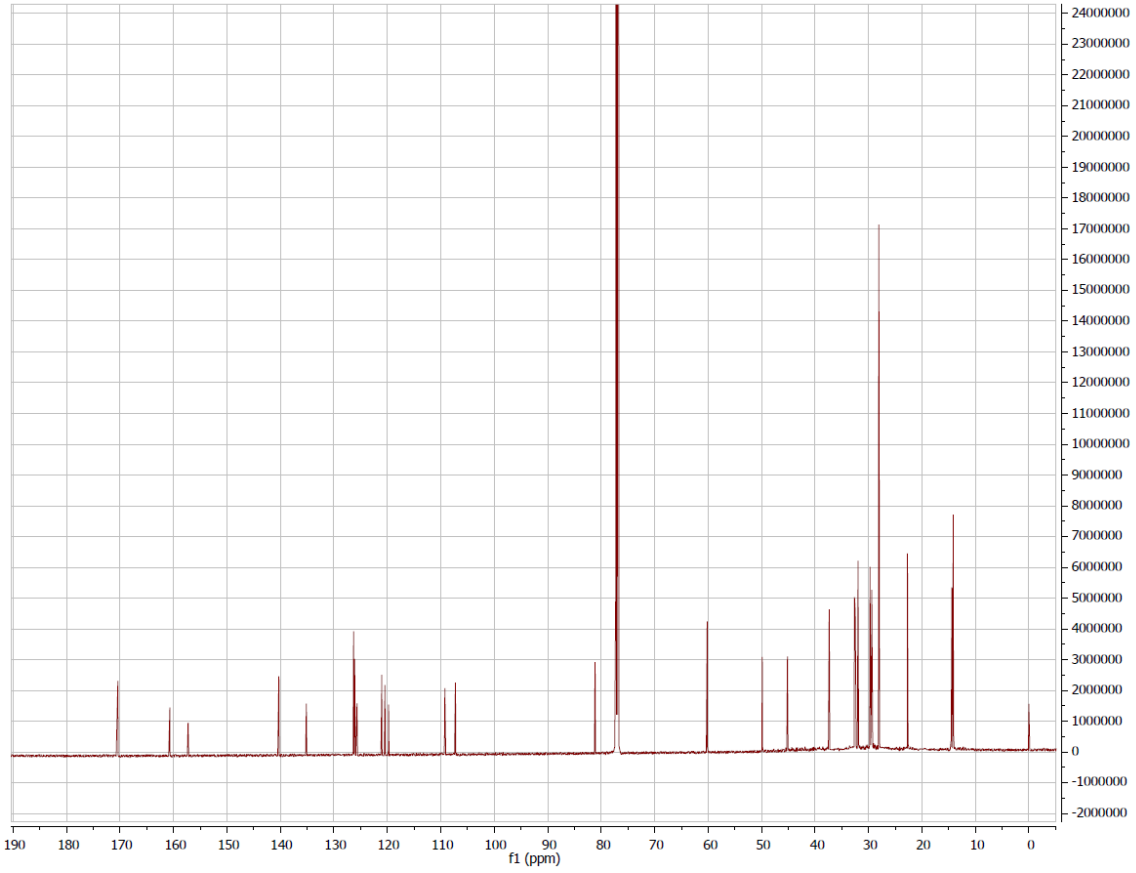

Figure S. ^{13}C of N-tert Butyl ADH-103

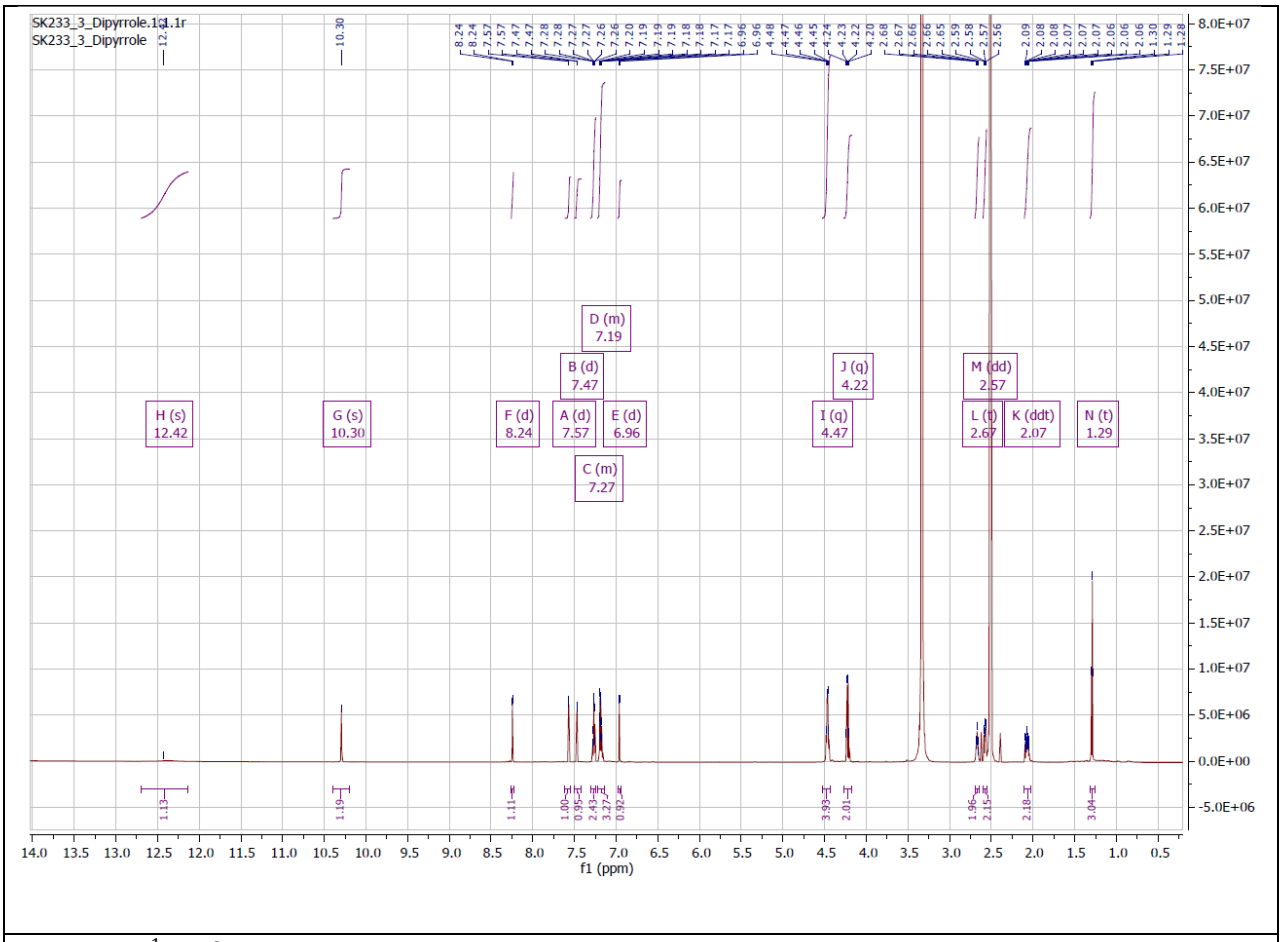

Figure S. ^{1}H of ADH-103

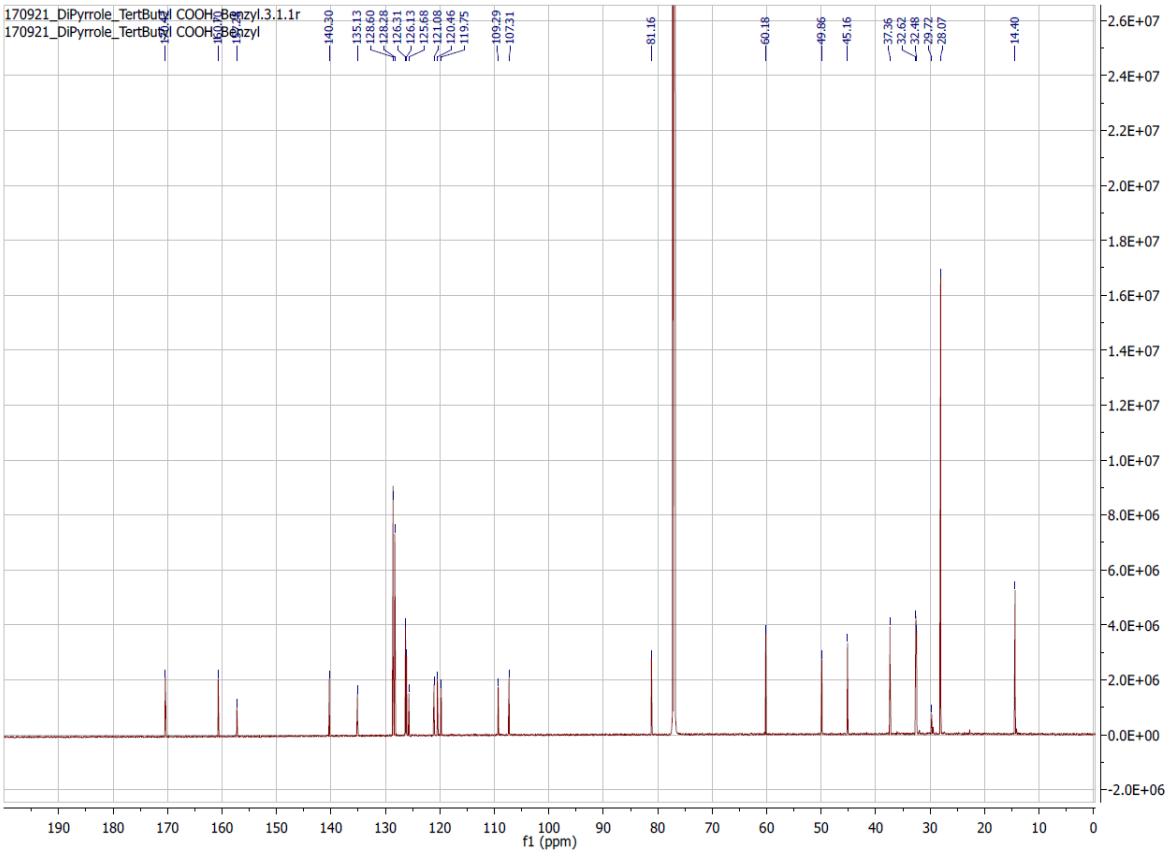

Figure S. ^{13}C of ADH-103

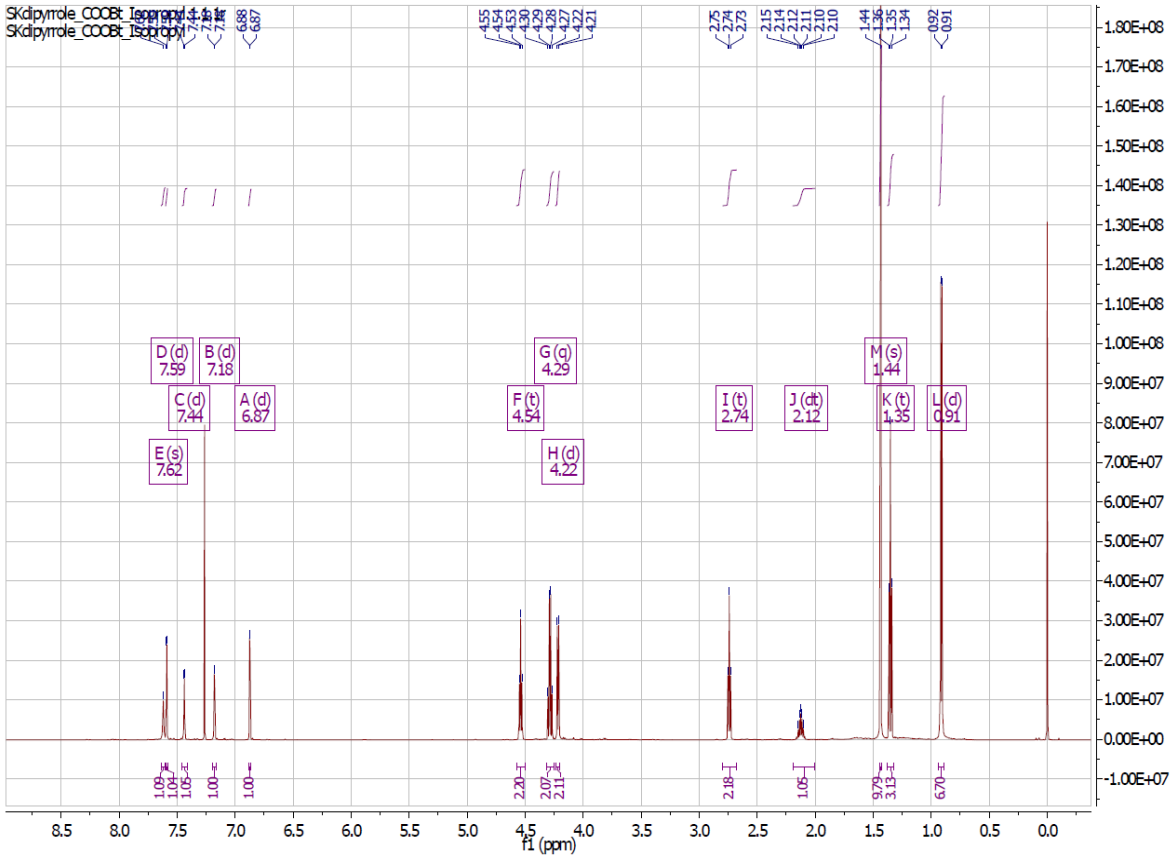

Figure S. ^{1}H of tert butyl ADH-104

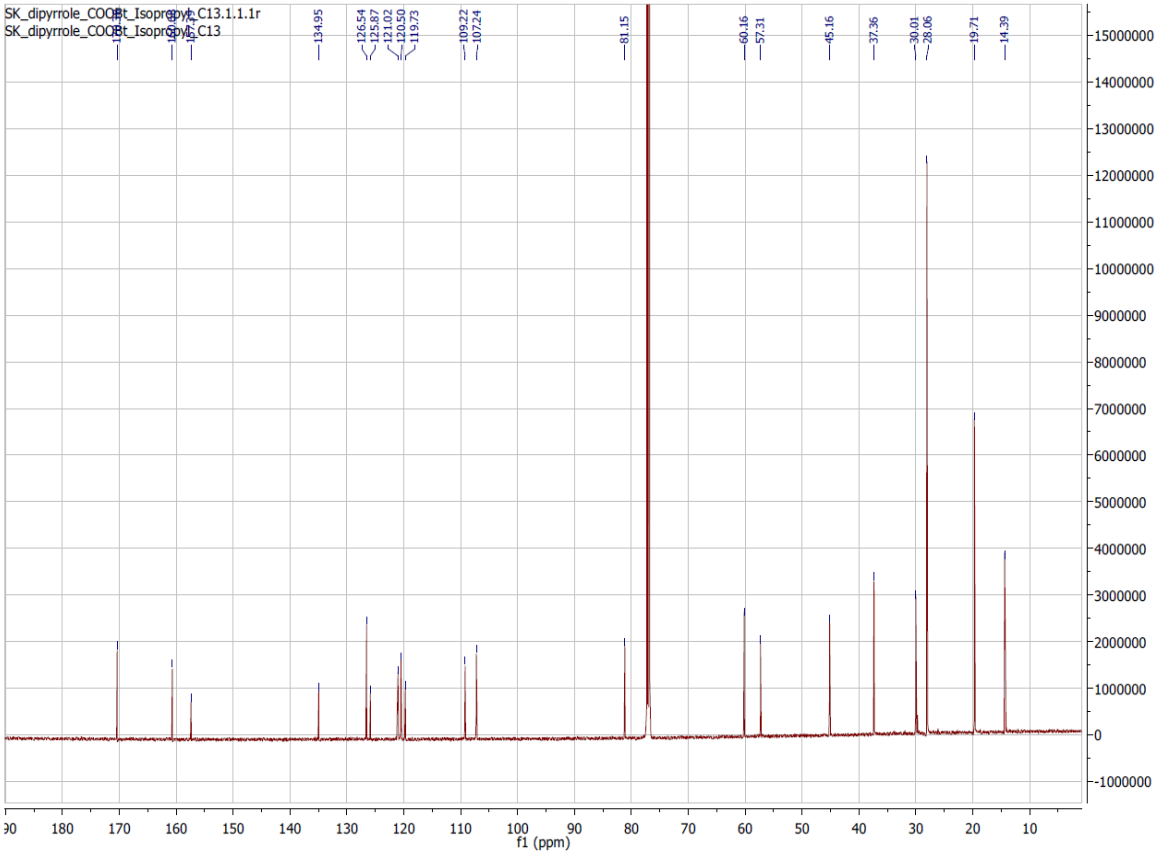

Figure S. ^{13}C of tert butyl ADH-104

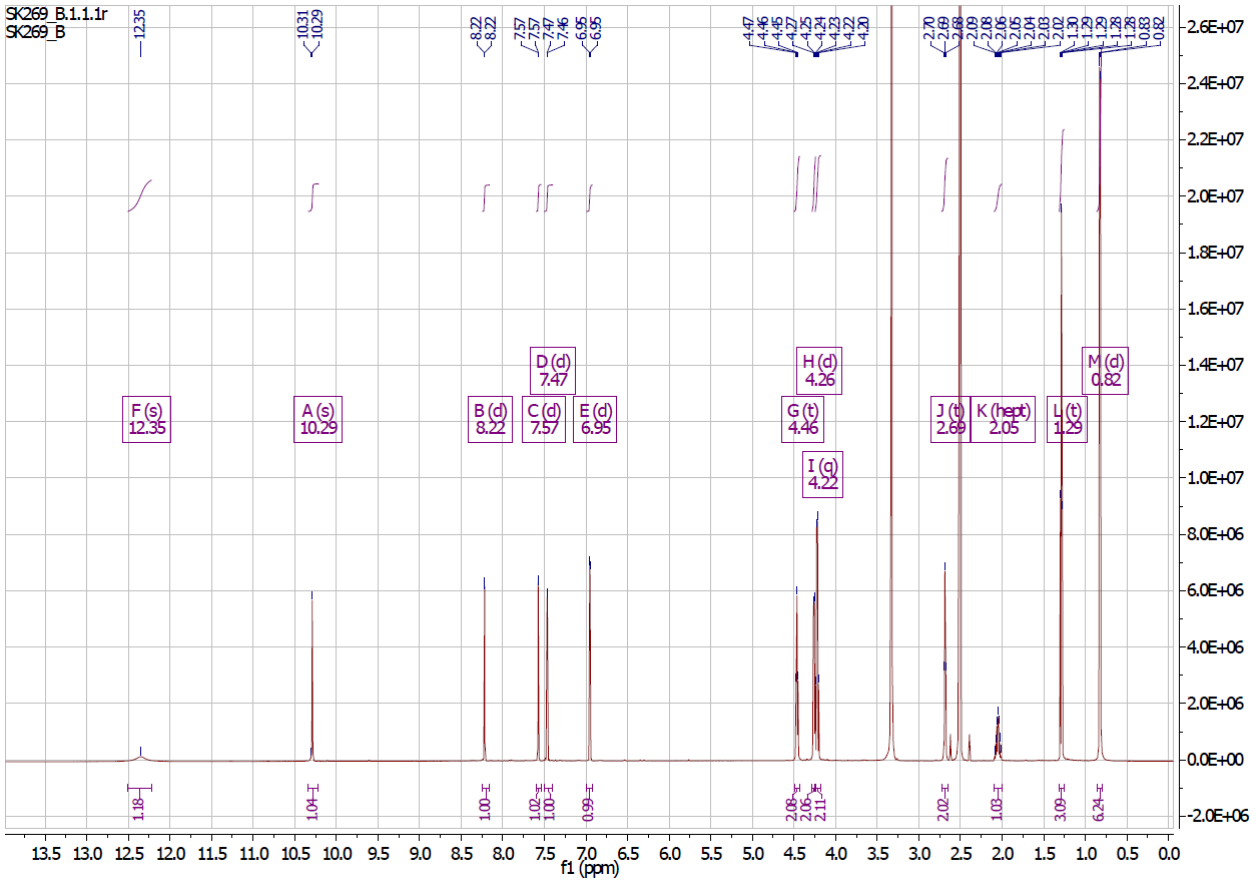

Figure S. ^{1}H of ADH-104

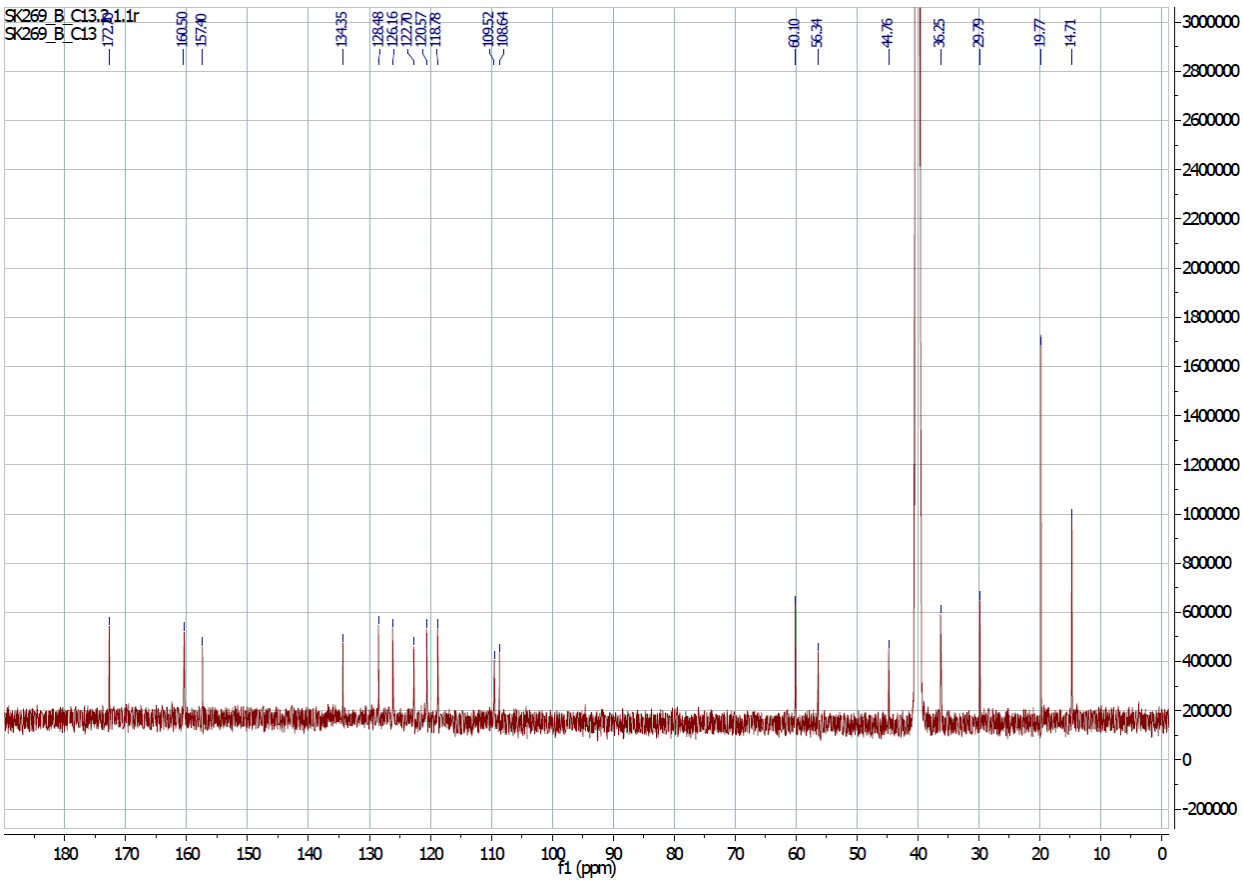

Figure S. ^{13}C of ADH-104

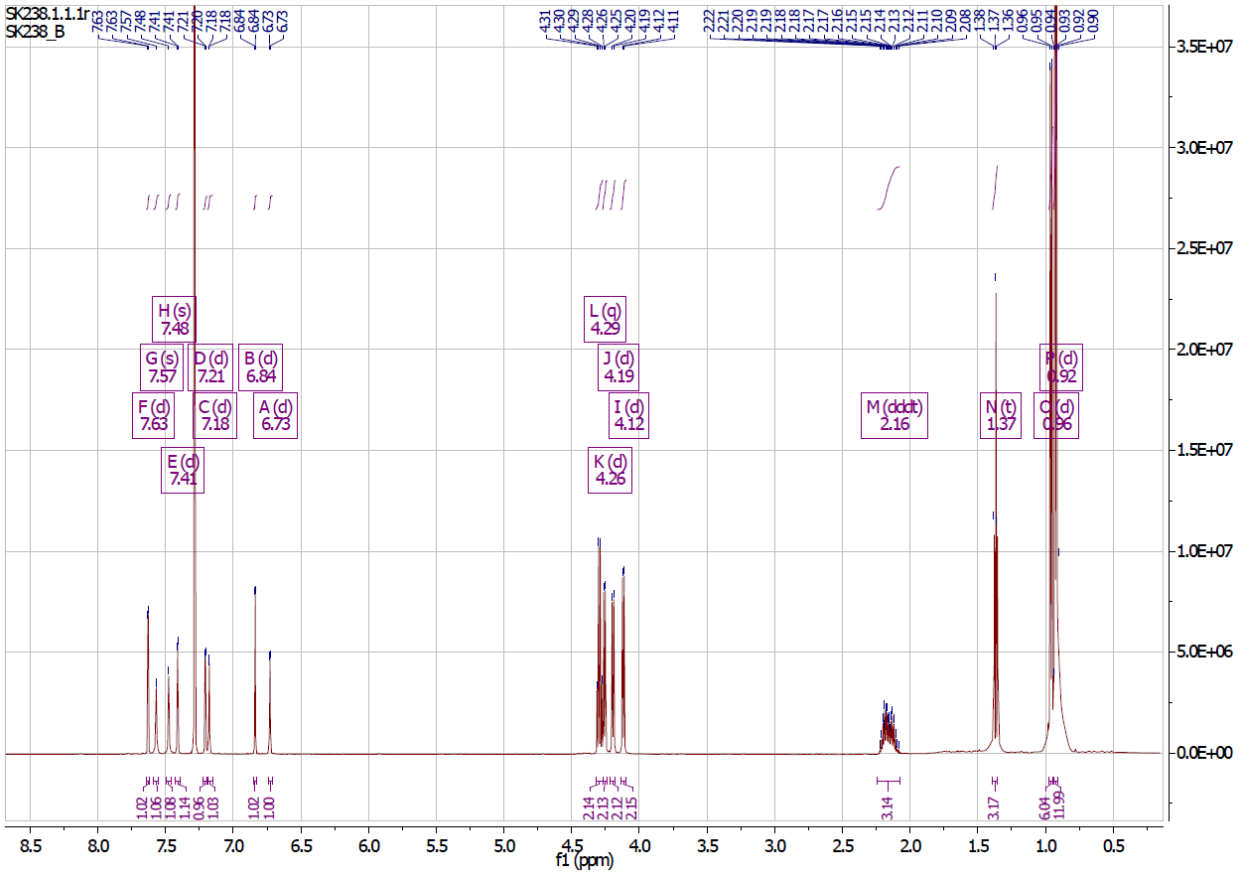

Figure S. ^{1}H of ADH-105

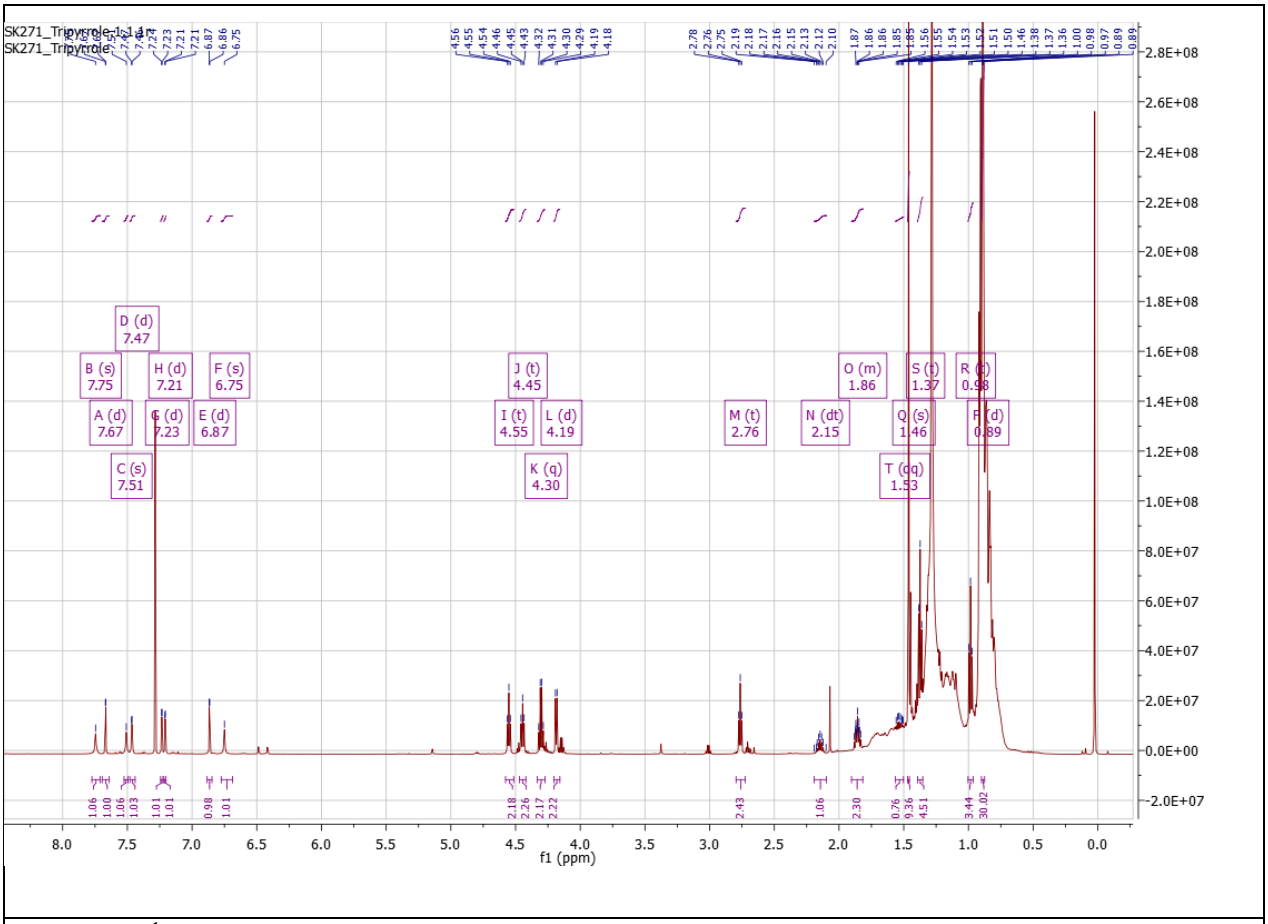

Figure S. ^{1}H of N-tert butyl ADH-106

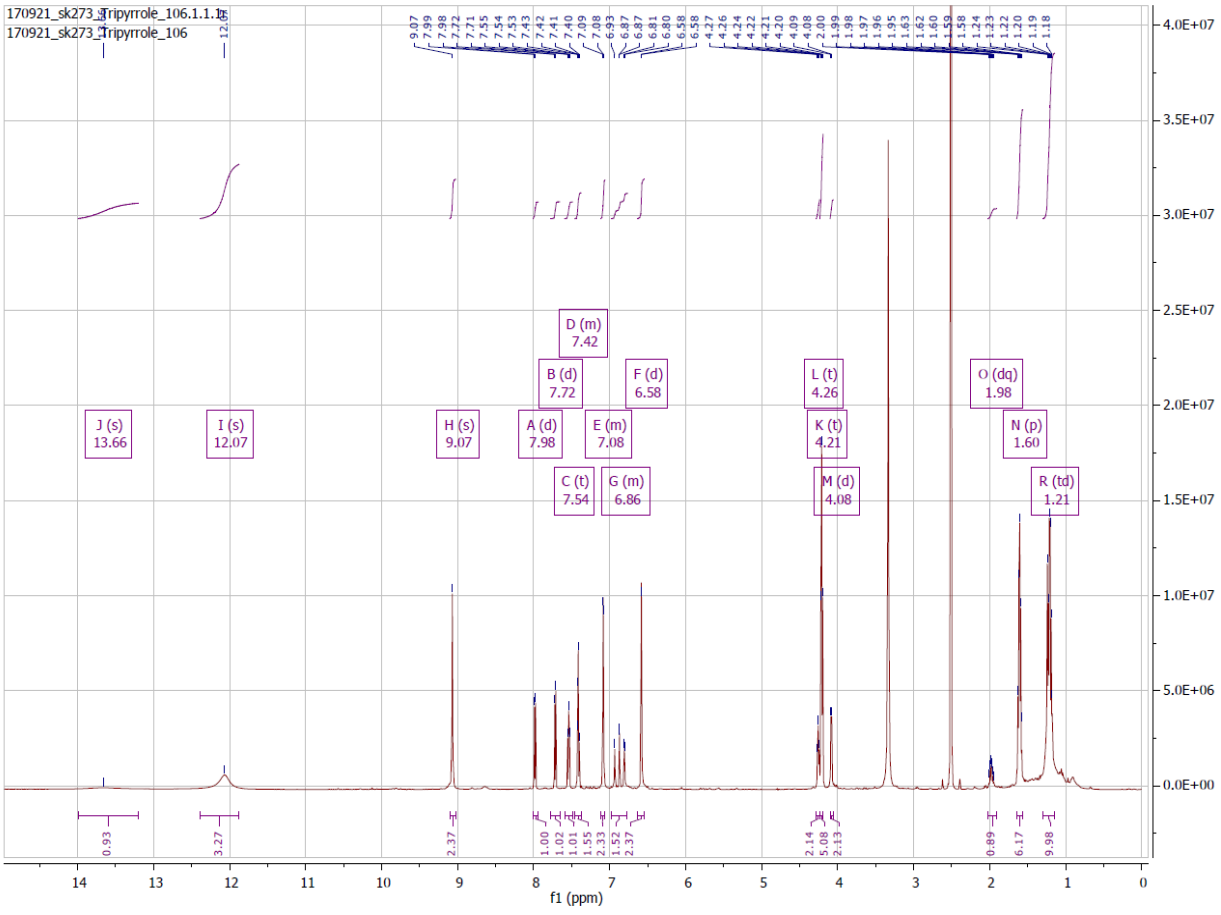

Figure S. ^{1}H of ADH-106

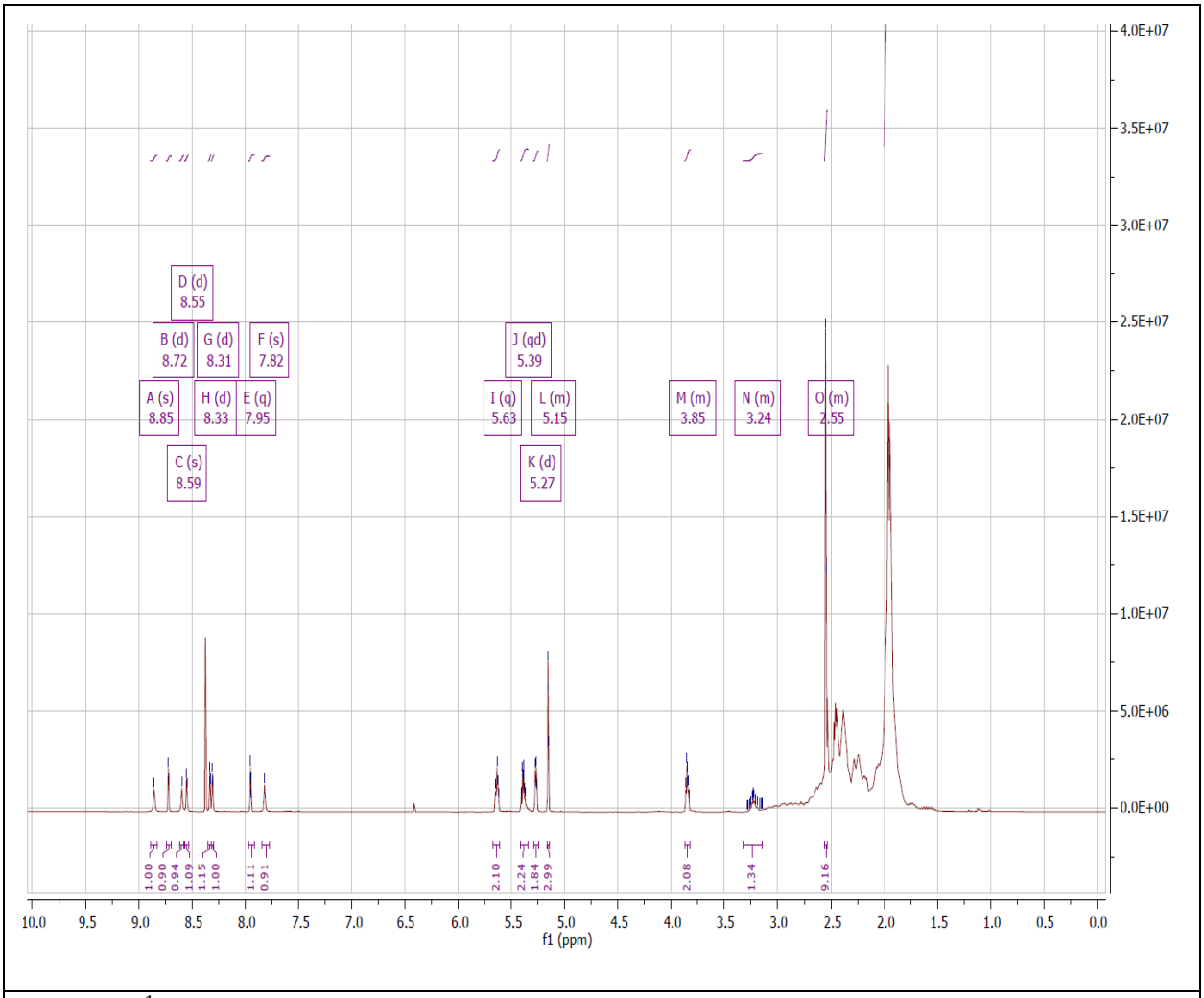

Figure S. ^{1}H of N-tert butyl ADH-107

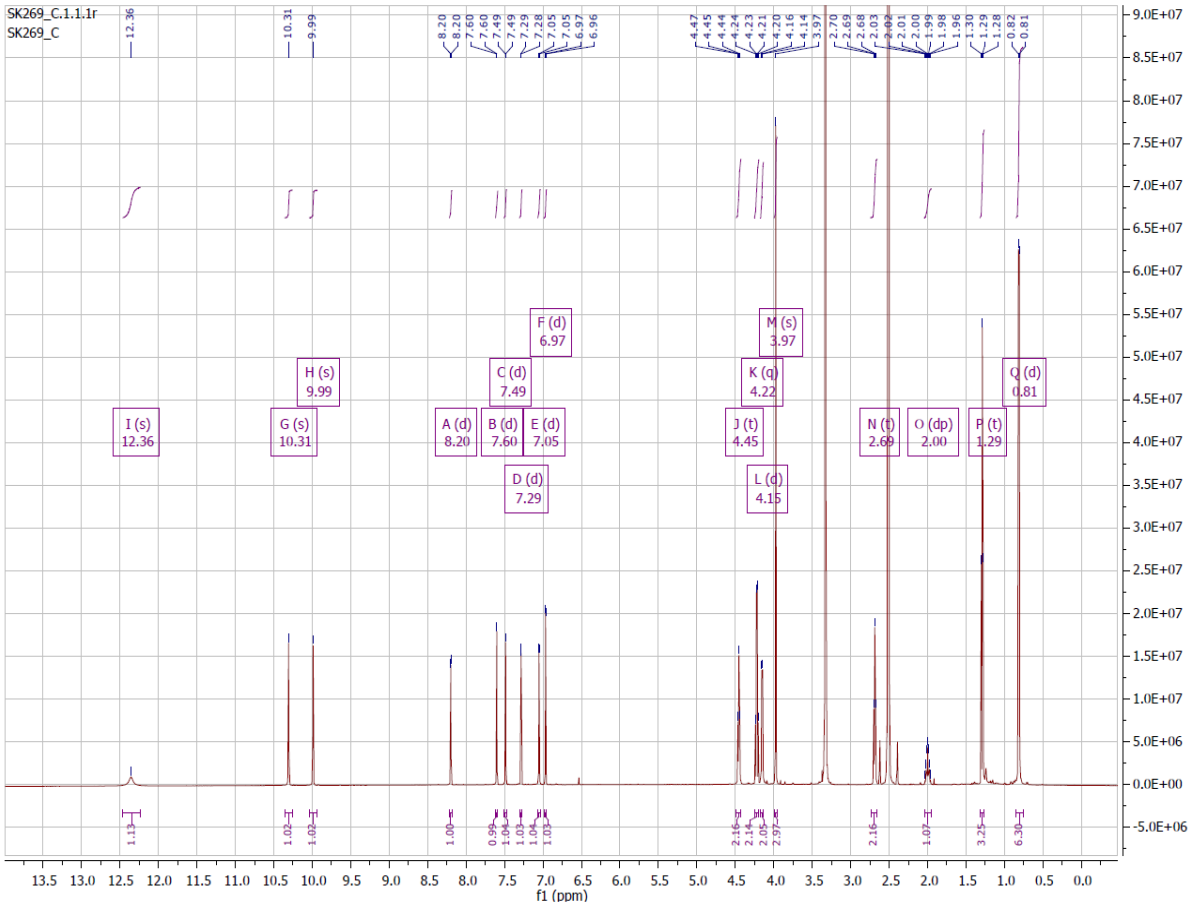

Figure S. ^{1}H of ADH-107

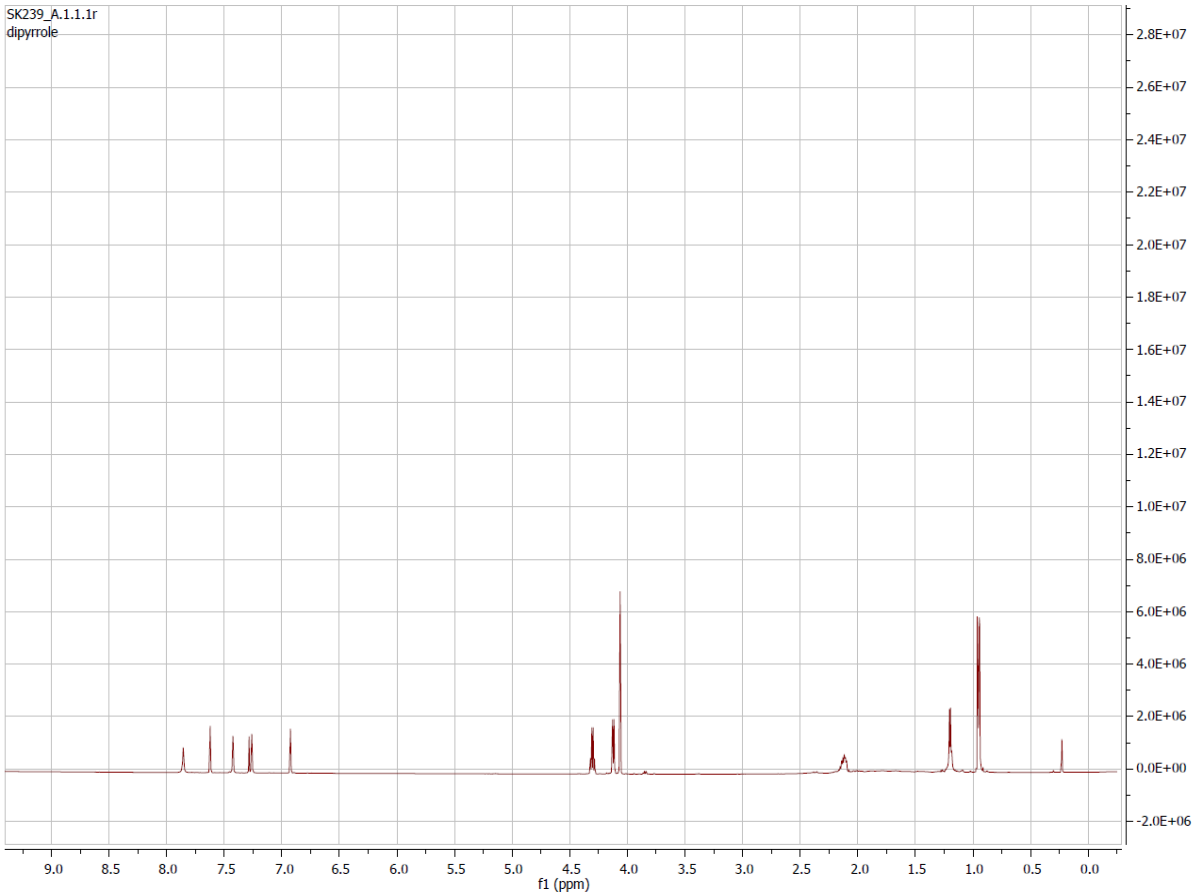

Figure S. ^{1}H of ADH-108

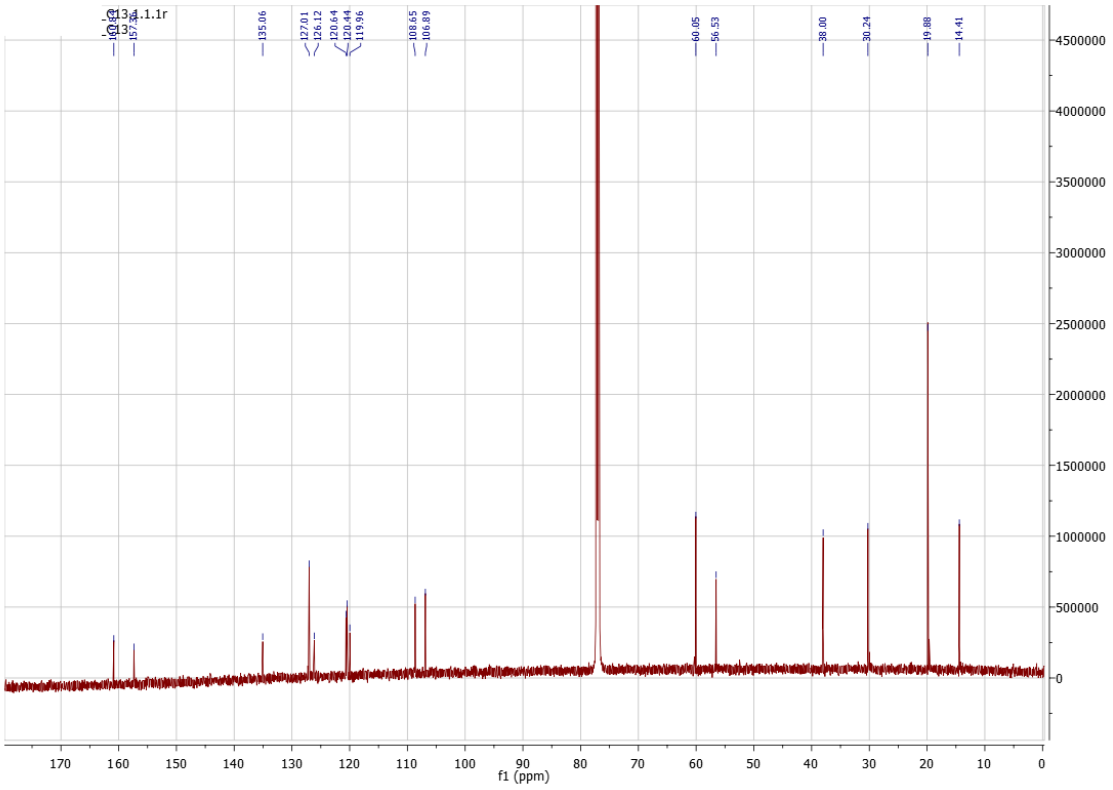

Figure S. ^{13}C of ADH-108

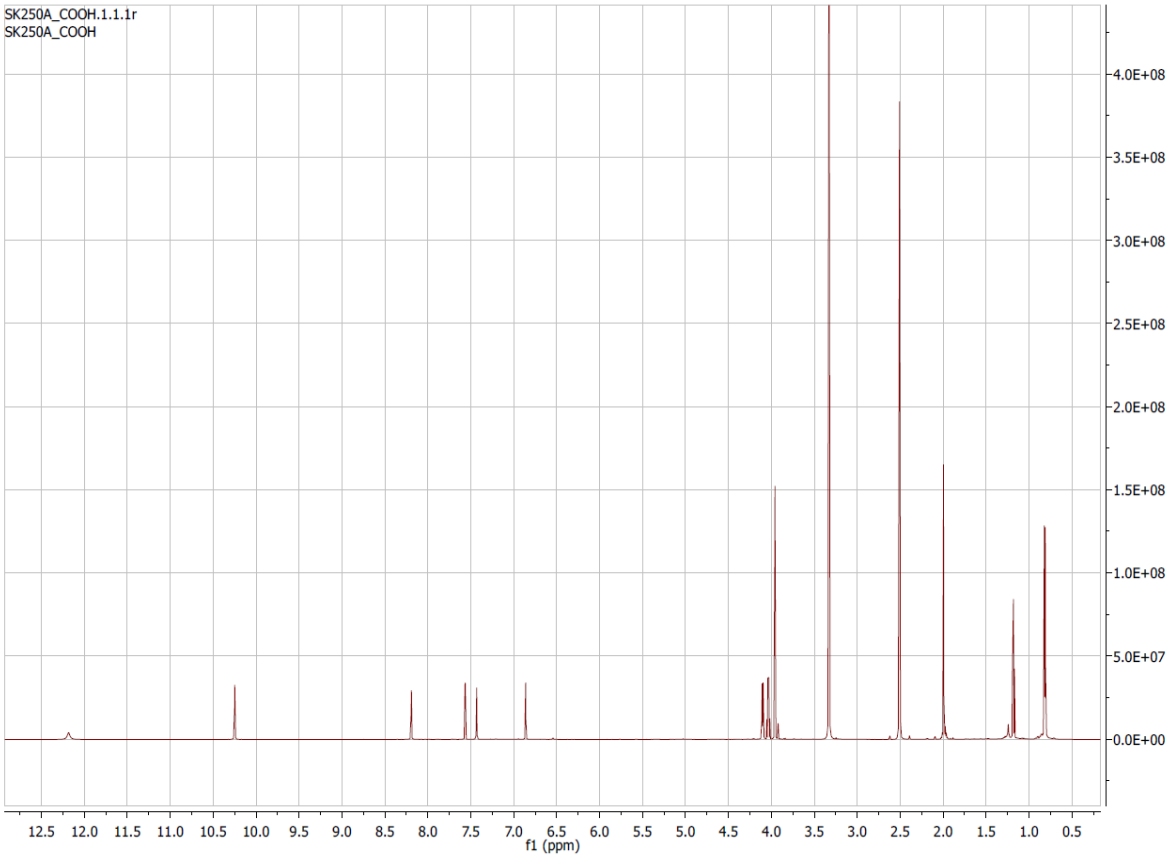

Figure S. ^{1}H of ADH-108_COOH

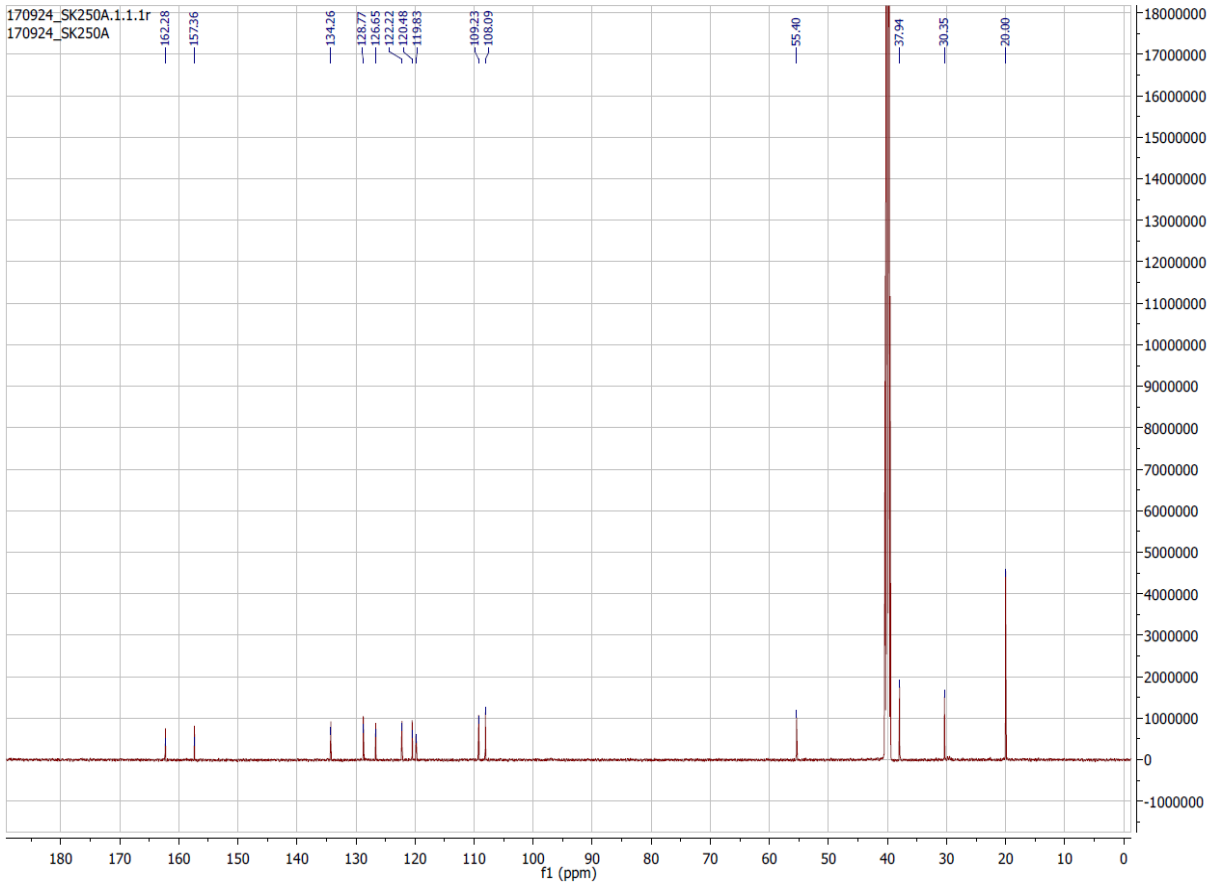

Figure S. ^{13}C of ADH-108_COOH

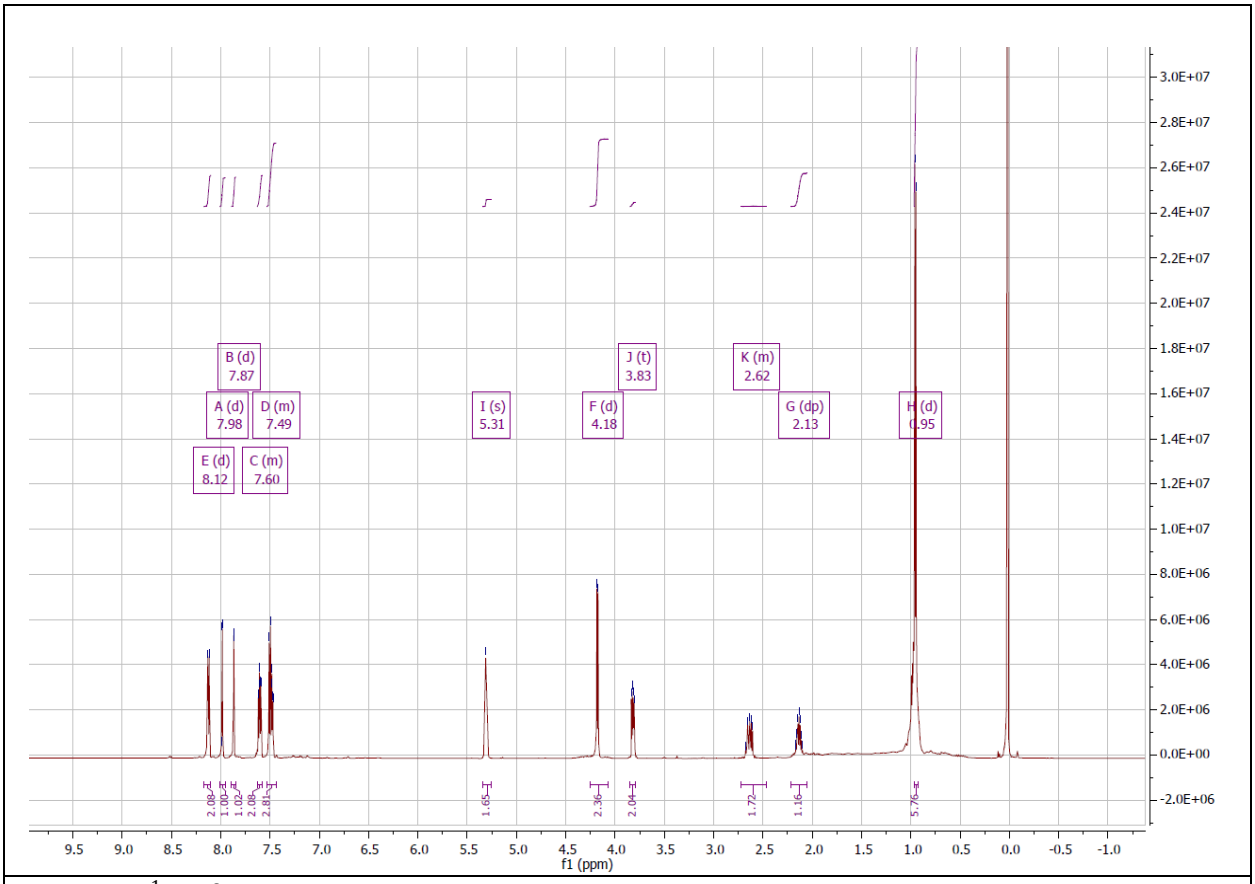

Figure S. ^{1}H of ADH-109

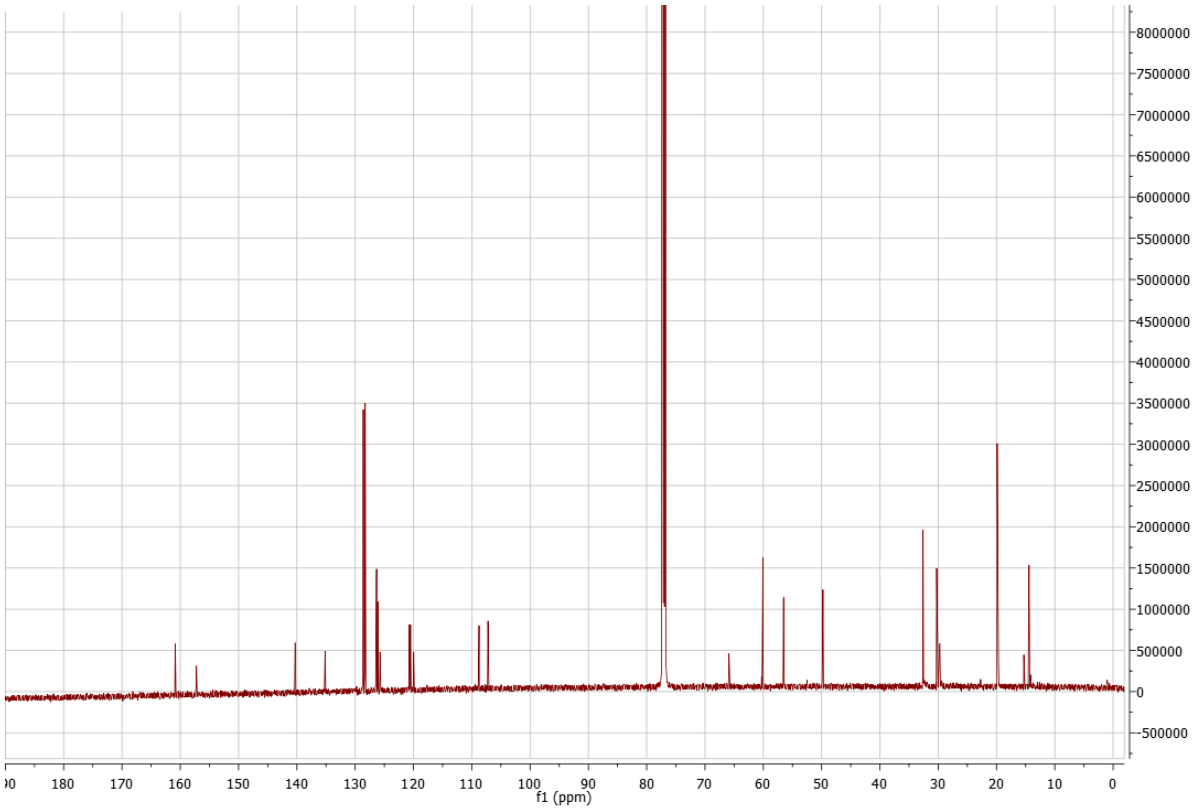

Figure S. ^{13}C of ADH-109

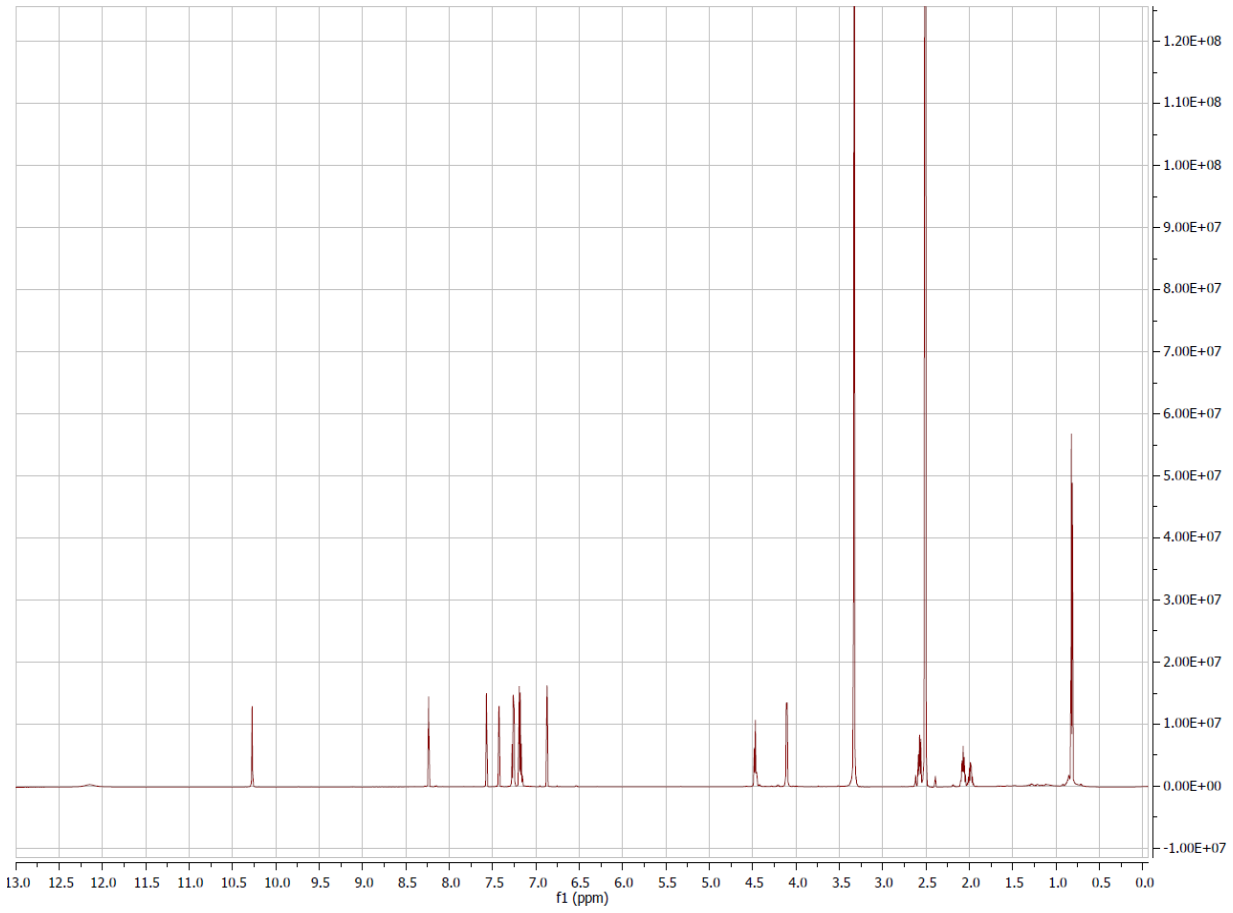

Figure S. ^{1}H of ADH-109_COOH

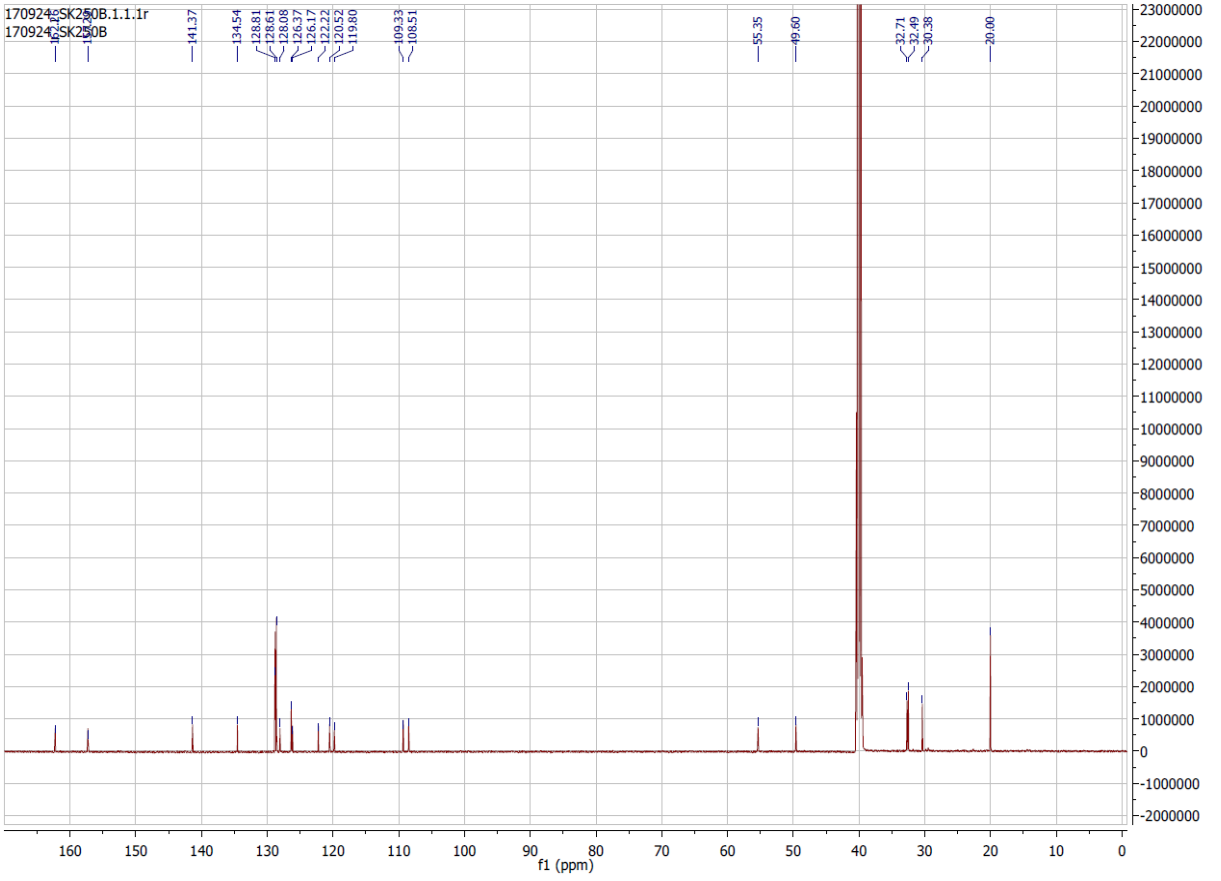

Figure S. ^{13}C of ADH-109_COOH

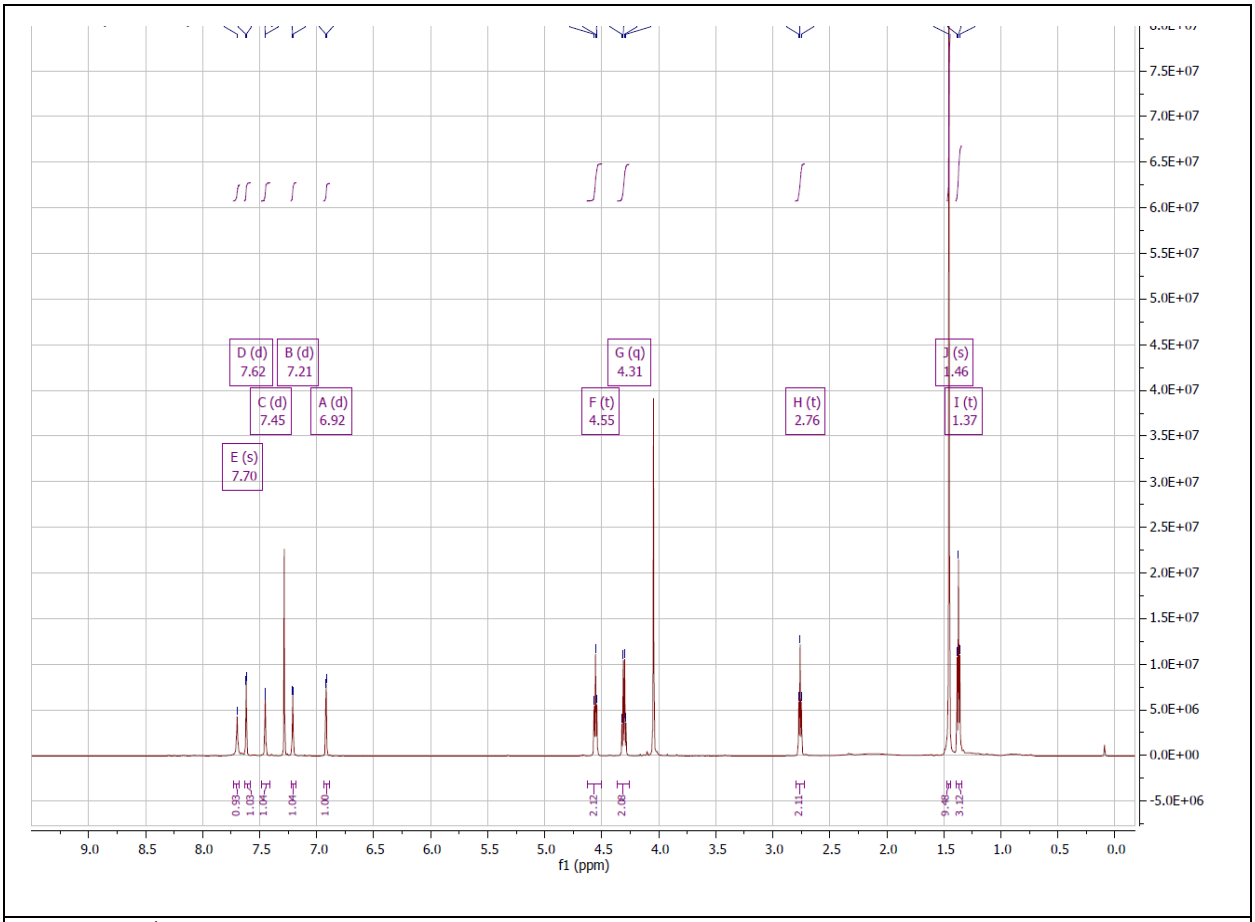

Figure S. ^{1}H of N-tert butyl ADH-110

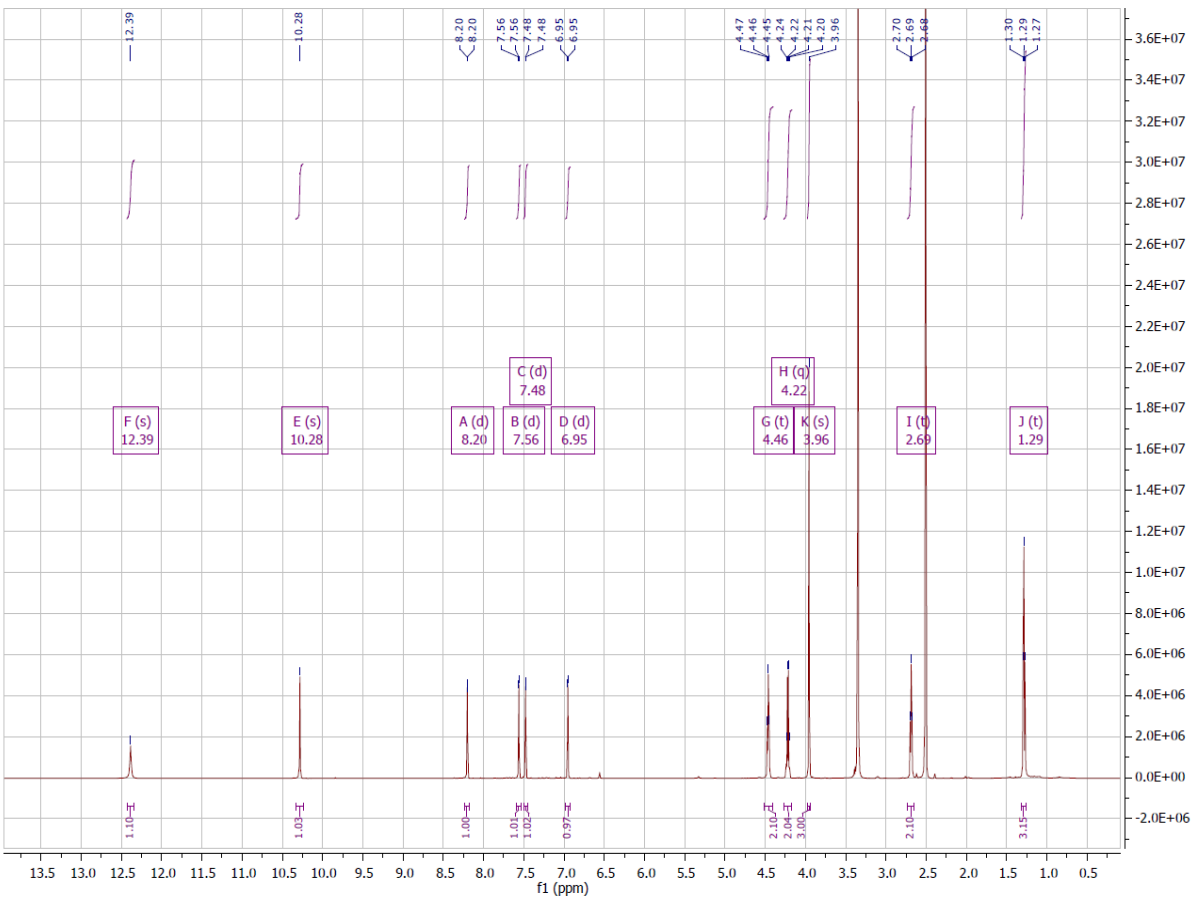

Figure S. ^{1}H of ADH-110

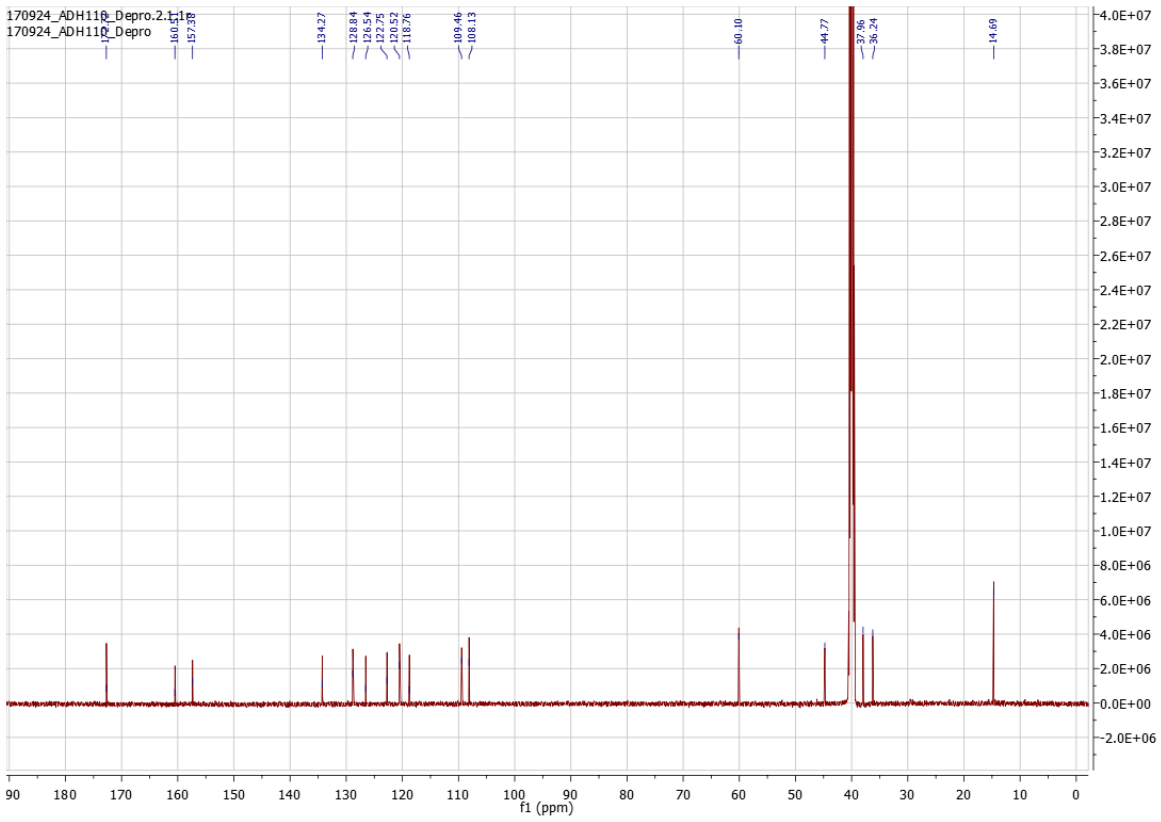

Figure S. ^{13}C of ADH-110

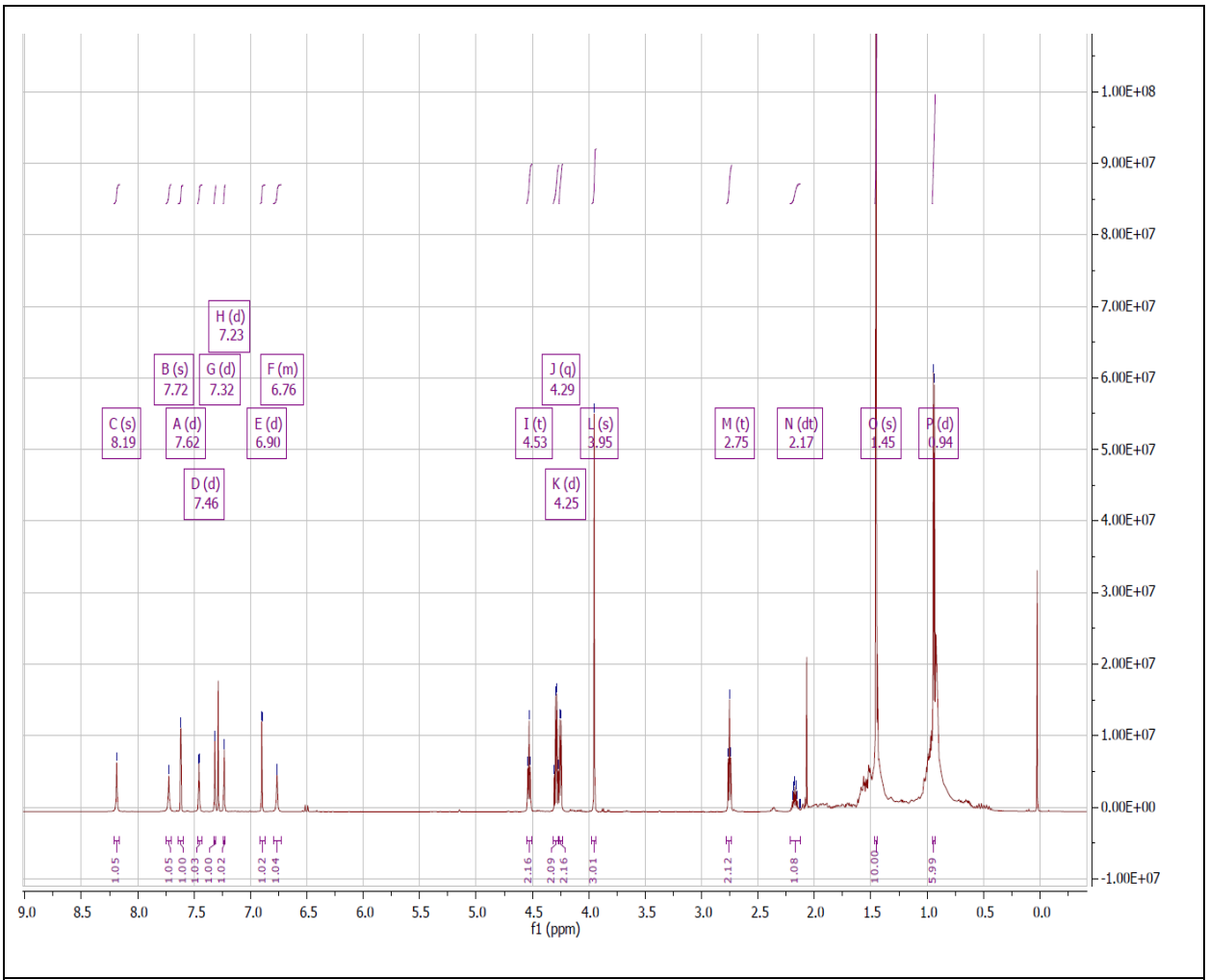

Figure S. ^{1}H of N-tert butyl ADH-111

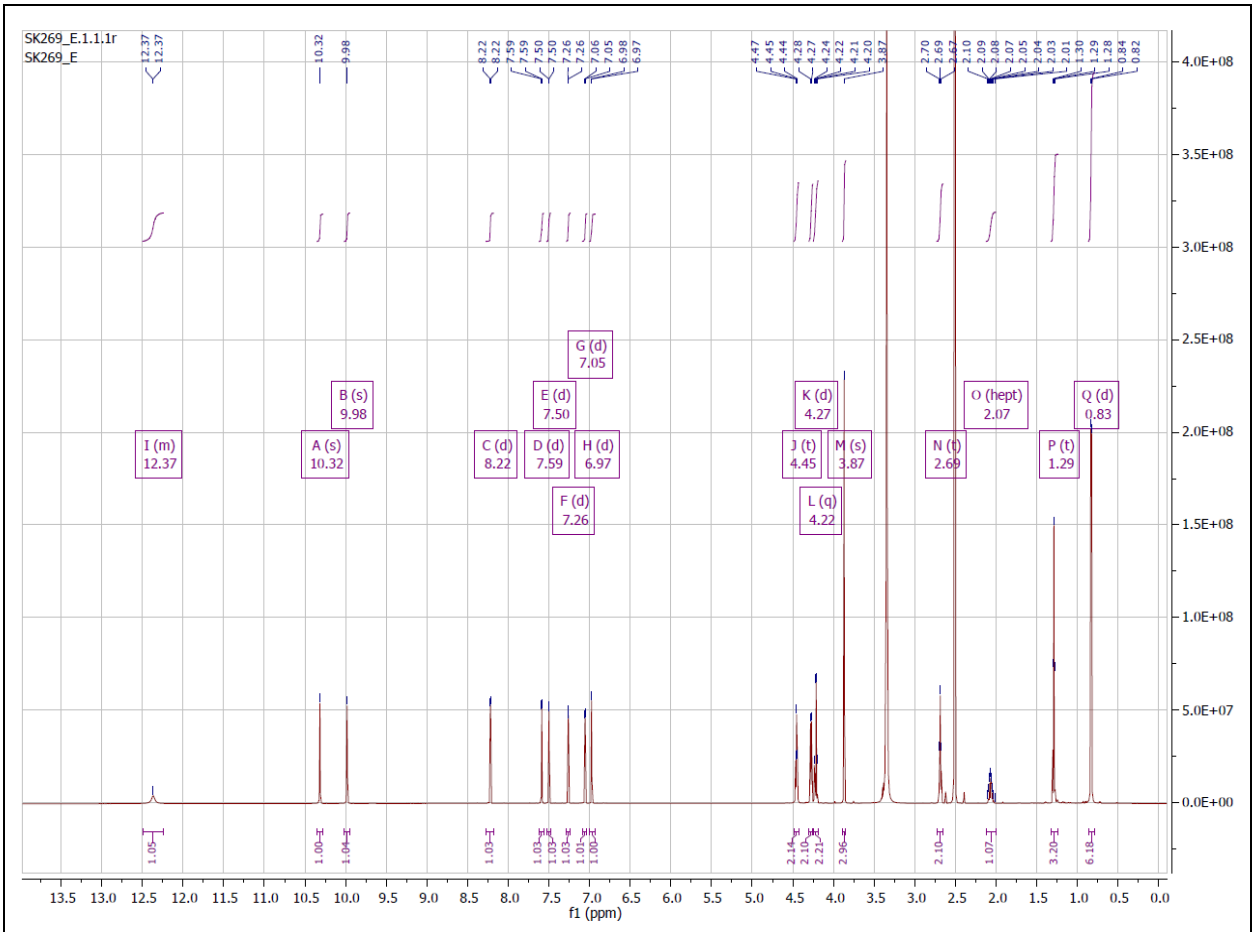

Figure S. ^{1}H of ADH-111

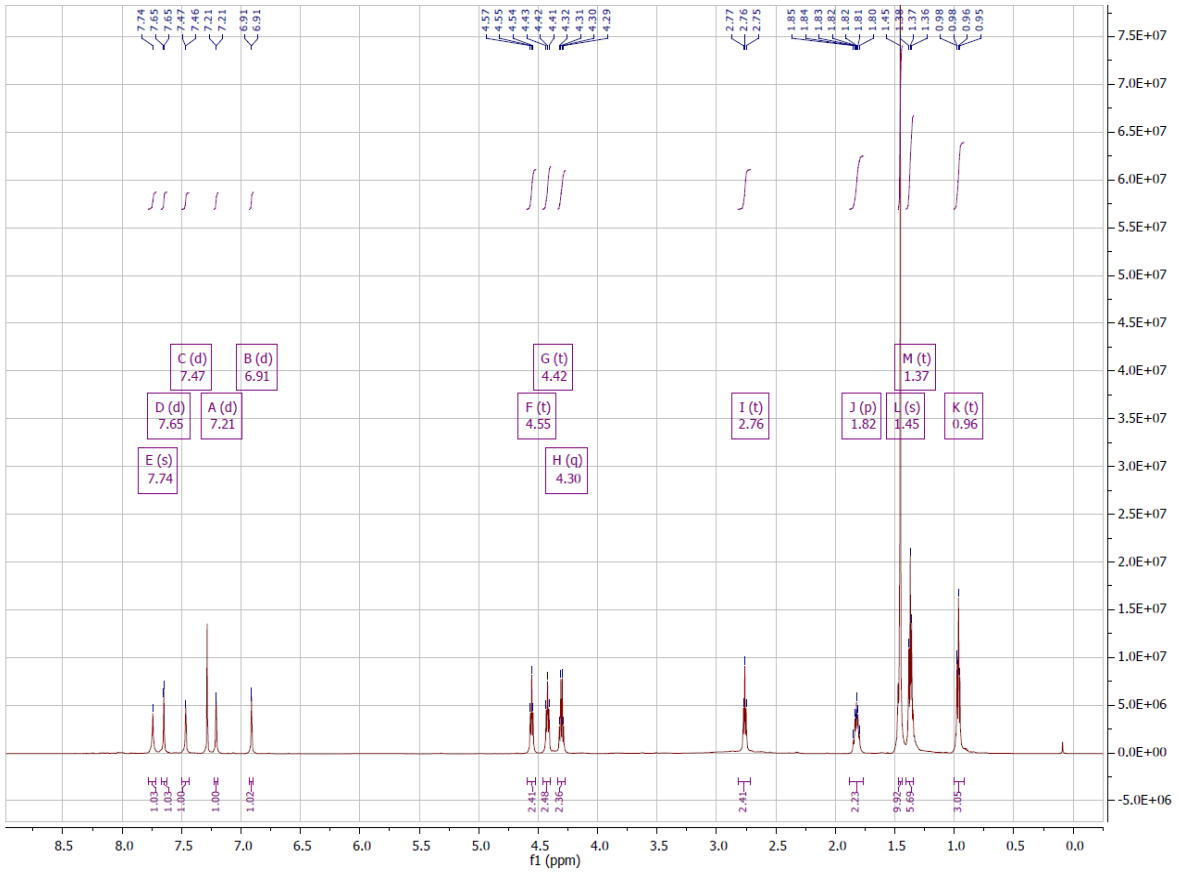

Figure S. ^{1}H of N-tert butyl ADH-112

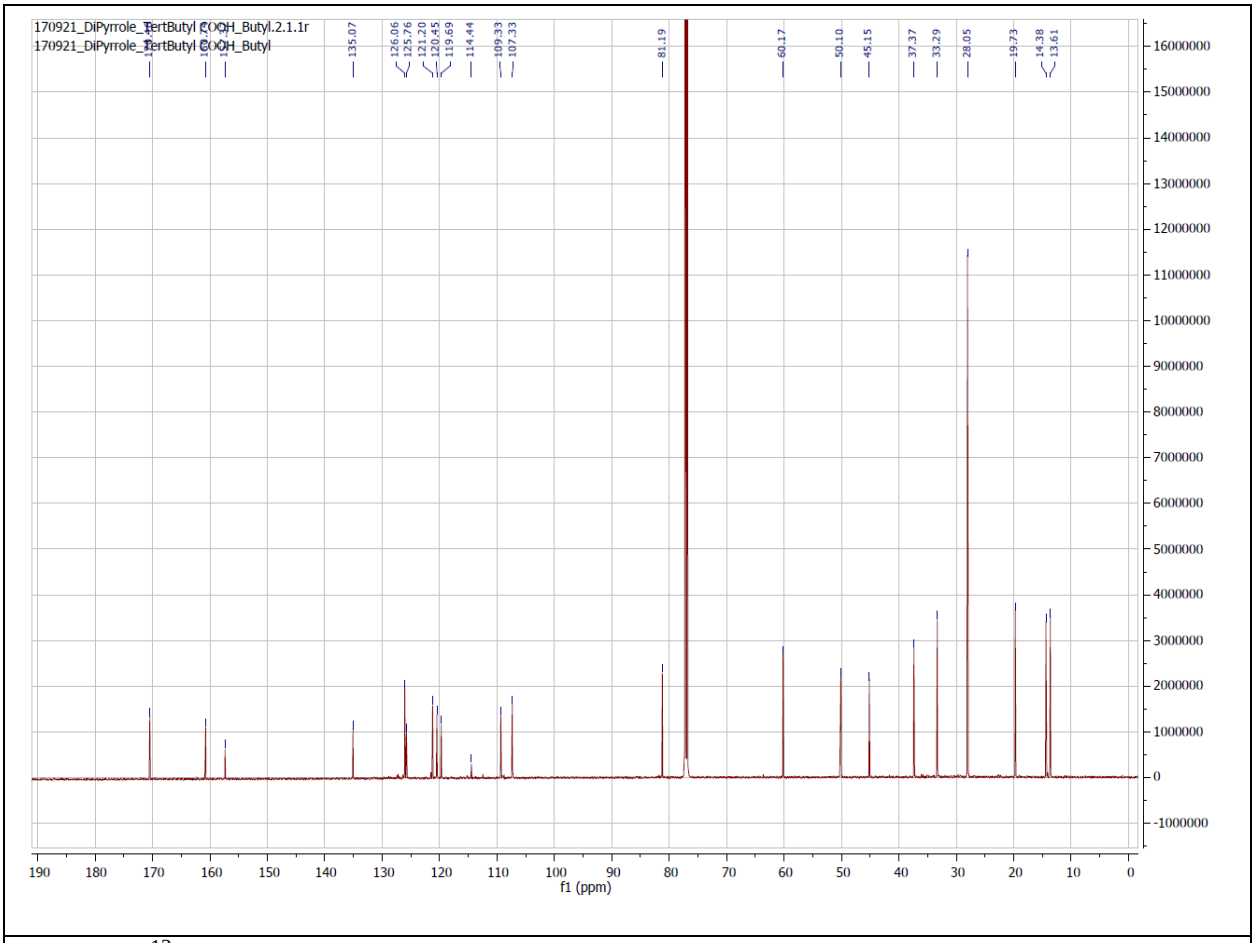

Figure S. ^{13}C of N-tert butyl ADH-112

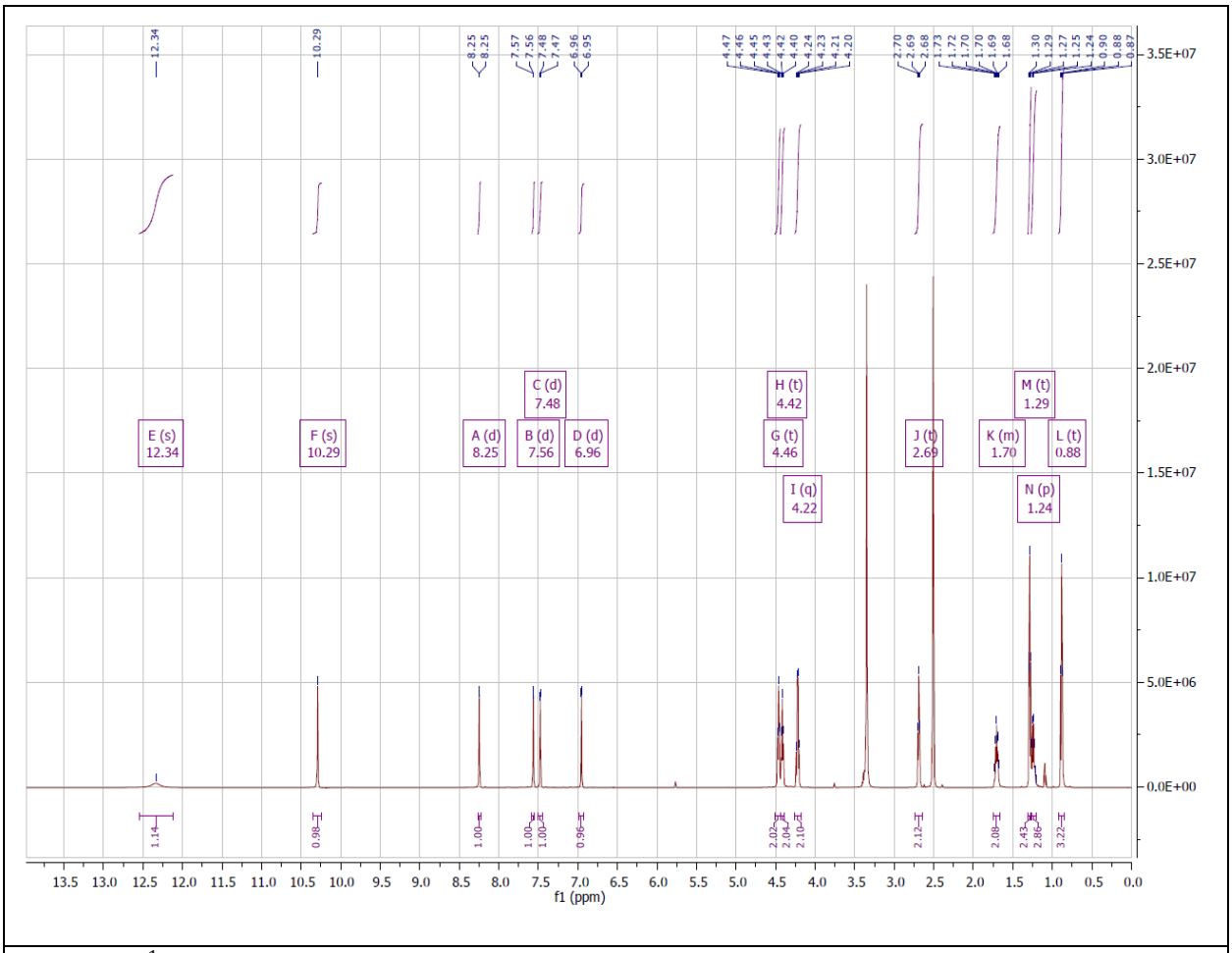

Figure S. ^{1}H of ADH-112

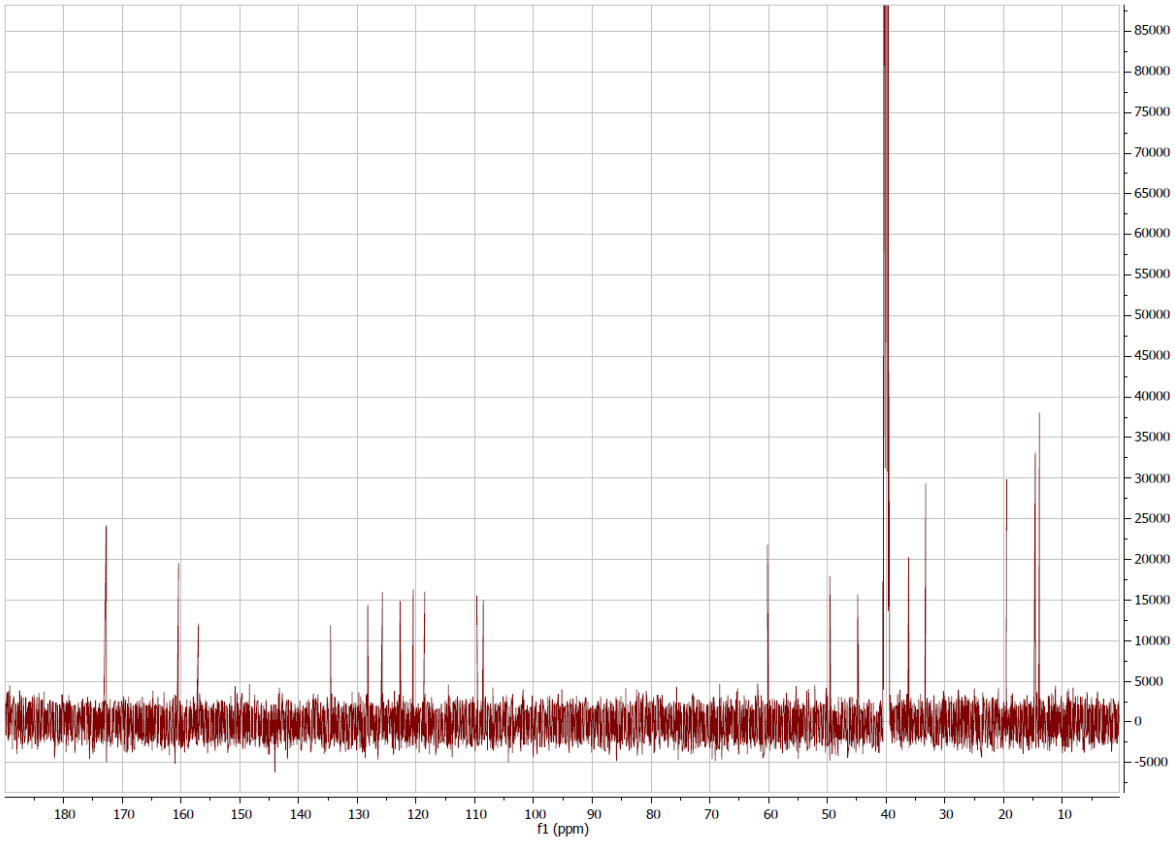

Figure S. ^{13}C of ADH-112

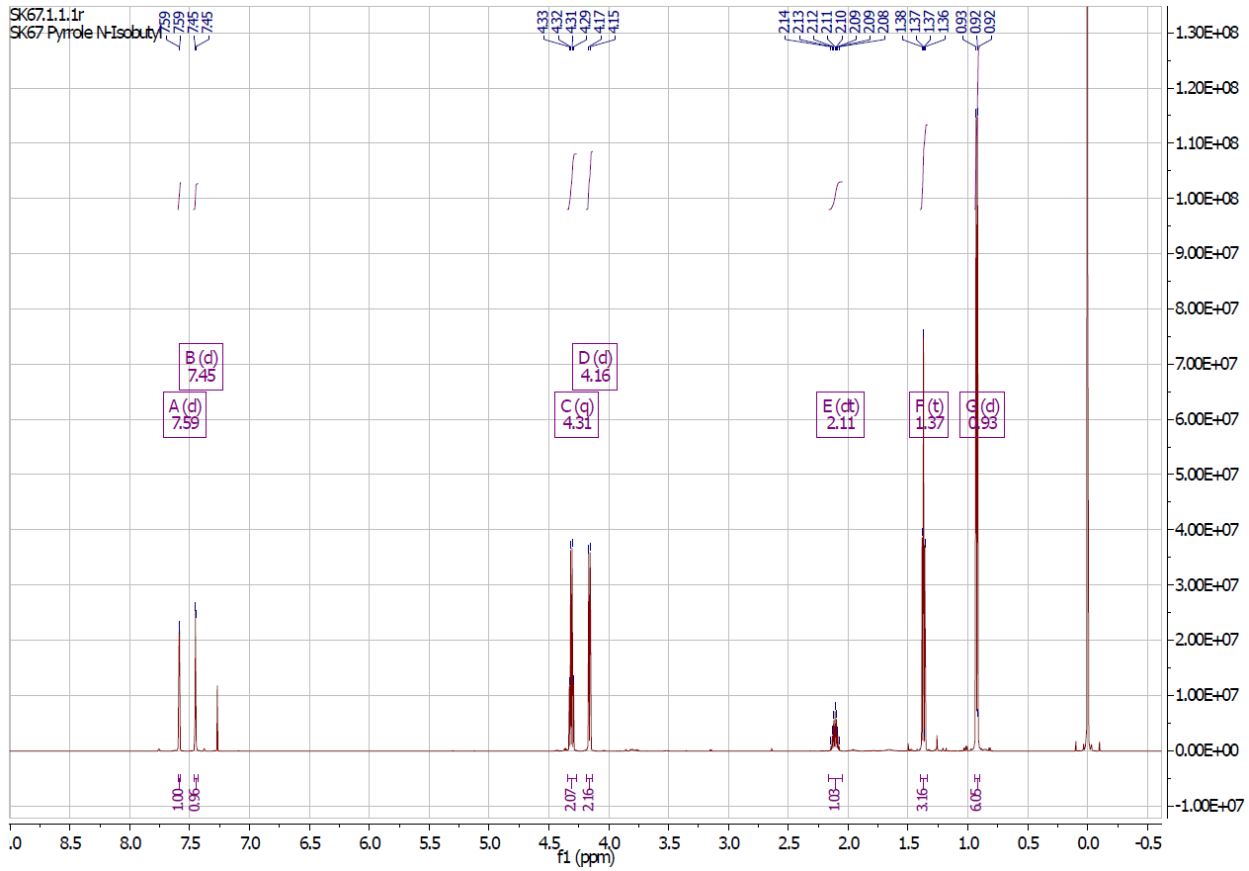

Figure S. ^{1}H of ADH-113

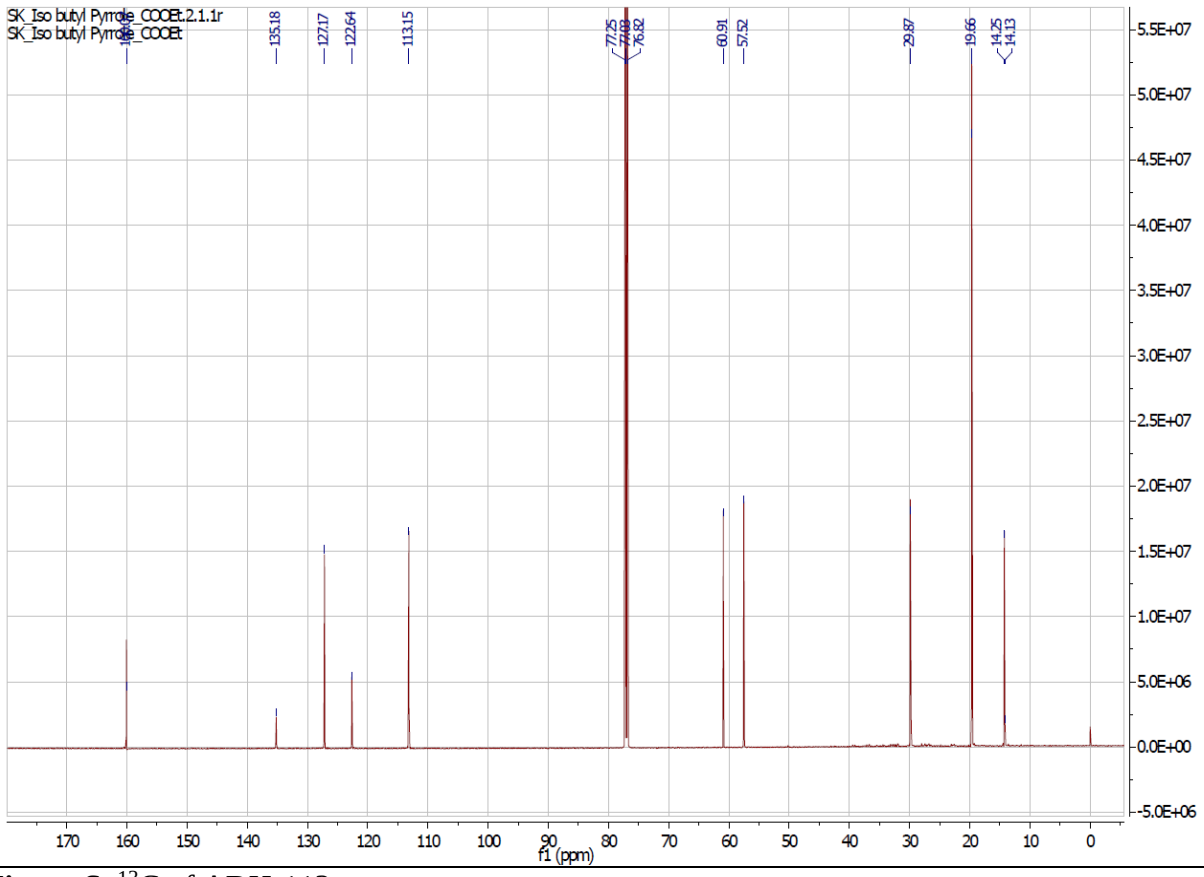

Figure S. ^{13}C of ADH-113

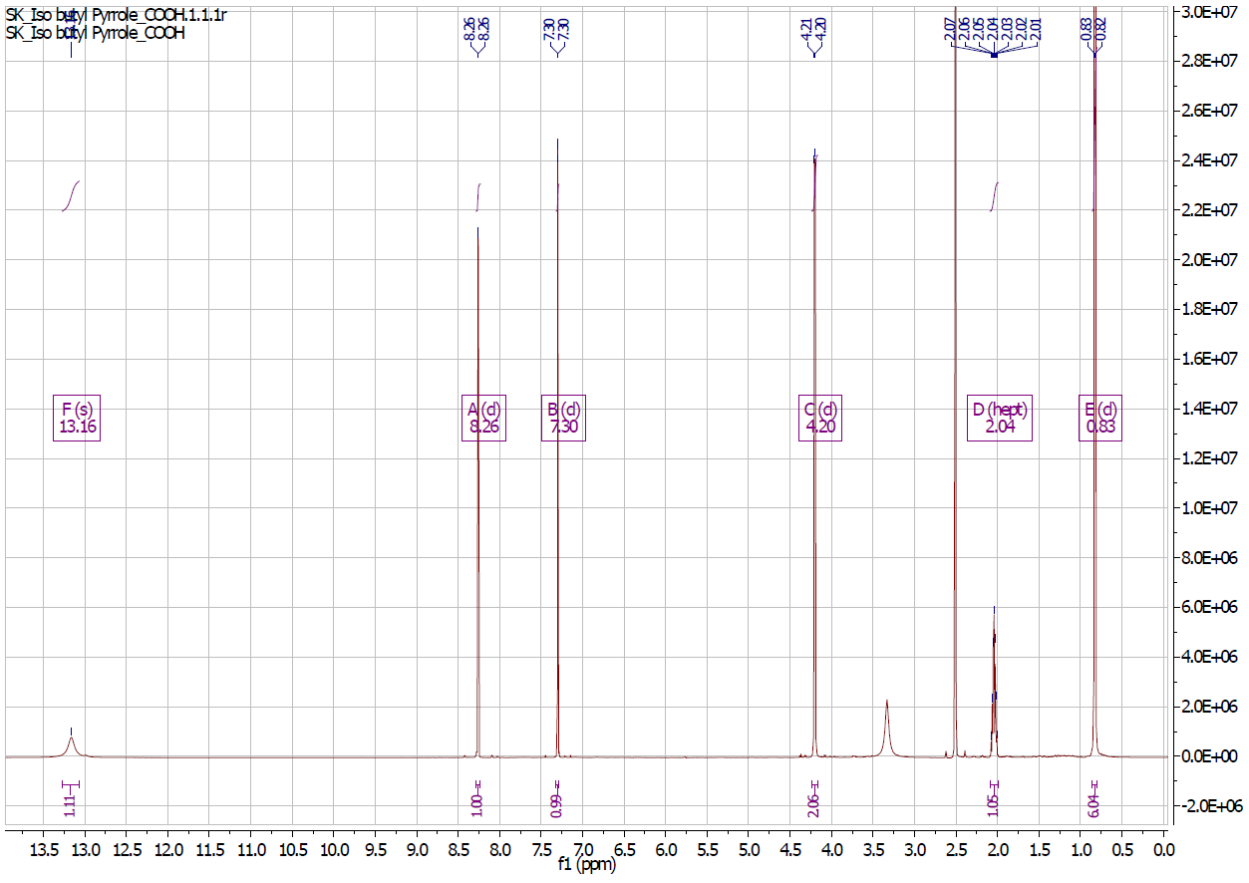

Figure S. ^{1}H of ADH-113_COOH

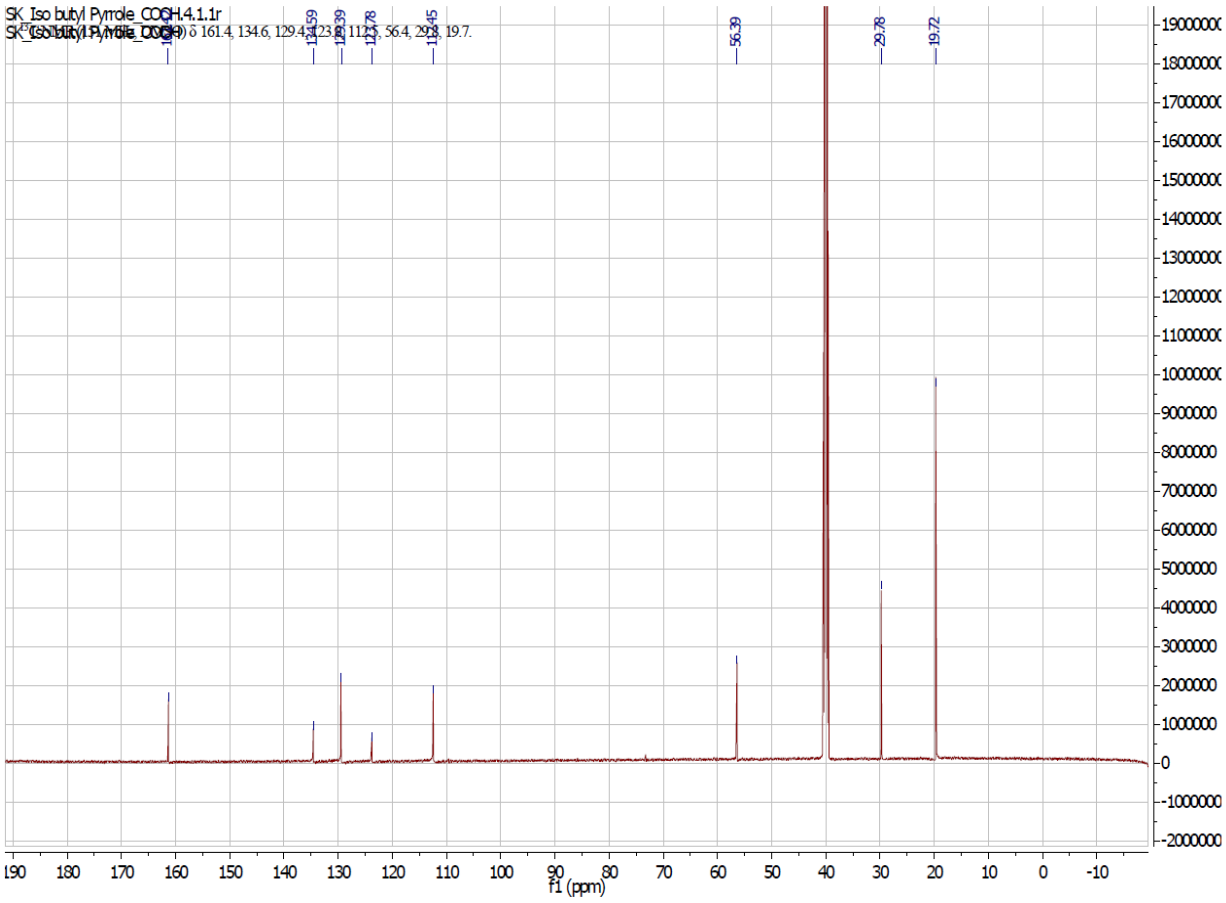

Figure S. ^{13}C of ADH-113_COOH

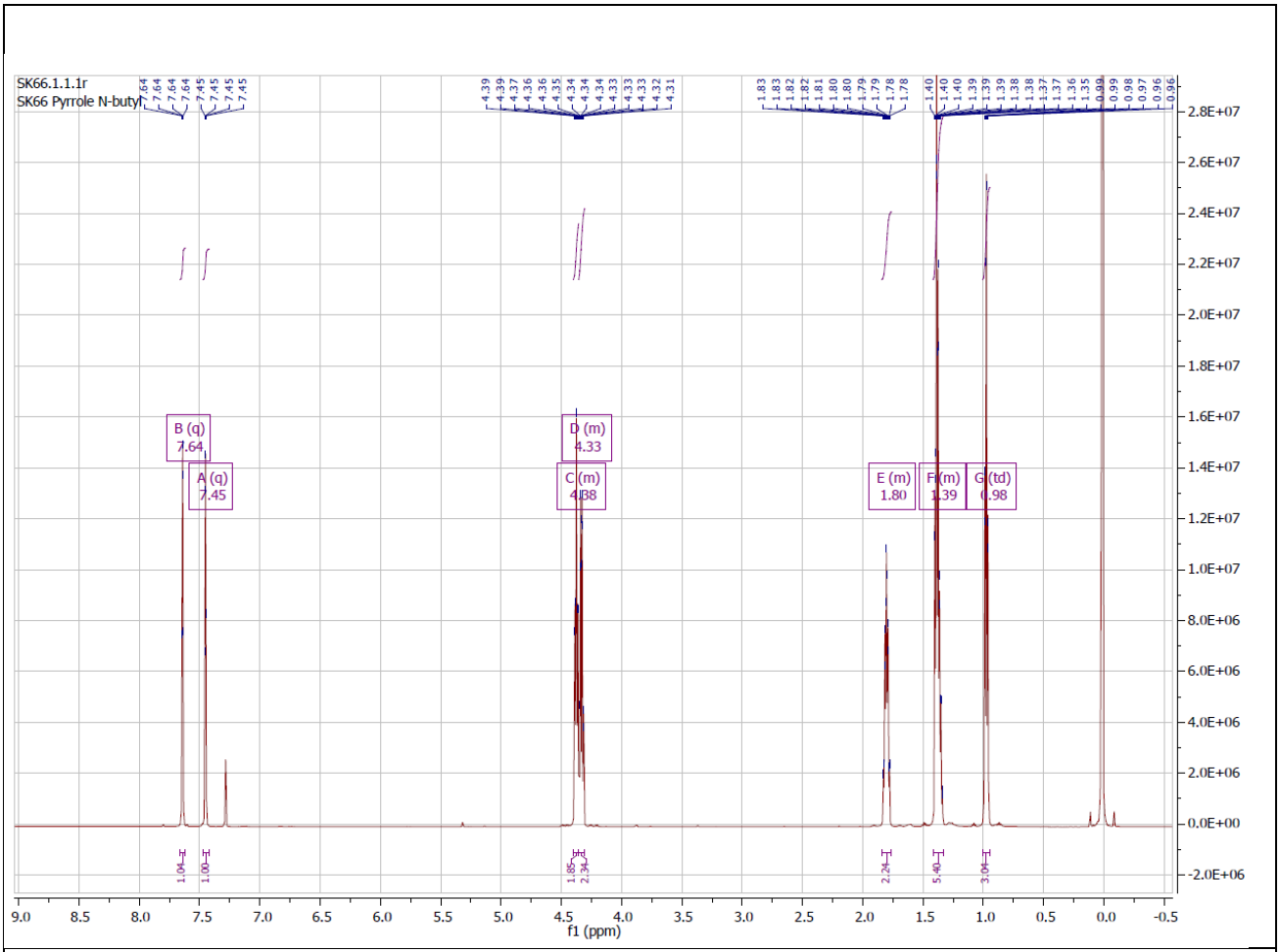

Figure S. ^{1}H of ADH-114

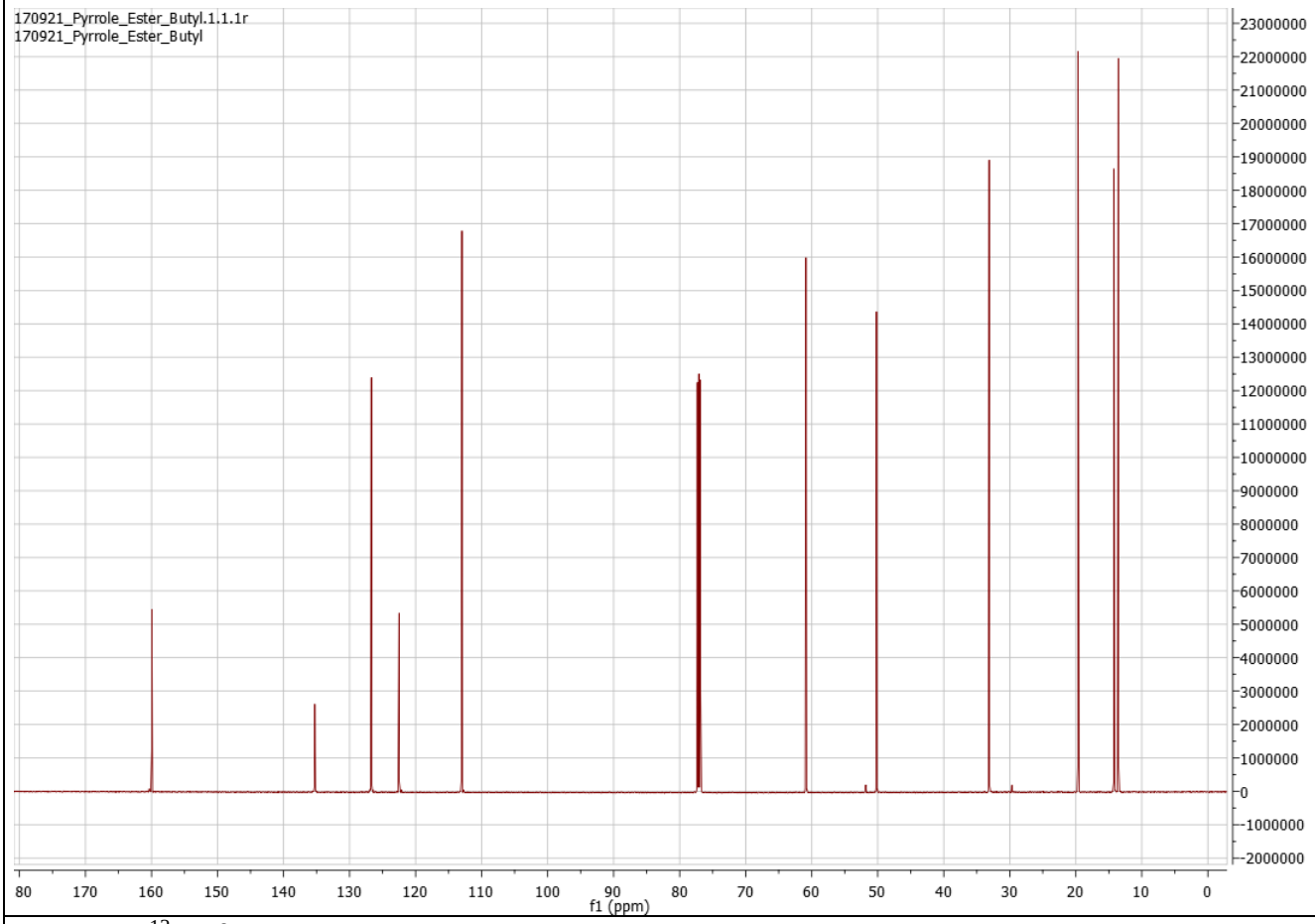

Figure S. ^{13}C of ADH-114

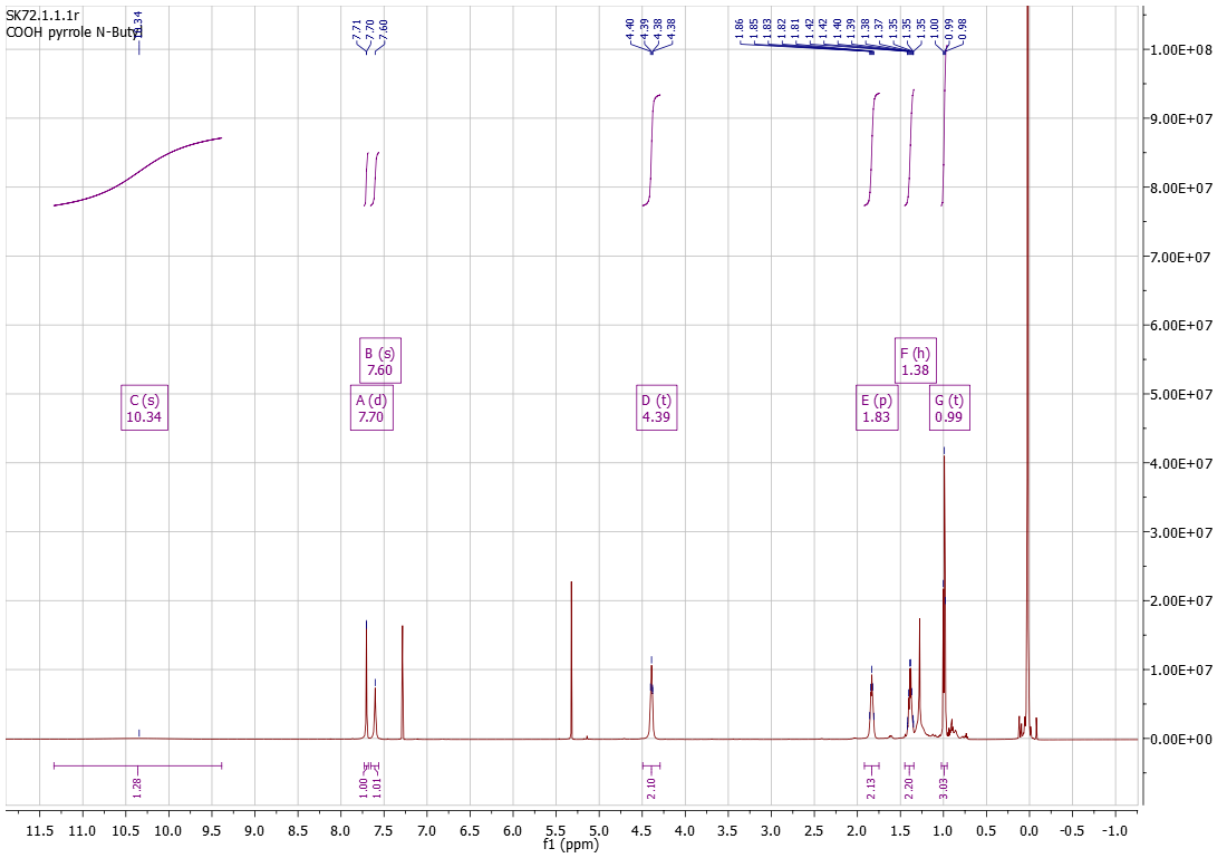

Figure S. ^{1}H of ADH-114_COOH

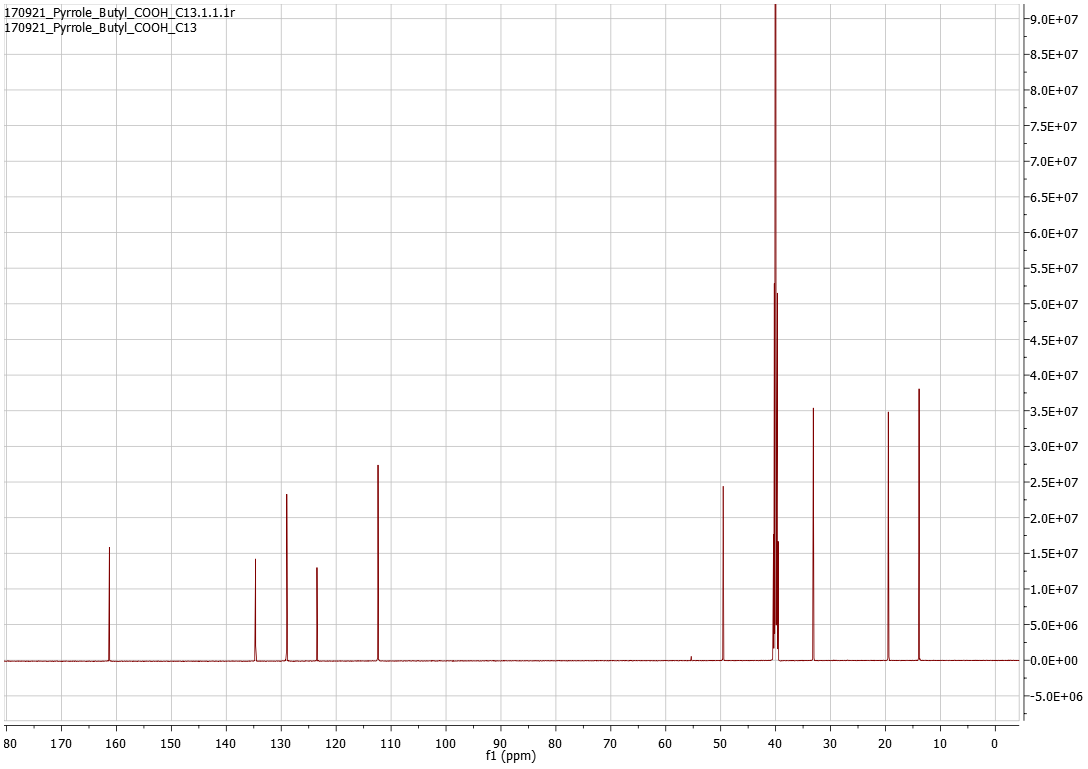

Figure S. ^{13}C of ADH-114_COOH

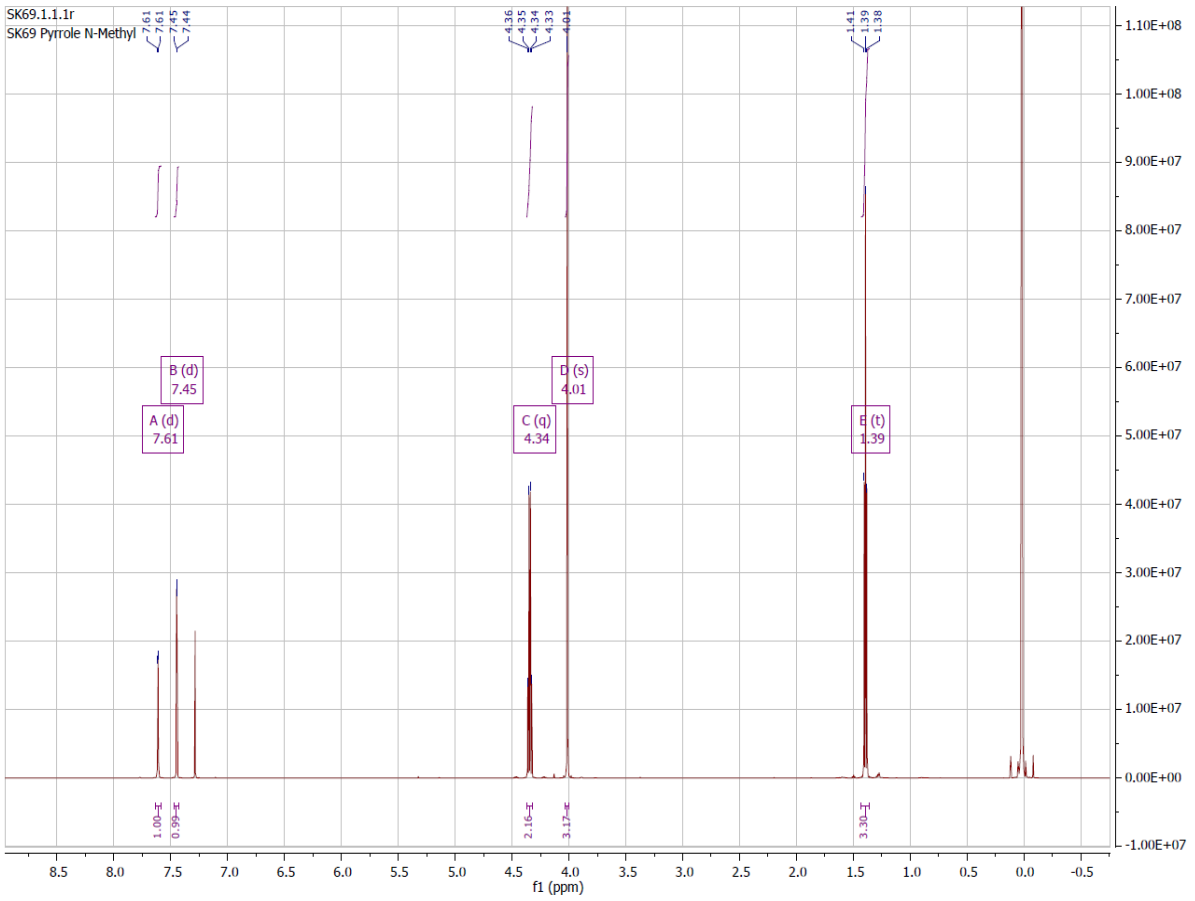

Figure S. ^{1}H of ADH-115

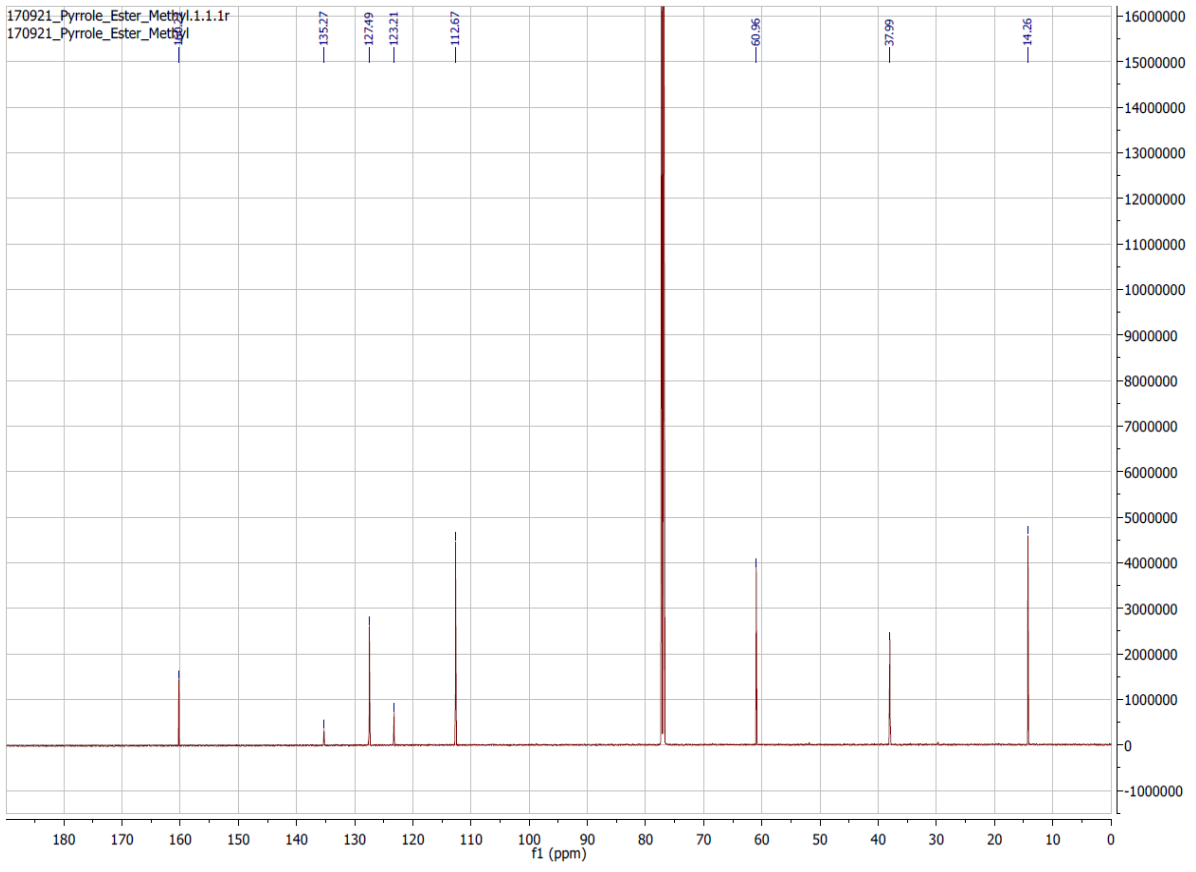

Figure S. ^{13}C of ADH-115

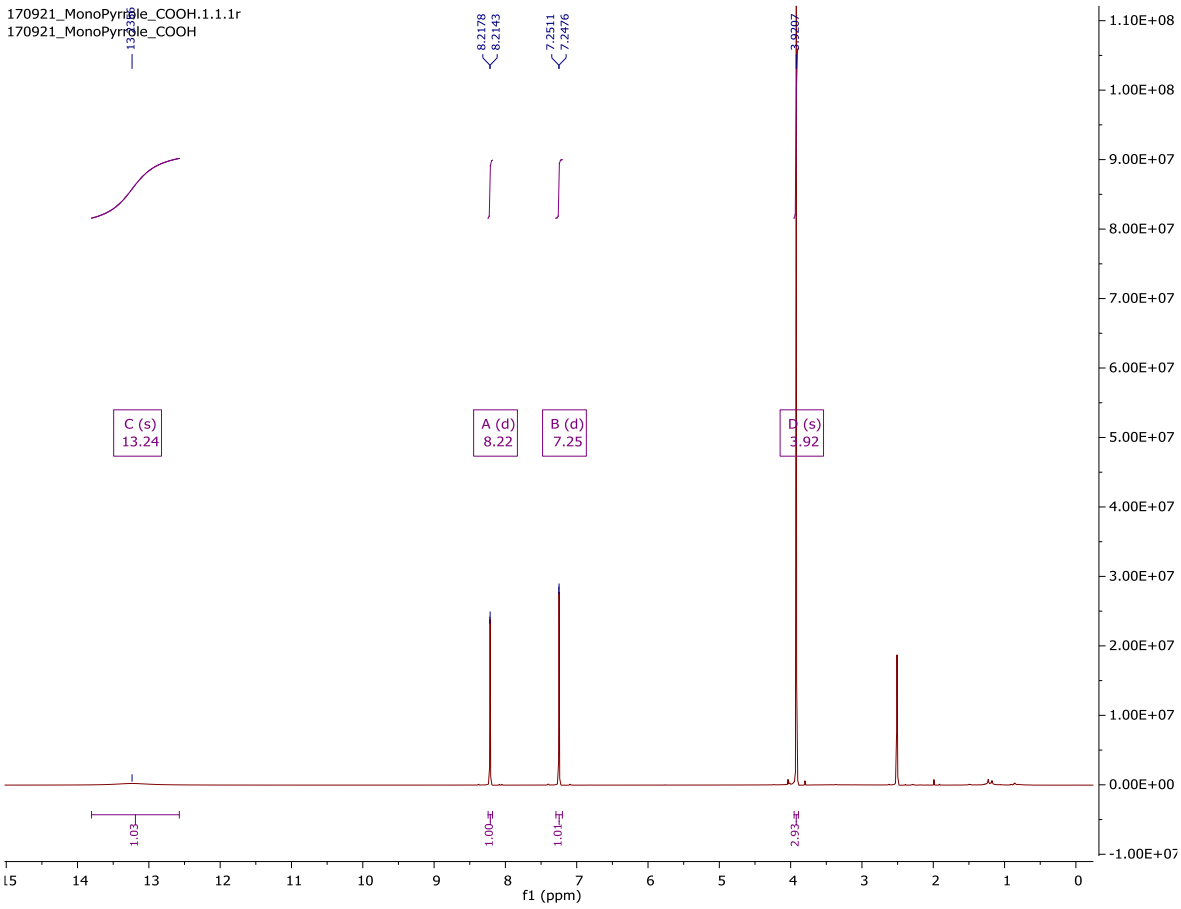

Figure S. ^{1}H of ADH-115_COOH

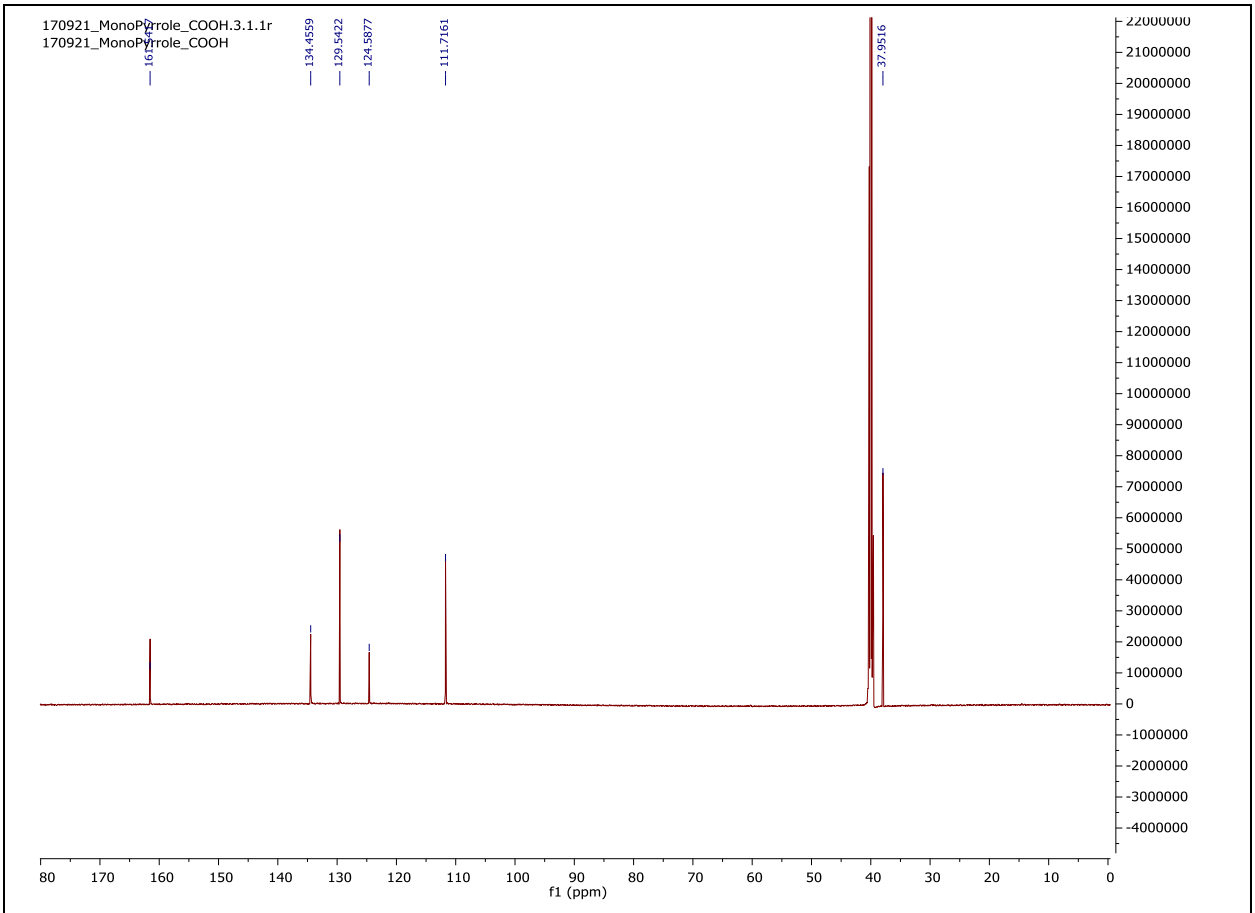

Figure S. ^{13}C of ADH-115_COOH

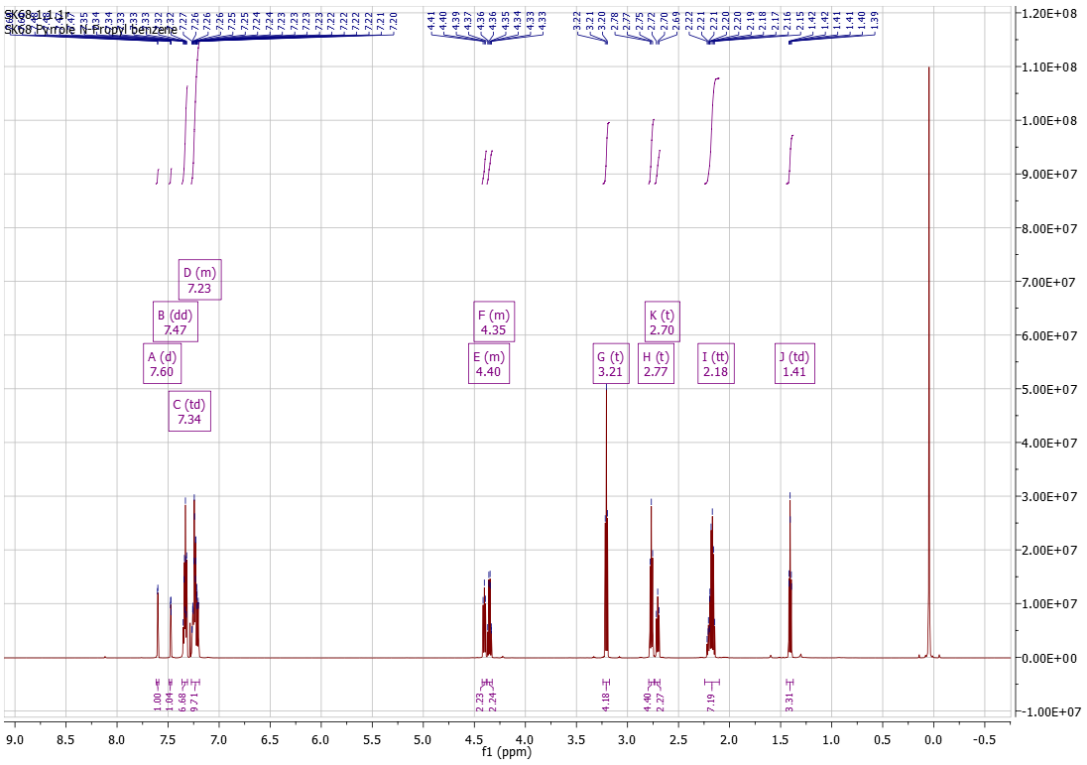

Figure S. ^{1}H of ADH-116

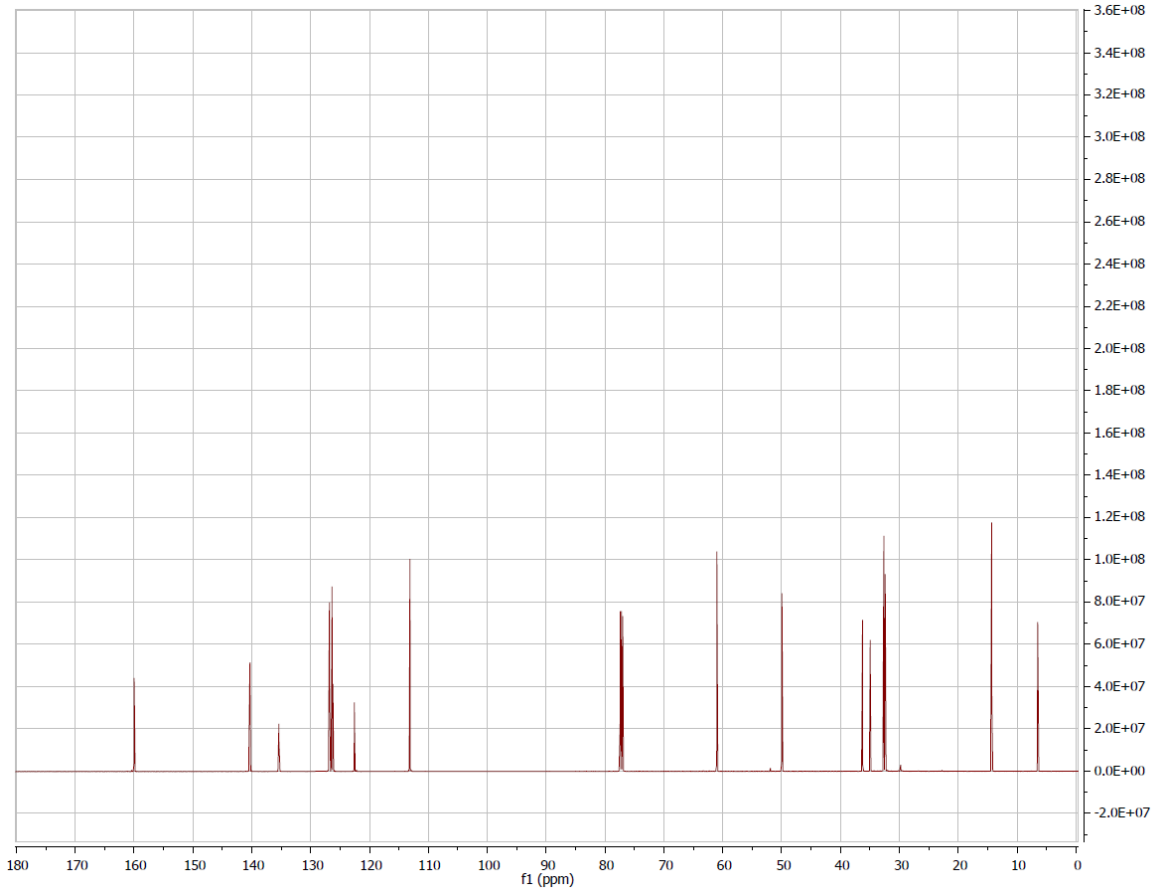

Figure S. ^{13}C of ADH-116

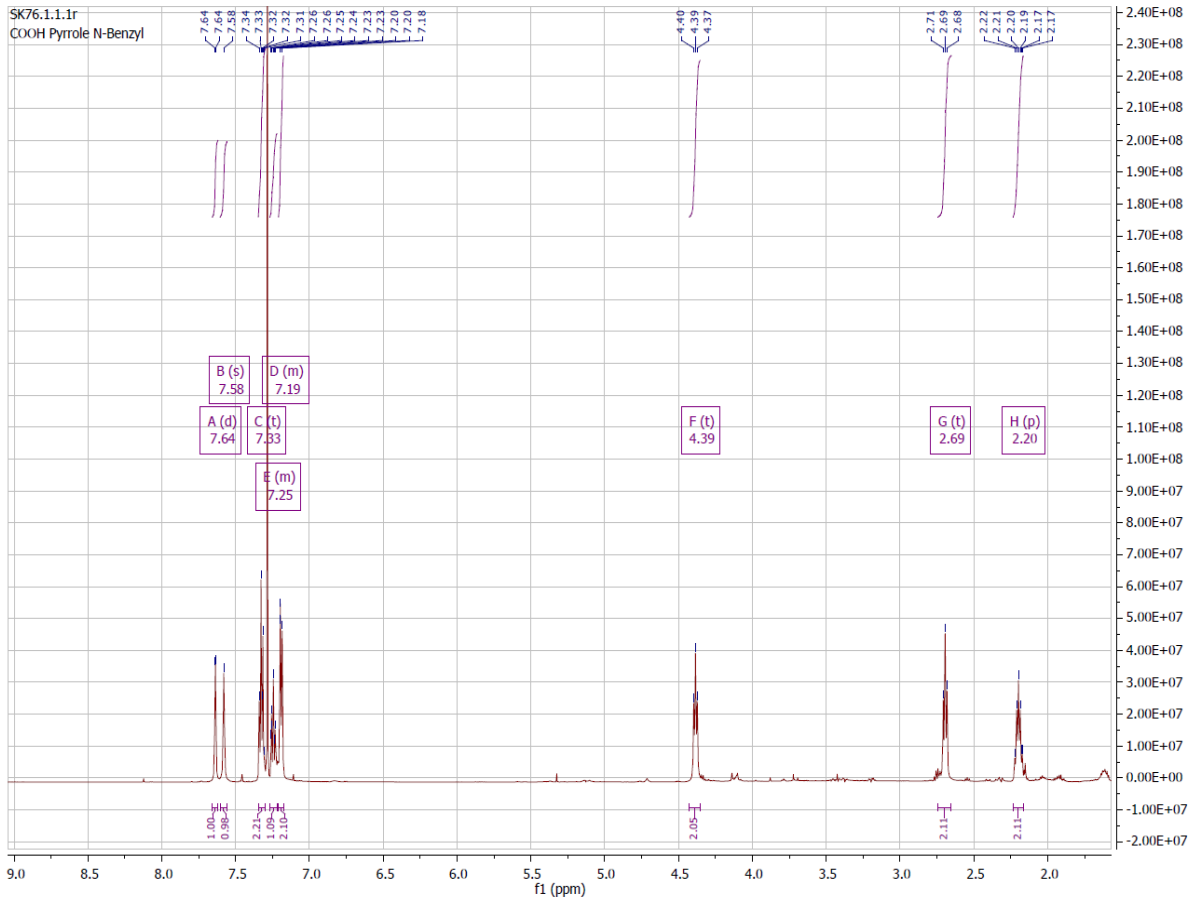

Figure S. ^{1}H of ADH-116_COOH

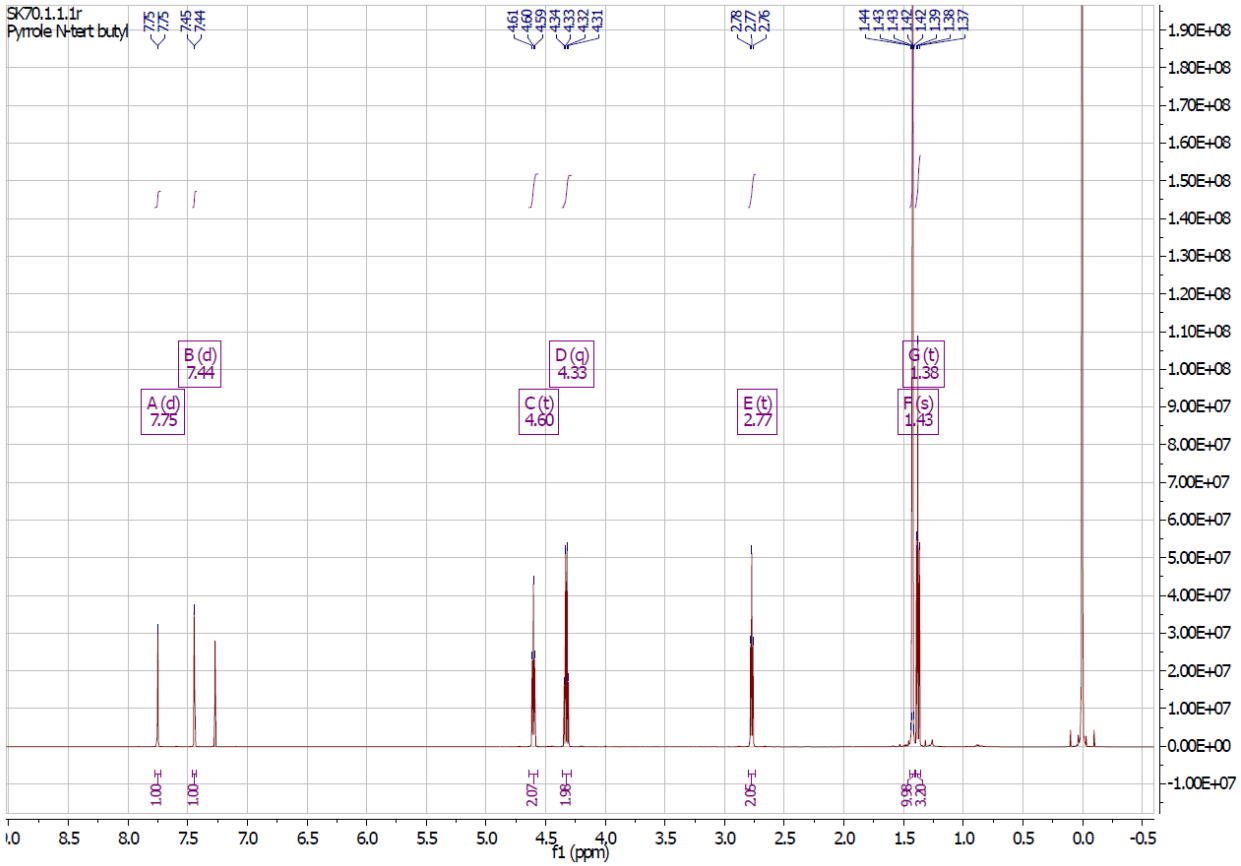

Figure S. ^{1}H of tert butyl ADH-117

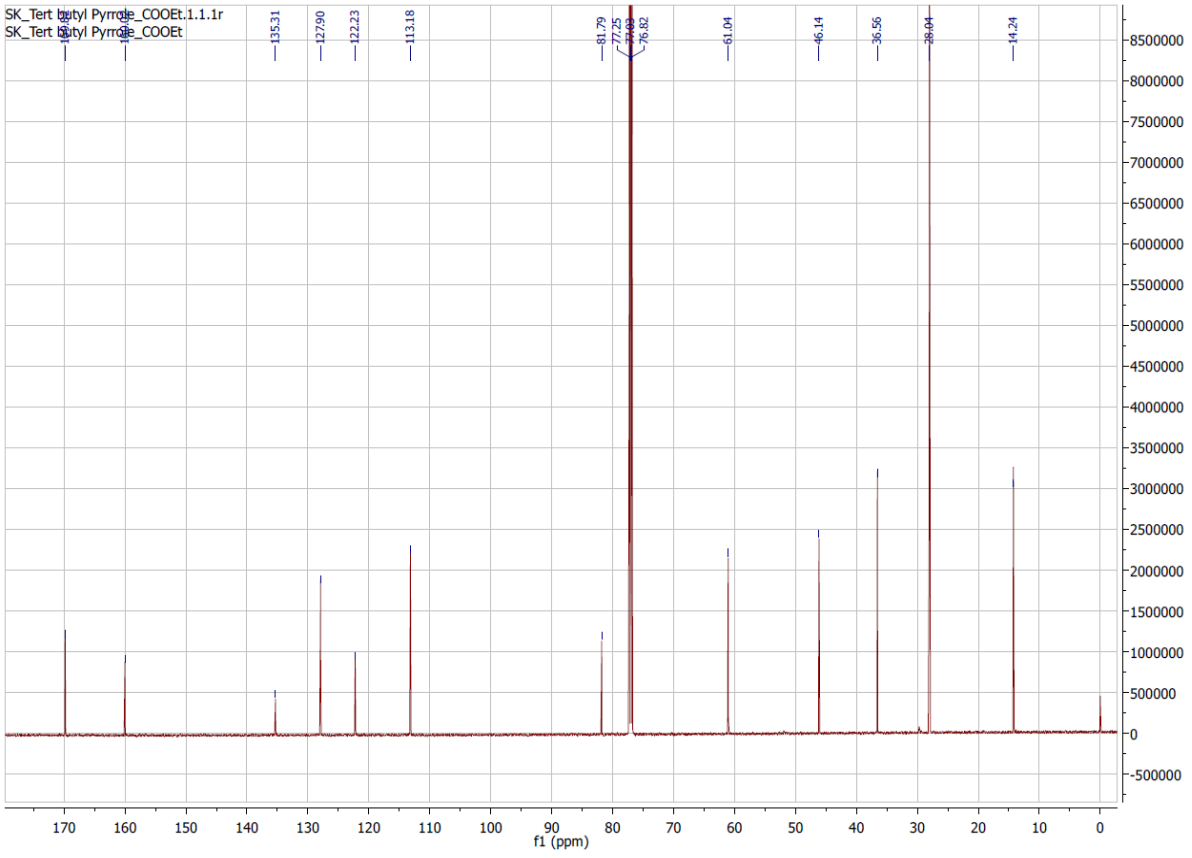

Figure S. ^{13}C of tert butyl ADH-117

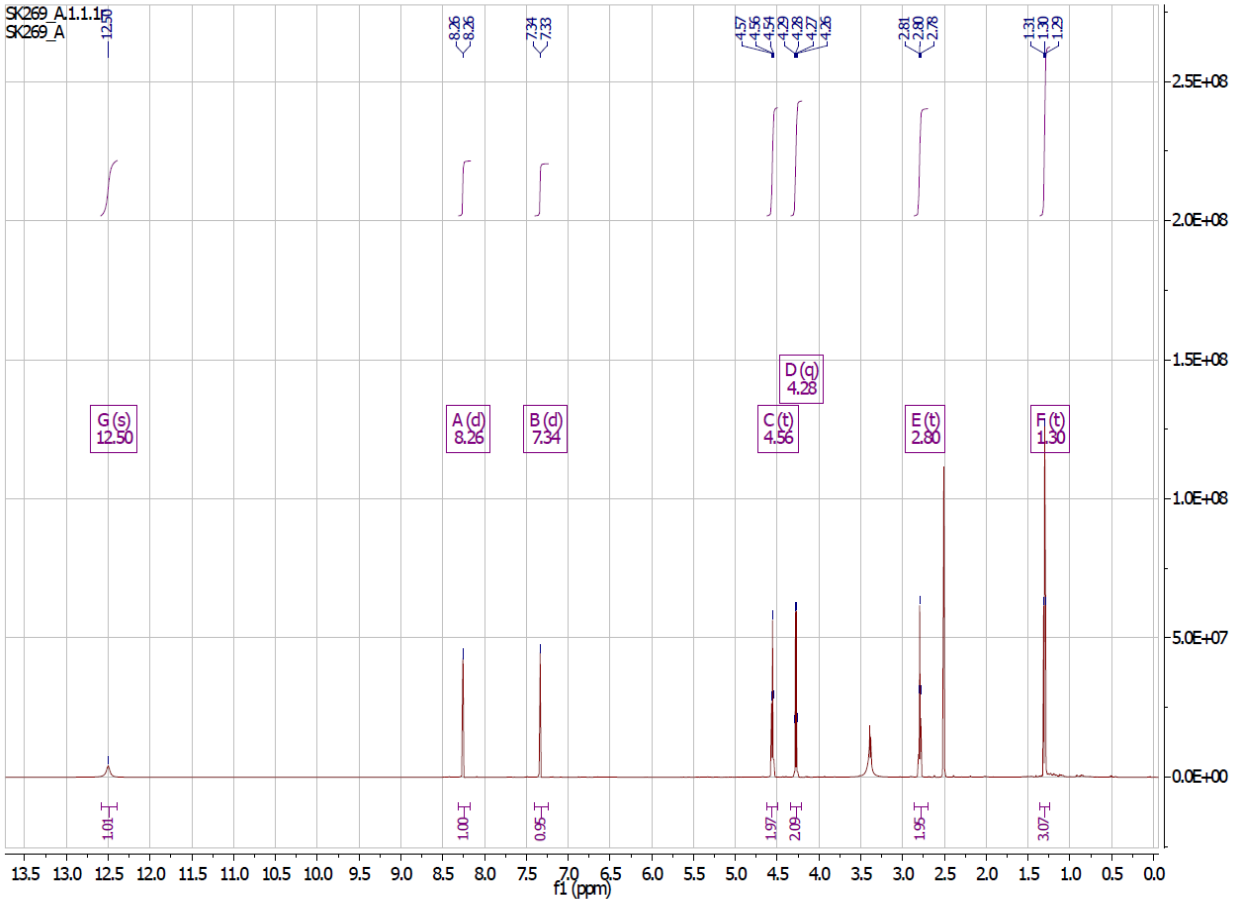

Figure S. ^{1}H of ADH-117

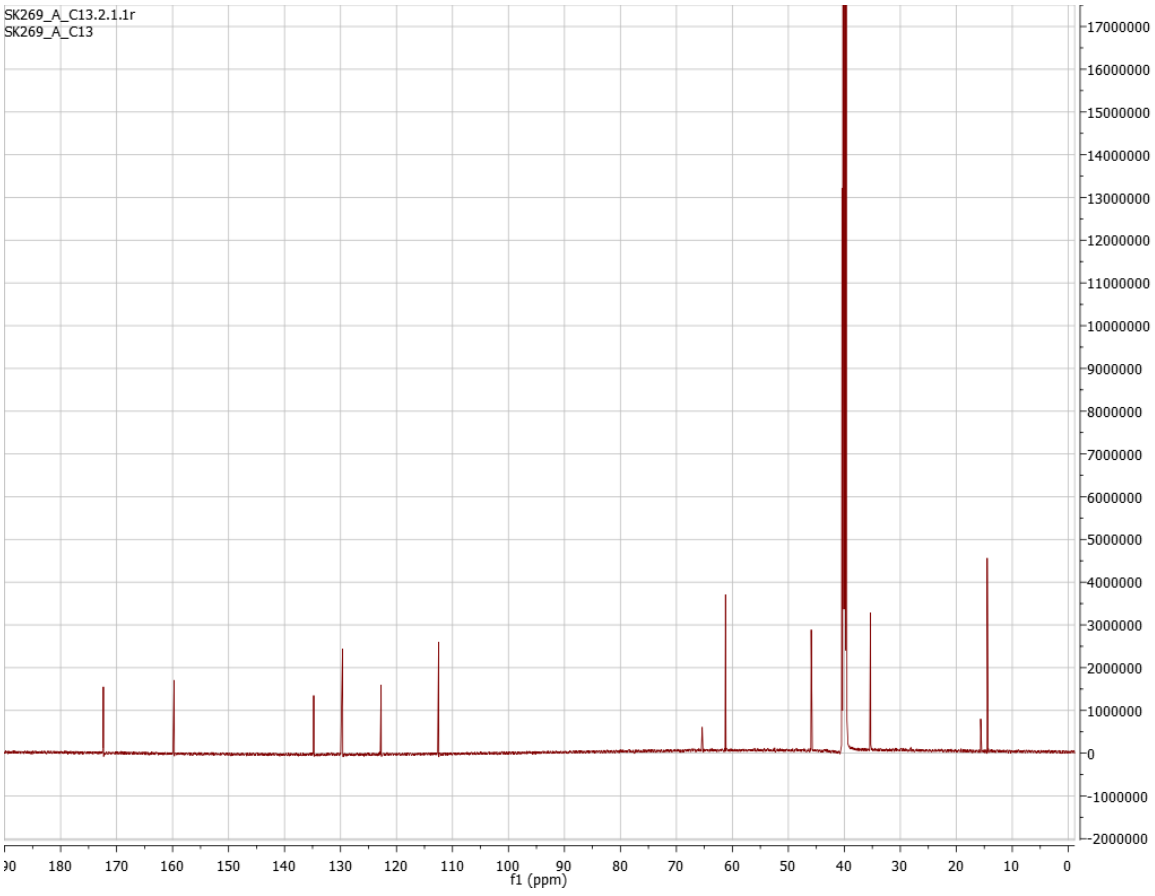

Figure S. ^{13}C of ADH-117

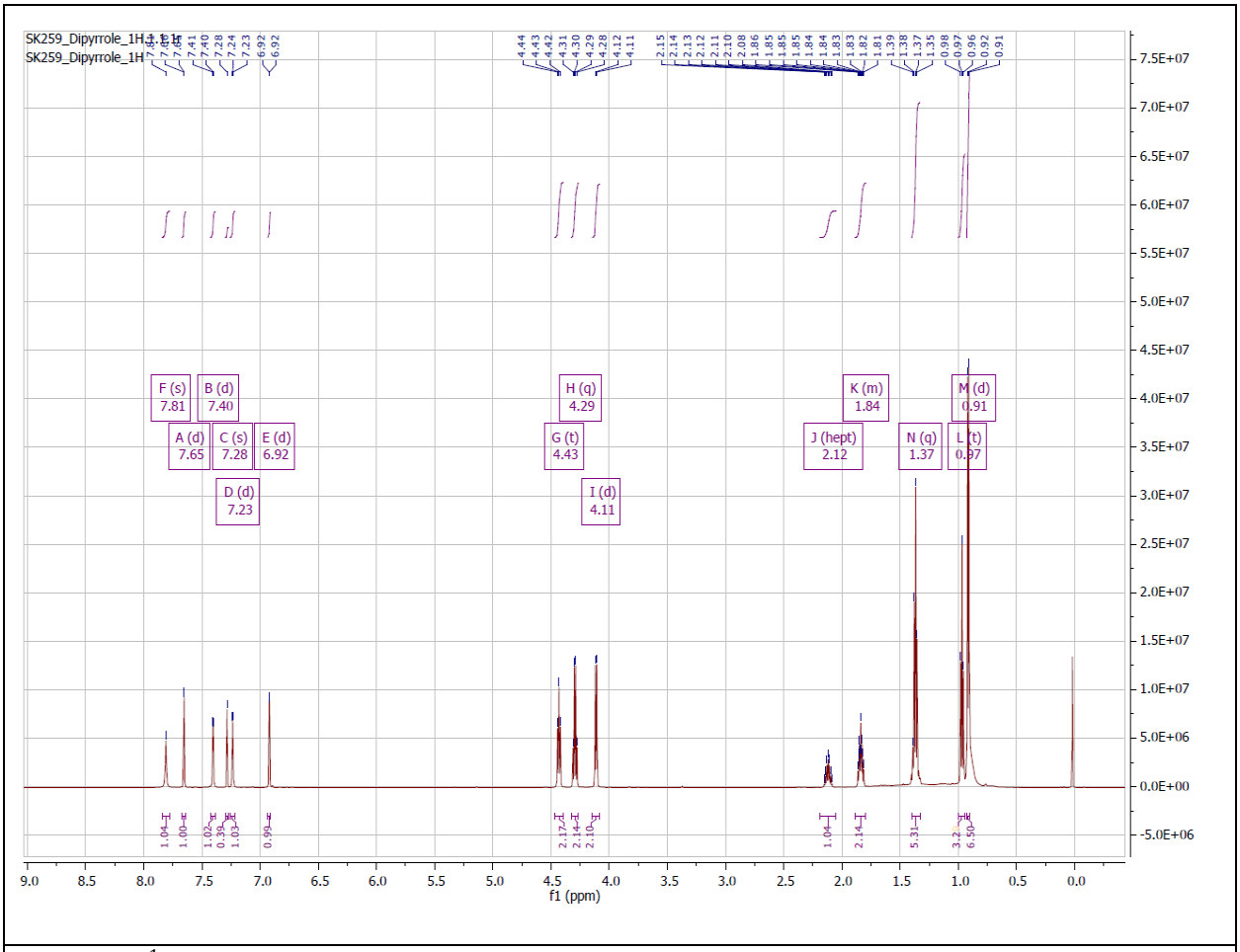

Figure S. ^{1}H of ADH-118

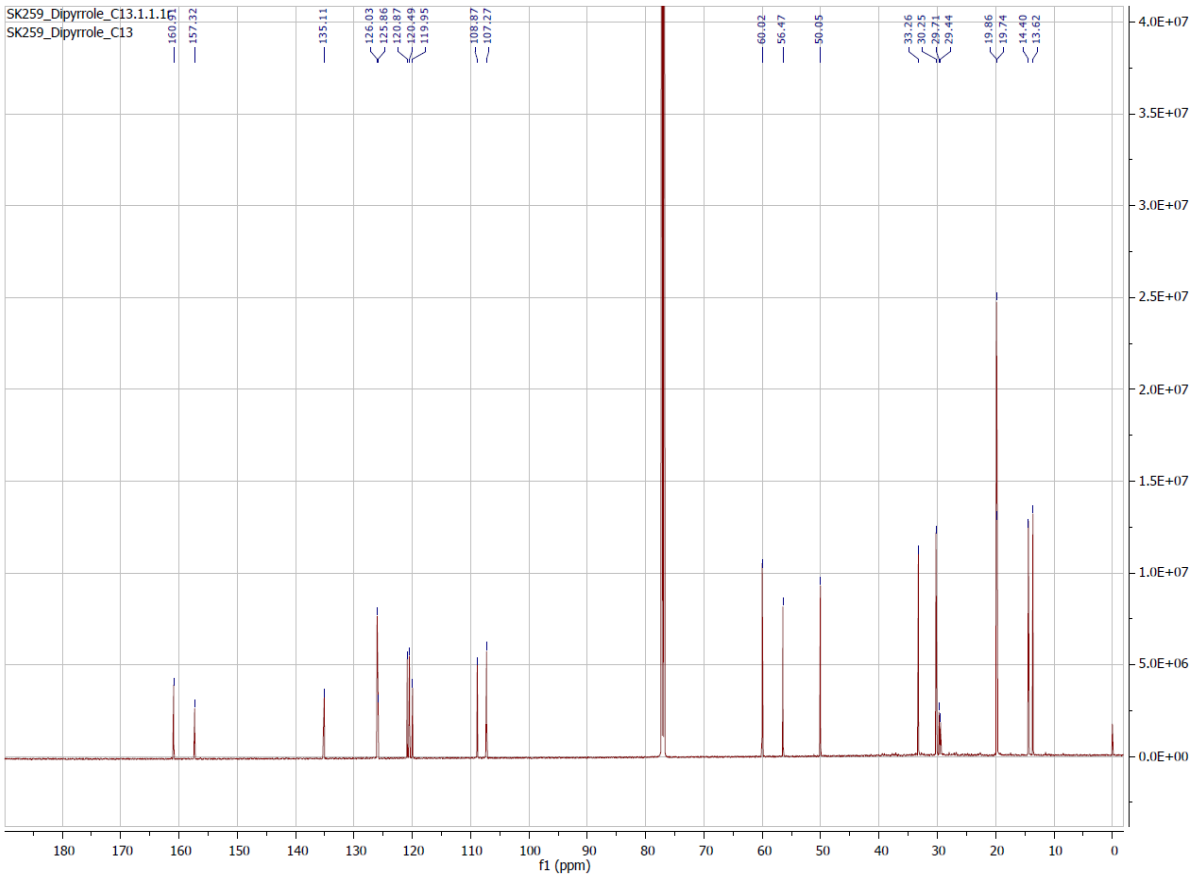

Figure S. ^{13}C of ADH-118

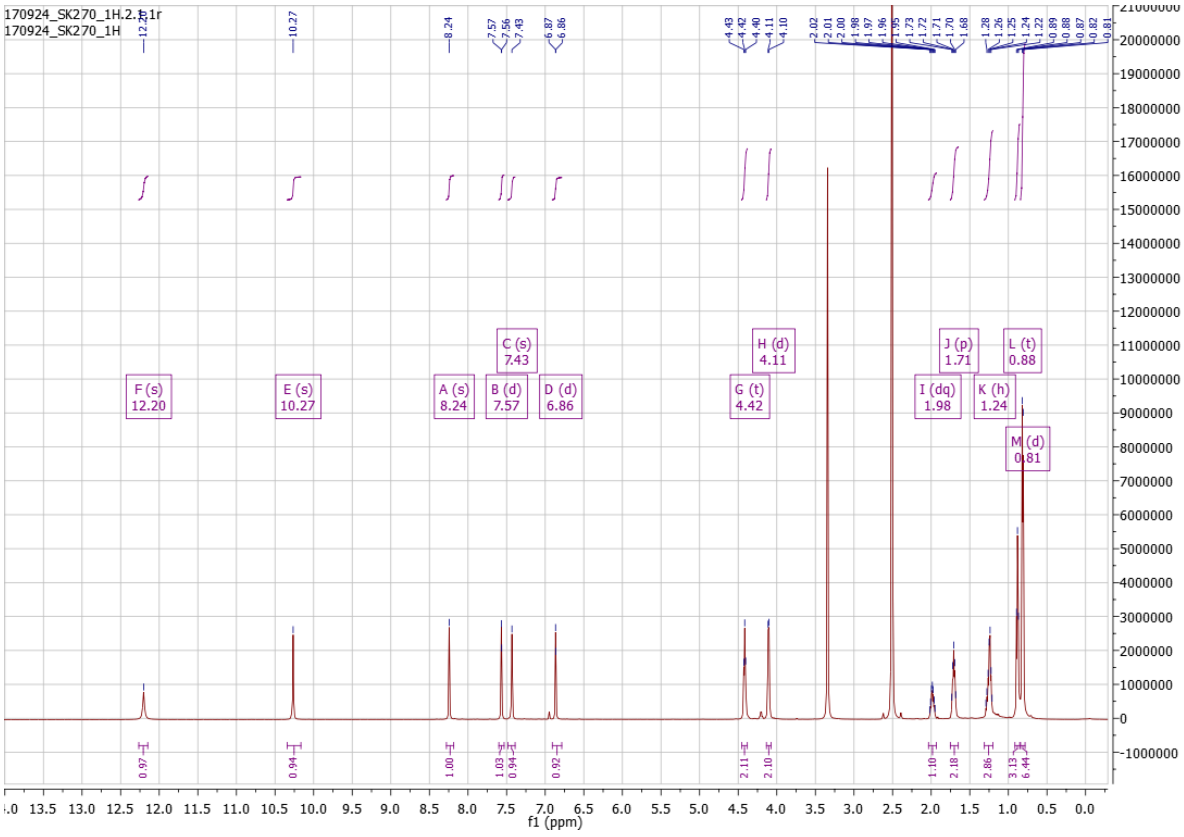

Figure S. ^{1}H of ADH-118_COOH

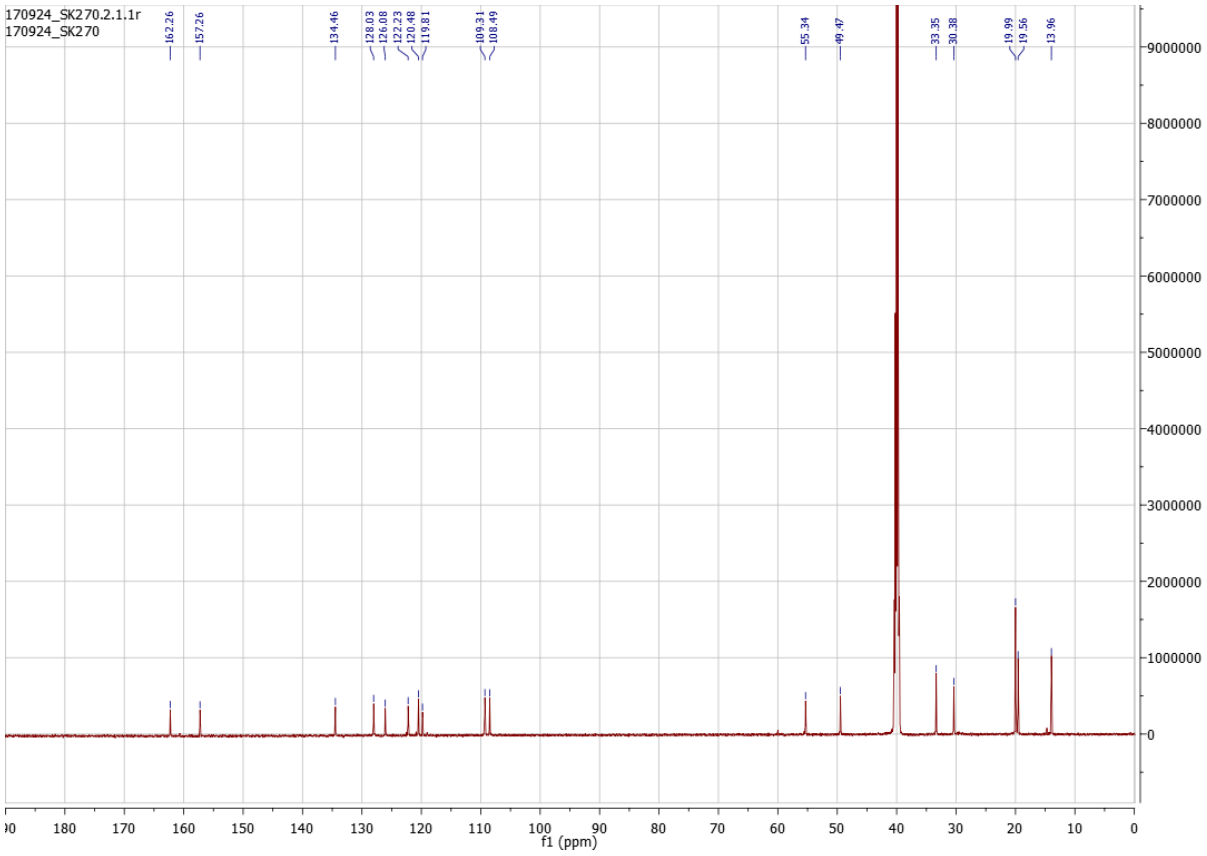

Figure S. ^{13}C of ADH-118_COOH

Figure S. ^{1}H of ADH-119

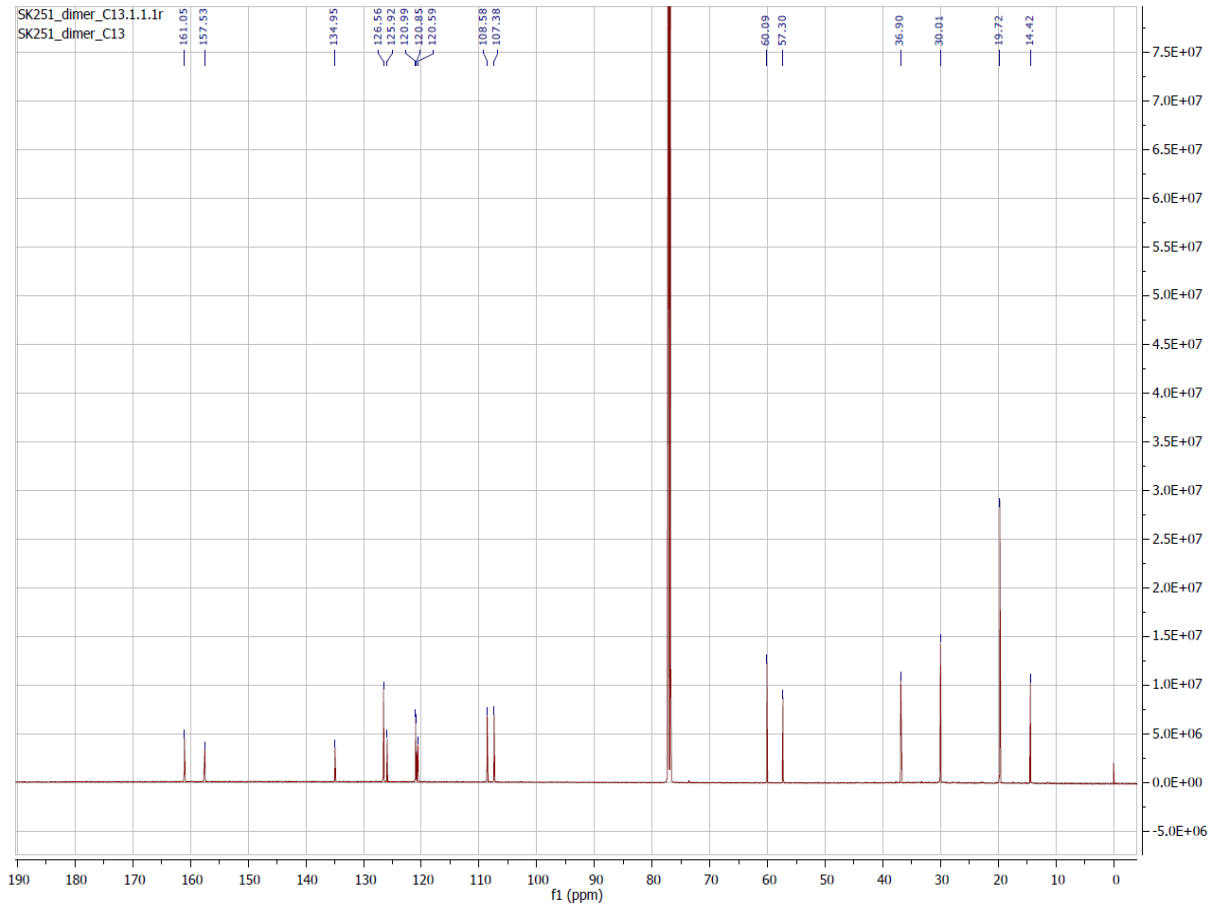

Figure S. ^{13}C of ADH-119

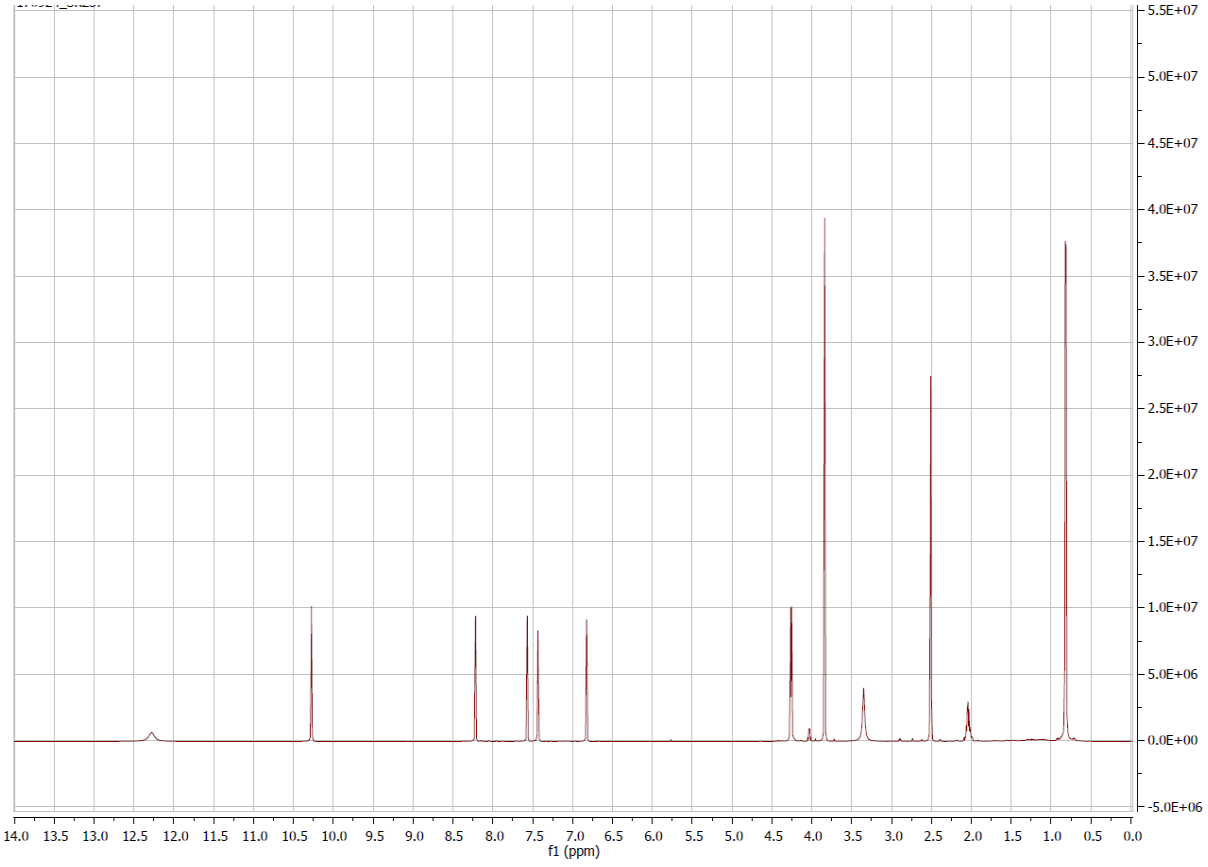

Figure S. ^{1}H of ADH-119_COOH

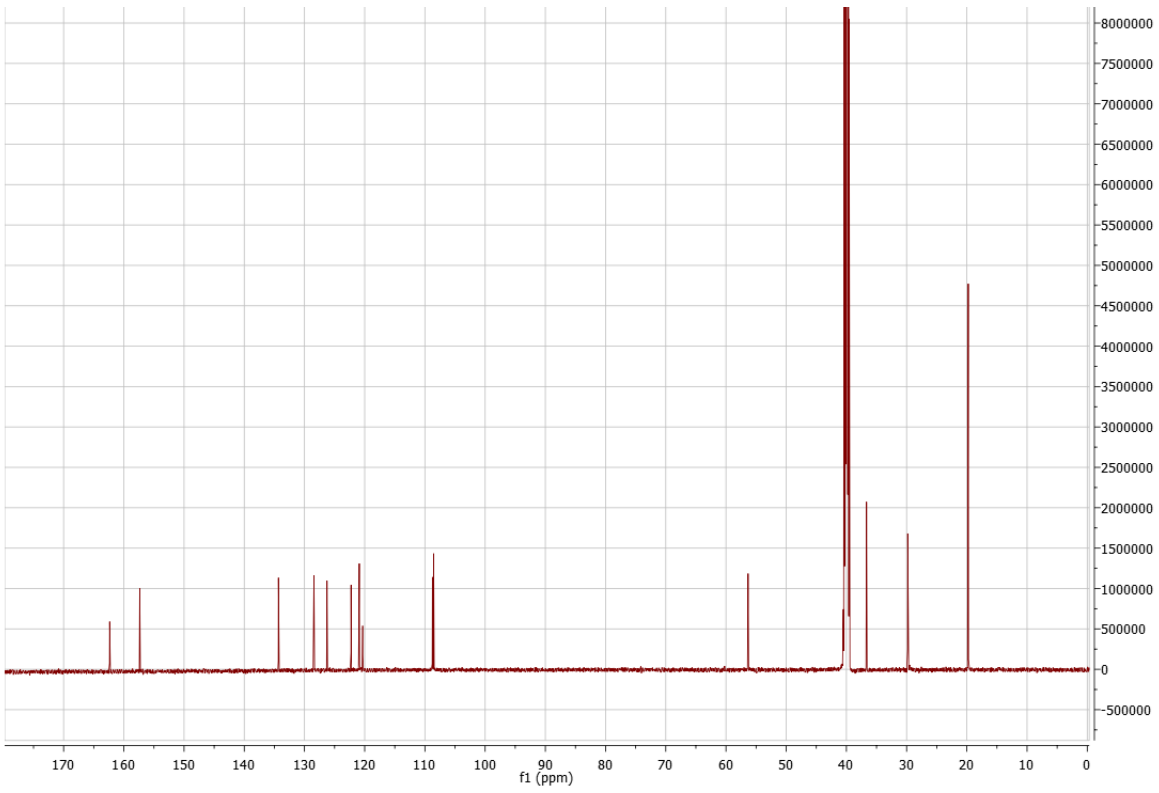

Figure S. ^{13}C of ADH-119_COOH

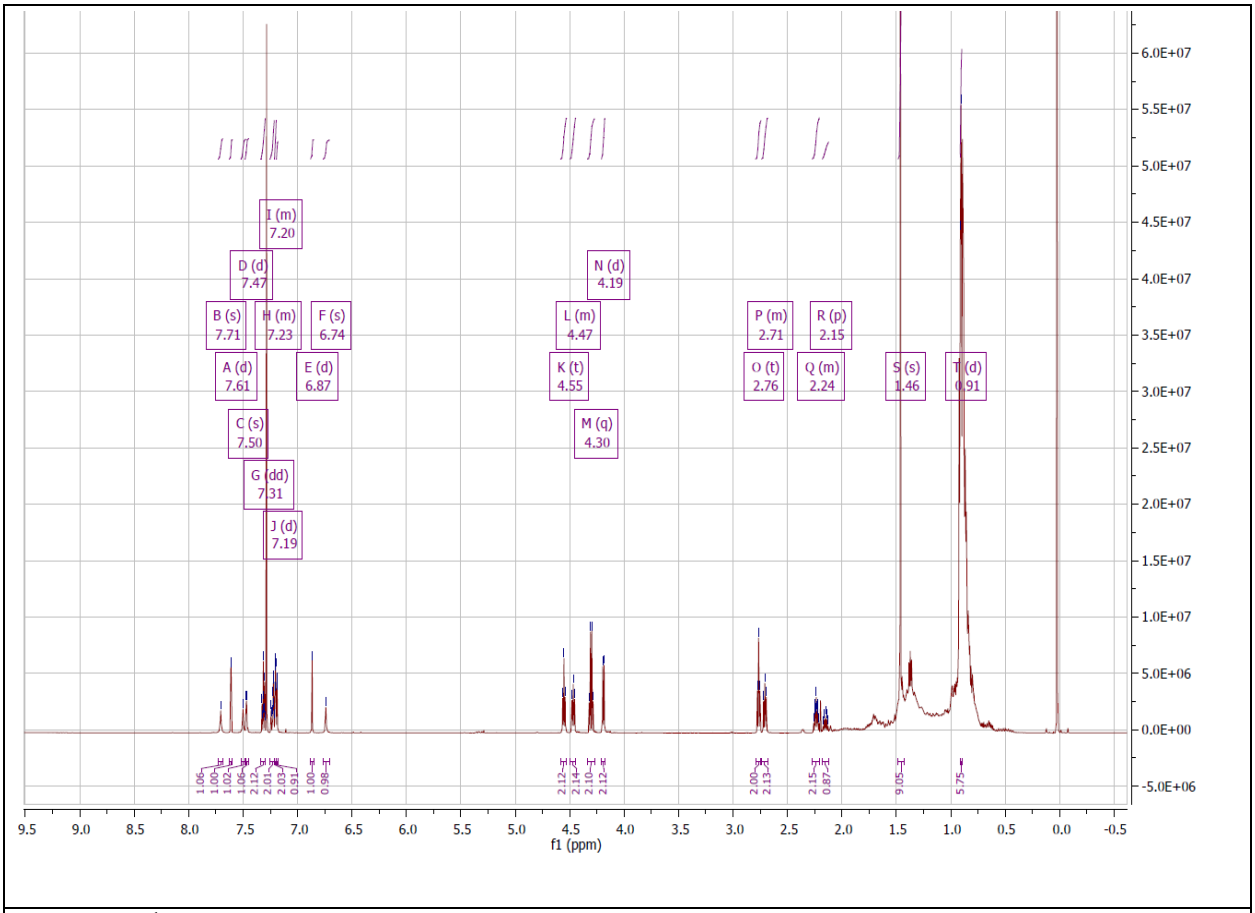

Figure S. ^{1}H of N-tert Butyl ADH-120

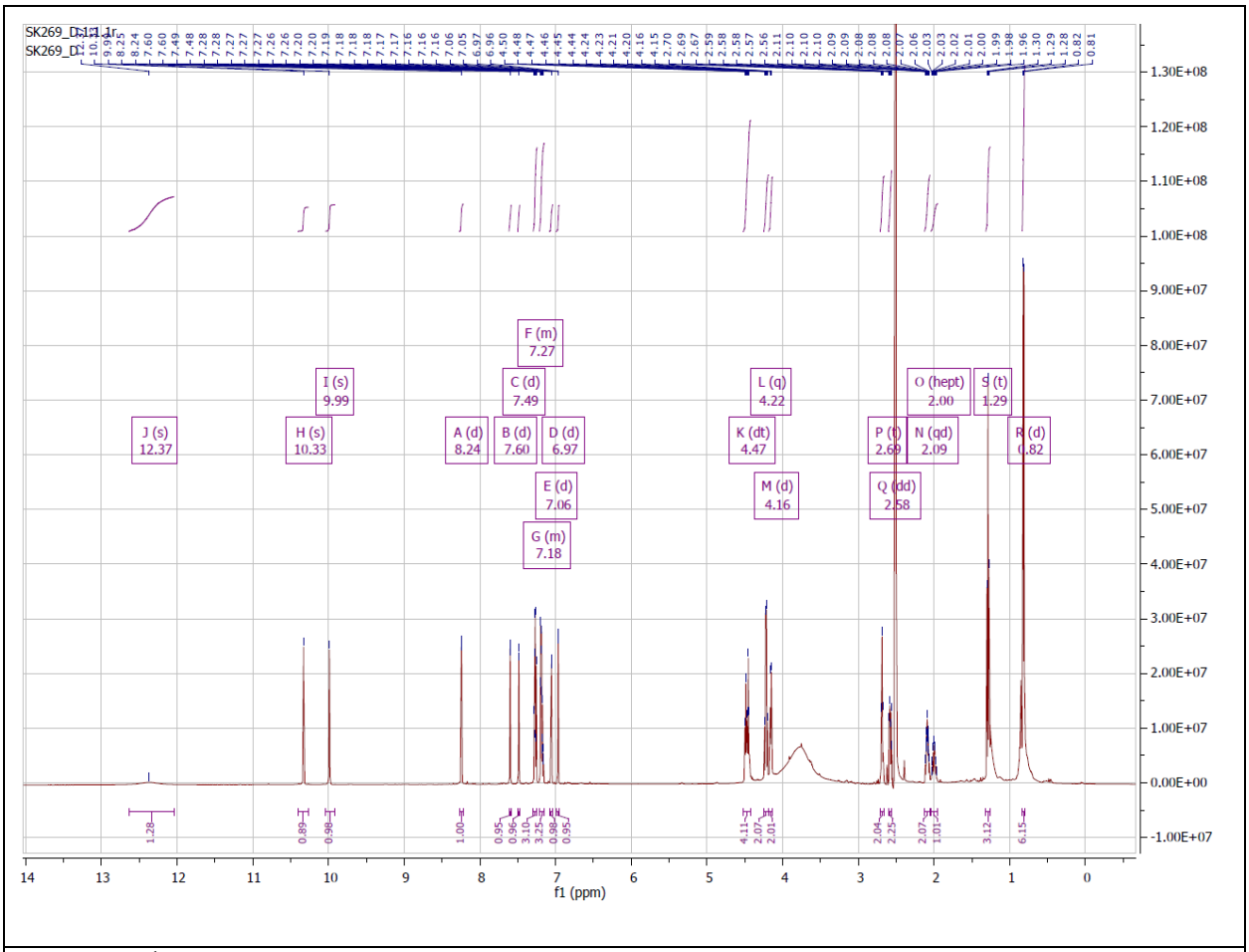

Figure S. ^{1}H of ADH-120